

**APICAL M2 PROTEIN IS REQUIRED FOR EFFICIENT INFLUENZA
A VIRUS REPLICATION**

by

Nicholas Wohlgemuth

A dissertation submitted to Johns Hopkins University in conformity with the
requirements for the degree of Doctor of Philosophy

Baltimore, Maryland

October, 2017

© Nicholas Wohlgemuth 2017

All rights reserved

ABSTRACT

Influenza virus infections are a major public health burden around the world. This dissertation examines the influenza A virus M2 protein and how it can contribute to a better understanding of influenza virus biology and improve vaccination strategies. M2 is a member of the viroporin class of virus proteins characterized by their predicted ion channel activity. While traditionally studied only for their ion channel activities, viroporins frequently contain long cytoplasmic tails that play important roles in virus replication and disruption of cellular function.

The currently licensed live, attenuated influenza vaccine (LAIV) contains a mutation in the M segment coding sequence of the backbone virus which confers a missense mutation (alanine to serine) in the M2 gene at amino acid position 86. Previously discounted for not showing a phenotype in immortalized cell lines, this mutation contributes to both the *attenuation* and *temperature sensitivity* phenotypes of LAIV in primary human nasal epithelial cells. Furthermore, viruses encoding serine at M2 position 86 induced greater IFN- λ responses at early times post infection. Reversing mutations such as this, and otherwise altering LAIV's ability to replicate *in vivo*, could result in an improved LAIV development strategy.

Influenza viruses infect at and egress from the apical plasma membrane of airway epithelial cells. Accordingly, the virus transmembrane proteins, HA, NA, and M2, are all targeted to the apical plasma membrane

and contribute to egress. When M2 is targeted away from the apical plasma membrane, virus replication and budding are significantly diminished. Consequently, viruses encoding M2 targeted away from the apical plasma membrane could be developed as vaccine candidates or used to improve systemic influenza virus models.

Together these studies demonstrate that non-immunodominant viral proteins, like M2, can be modified and used to drastically affect virus replication and function while potentially leading to new therapeutics and prophylactics.

Thesis Readers:

| | |
|-------------------------------|--|
| Adviser: Andrew Pekosz | Molecular Microbiology and Immunology – BSPH |
| Isabelle Coppens | Molecular Microbiology and Immunology – BSPH |
| Anna P. Durbin | International Health – BSPH |
| Diane E. Griffin | Molecular Microbiology and Immunology – BSPH |
| Carolyn E. Machamer | Cell Biology - SOM |

Alternates:

| | |
|-------------------|--|
| Sabra L. Klein | Molecular Microbiology and Immunology – BSPH |
| Kellogg J. Schwab | Environmental Health and Engineering – BSPH |

PREFACE

For Rosalind

The journey is difficult, immense, at times impossible, yet that will not deter some of us from attempting it. We cannot know all that has happened in the past, or the reason for all of these events, any more than we can with surety discern what lies ahead. We have joined the caravan, you might say, at a certain point; we will travel as far as we can, but we cannot in one lifetime see all that we would like to see or learn all that we hunger to know.

– Loren Eiseley, from *The Immense Journey*, 1946

ACKNOWLEDGEMENTS

This dissertation could not have been accomplished without the guidance, help, and support of many individuals. First, I would like to thank my thesis advisor, Dr. Andrew Pekosz. Andy is an incredible scientist, role model, and friend. Under his mentorship I have grown both professionally and personally. During my rotation, Andy spent the time to personally train me in several basic lab techniques. He taught me to think critically and like a scientist. Andy was perfect at giving me the space to have my own ideas and make mistakes (and learn from them) while also helping to guide me down the best path to the next, interesting experiment.

Additionally, I need to express gratitude for the people I worked with in Andy's lab. Drs. Erin Lalime and Melissa Hayes were great mentors who helped train me and answered many questions, even if their favorite answer was, "Did you check the protocol book?" (and yes, the answer was usually in there). Eric Jesteadt was a one-of-a-kind master's degree student who was a thorough teacher when it came to training me on the FACScalibur. Drs. Deena Blumenkrantz, Katherine Fenstermacher, and Hsuan Liu, all joined the lab during the middle of my tenure and provided excellent sources of knowledge and advice. Deena, was always generous with both her time and encyclopedic knowledge of influenza virus research. Katherine and Hsuan, both of whom did graduate training in other viral systems, were amazing sounding boards for ideas and provided keen insight from their unique

perspectives. Katherine's artistic eye and Illustrator skills proved invaluable for making and optimizing figures and schematics. Hsuan and I's projects were the most similar, and it was excellent to have another molecularly minded person in the lab to chat with about techniques. I also need to thank Brendan Smith, Harrison Powell, and James Stanton. Brendan's unique experience in industry and chemistry made him very helpful when troubleshooting assays, and it was great to have another dad in the lab to commiserate with about balancing child care and lab life. Harry and Jim were both fun to have around in the lab, but also great scientists with whom to discuss ideas. Drs. Farah El Najjar and Kathryn Shaw Saliba both joined the lab during the last couple years of my tenure and provided excellent fonts of knowledge and experience for troubleshooting experiments. The last labmate I need to thank is Yang "Eddy" Ye. Mentoring Eddy was an excellent opportunity to both grow as a teacher and work with a very talented scientist. Eddy had excellent "lab hands" and was instrumental to the work in Chapter 2 of this dissertation. I cannot thank him enough for his contributions to my growth as a mentor and scientist.

I would also like to thank Dr. Sabra Klein, an excellent "vice-mentor". Between sharing lab space, common resources, and a lab meeting, Sabra has always supported my growth as scientist. Her questions after my presentations often led to new experiments and ways of interpreting my data that I would never have thought of otherwise. I also need to thank all of the

members of the Klein lab that I had the pleasure of working with, especially Dr. Oliva Hall and Landon Vom Steeg. Having Oliva a year ahead of me in the program and Landon a year behind, provided great opportunities to receive advice, give advice, and chat about courses and departmental requirements.

I also need to thank my oral exam committee, thesis committee, thesis readers and alternates: Drs. Diane Griffin, Carolyn Machamer, Isabelle Coppens, Anna Durbin, and Kellogg Schwab. Their advice on the project at regular intervals has drastically improved this dissertation and helped facilitate my training. Dr. Griffin was a great mentor as a rotation advisor, as a member of my thesis committee, and for the three years I was her teaching assistant in Fundamental Virology. I have known for years that I wanted to be a virologist, and outside of Andy, Diane was the person most responsible for turning me into one. I would also like to specifically thank Drs. Coppens and Machamer for experimental help, both with techniques and reagents.

Many people within the MMI department also contributed to either this dissertation or my experience at Johns Hopkins. I would especially like to thank my cohort: Amanda Balaban, Tyler Henning, Jason Huska, Ross McFarland, Raúl Saraiva, and Drs. Natapong Tui, Nina Martin, and Ashley Nelson. Thanks for the directions while getting lost in Hershey, help finishing my hubcap margarita, and the late night study sessions. I also need to thank Gail O'Connor and Thom Hitzelberger. Gail was my primary go-to

for any questions about academics and always happy to chat about any problems I had. Thom was my go-to for questions about anything else. I have to believe that I set the MMI record for most package deliveries, and I thank Thom for taking it in good stride.

Next, I need to thank my Baltimore friends that helped keep me sane during my Hopkins tenure. I would first like to thank Rev. James and Angela Sharp for inviting us into their home weekly for Sausage Thursday where we got connected to most of our Baltimore friends. I especially need to thank Andrew Daugherty, Nelson Vasconcelos, Kevin Hentz, Sammy Grimsley, Patrick and Jocelyn Broadwick, Patrick and Jennie McCollum, Dave and Katie Reid, Samira Laniyan, and Dr. Christiana Salama. James, Ashley, and R.J. Gordy were great family friends with whom it was a pleasure to begin our families in parallel. I'm also thankful that one of my best friends, Davy Foote, moved from Nebraska to also get his PhD in the same state.

Finally, I need to thank my family for their constant support during my education. My parents helped raise me into the person I am, and I couldn't have finished my thesis without their support. I also need to thank my in-laws for their support and for helping take care of my family when I had to travel for conferences. Most importantly, I need to thank my wife Alexandra, whose support and love over these years has been the most critical to my success.

TABLE OF CONTENTS

| | |
|--|-------|
| ABSTRACT | ii |
| PREFACE..... | iv |
| ACKNOWLEDGEMENTS..... | v |
| TABLE OF CONTENTS | ix |
| LIST OF FIGURES..... | xv |
| LIST OF TABLES | xvii |
| LIST OF ABBREVIATIONS | xviii |
| CHAPTER 1: INTRODUCTION | 1 |
| BACKGROUND..... | 2 |
| INFLUENZA A VIRUS GENERAL BIOLOGY..... | 2 |
| LIVE-ATTENUATED INFLUENZA VACCINES | 5 |
| VIRAL MEMBRANE PROTEIN LOCALIZATION..... | 8 |
| VIROPORINS MEDIATE REPLICATION THROUGH ION CHANNEL DEPENDENT AND INDEPENDENT MECHANISMS | 10 |
| ABSTRACT | 10 |
| INTRODUCTION | 11 |
| GENERAL CHARACTERISTICS | 12 |
| CLASSIFICATION..... | 12 |
| ION CHANNEL ACTIVITY..... | 13 |

| | |
|---|----|
| ION CHANNEL DEPENDENT AND INDEPENDENT EFFECTS ON VIRUS REPLICATION AND CELLULAR FUNCTION | 15 |
| Influenza virus M2 | 15 |
| HIV-1 Vpu..... | 19 |
| HCV p7 | 21 |
| Coronavirus E..... | 23 |
| Other viroporins | 25 |
| VIROPORIN TARGETED TREATMENTS AND VACCINES | 29 |
| Inhibitors of viroporins | 29 |
| Vaccines targeted against viroporins | 31 |
| CONCLUSIONS AND FUTURE PERSPECTIVES..... | 33 |
| FIGURES AND TABLES | 35 |

| | |
|--|----|
| CHAPTER 2: THE M2 PROTEIN OF LIVE, ATTENUATED INFLUENZA VACCINE ENCODES A MUTATION THAT REDUCES REPLICATION IN HUMAN NASAL EPITHELIAL CELLS..... | 43 |
| ABSTRACT..... | 44 |
| INTRODUCTION..... | 45 |
| MATERIALS AND METHODS | 48 |
| Plasmids | 48 |
| Cell culture..... | 48 |
| Viruses..... | 49 |

| | |
|---|----|
| Plaque assays | 49 |
| 50% Tissue culture infectious dose (TCID ₅₀) assay | 50 |
| Low MOI infection | 51 |
| Interferon, cytokine and chemokine measurements | 52 |
| Statistical analyses | 53 |
| RESULTS | 53 |
| Rescue of recombinant viruses with mutations in the M2 cytoplasmic tail | 53 |
| Replication of rUd M2-83 mutants in MDCK cells and hNEC cultures.. | 54 |
| Replication of rUd M2-86 mutants in MDCK cells and hNEC cultures.. | 55 |
| Replication of rVic-LAIV M2-86 mutants in MDCK cells and hNEC cultures..... | 56 |
| Induction of chemokines, cytokines, and IFN- λ by rVic-LAIV M2-A86S in hNEC cultures..... | 56 |
| DISCUSSION..... | 57 |
| Acknowledgements..... | 61 |
| FIGURES AND TABLES | 62 |
| CHAPTER 3: INFLUENZA A VIRUS M2 PROTEIN APICAL TARGETING IS REQUIRED FOR EFFICIENT VIRUS BUDDING AND REPLICATION | 72 |
| ABSTRACT | 73 |
| IMPORTANCE | 73 |

| | |
|---|----|
| INTRODUCTION..... | 74 |
| MATERIALS AND METHODS | 76 |
| Plasmids | 76 |
| Cells | 77 |
| Antibodies..... | 78 |
| Stable cell line production and culture | 78 |
| Flow cytometry..... | 79 |
| Viruses..... | 80 |
| Plaque assays | 80 |
| 50% tissue culture infectious dose (TCID ₅₀) assay | 81 |
| Low MOI infection | 81 |
| High MOI infection | 83 |
| Microscopy | 83 |
| SDS-PAGE and western blotting | 84 |
| Statistical analyses | 85 |
| RESULTS | 86 |
| Expression of mistargeted M2 constructs..... | 86 |
| Complementation of viruses that do not express M2 | 87 |
| Replication of recombinant viruses expressing mistargeted M2 | 88 |
| High MOI infection and protein analysis of rVic M2-Baso in hNECs..... | 89 |
| rVic M2-baso replication and cell polarization | 90 |

| | |
|--|-----|
| High MOI infection and protein analysis of rVic M2-ER and rUdorn M2- Stop in MDCK cells..... | 91 |
| DISCUSSION | 92 |
| ACKNOWLEDGEMENTS | 98 |
| FIGURES..... | 99 |
| CHAPTER 4: GENERAL DISCUSSION | 109 |
| LAIV is no longer recommended in the USA due to problems with low effectiveness..... | 110 |
| Identification of novel determinants of LAIV replication..... | 114 |
| Identification of the mechanism behind the M2-86 mutation's role in <i>attenuation</i> | 115 |
| Optimizing LAIV replication and vaccine efficacy for diverse viruses and populations | 116 |
| Targeting M2 away from the apical plasma membrane decreases virus replication..... | 118 |
| Identification of the mechanism underlying the decrease in replication from mistargeting M2 | 119 |
| Identification of the M2 apical targeting sequence | 119 |
| Determine if mistargeting M2 has effects on early stages of virus gene expression..... | 121 |

| | |
|--|-----|
| Assessing the effects of mistargeting M2 on IAV assembly, budding, and cellular function | 122 |
| Systemic influenza virus model | 123 |
| Development of a mistargeted M2 vaccine..... | 125 |
| Conclusion..... | 128 |
| APPENDIX..... | 130 |
| REFERENCES..... | 131 |
| CURRICULUM VITAE..... | 209 |

LIST OF FIGURES

| | |
|---|-----|
| Figure 1.1. Influenza A virus biology | 36 |
| Figure 1.2. M2 schematic..... | 37 |
| Figure 1.3. The two-step process of influenza A virus assembly and budding | 38 |
| Figure 1.4. Targeting of proteins to the plasma membrane or ER in polarized epithelial cells | 40 |
| Figure 2.1. M2 cytoplasmic tail..... | 62 |
| Figure 2.2. Replication of M2-83 mutants on MDCK cells..... | 63 |
| Figure 2.3. Replication of M2-86 mutants in the rUd background on MDCK cells and hNECs | 65 |
| Figure 2.4. Replication of M2-86 mutants in the rVic-LAIV background in MDCK cells..... | 67 |
| Figure 2.5. Comparison of apical versus basolateral secretion of cytokines and chemokines | 69 |
| Figure 3.1. Localization of M2 proteins | 99 |
| Figure 3.2. Replication of IAV on MDCK II cells stably expressing different M2 proteins | 101 |
| Figure 3.3. Replication of recombinant viruses expressing different M2 constructs | 102 |
| Figure 3.4. Replication and protein expression of rVic M2-Baso and rVic M2- FLAG on hNECs | 103 |

| | |
|---|-----|
| Figure 3.5. The M2-Baso replication defect is dependent on the polarization of the hNEC culture | 105 |
| Figure 3.6. Replication and protein expression of rVic M2-ER on MDCK cells | 107 |
| Figure 3.7. Replication and protein expression of rUdorn M2-Stop on MDCK cells | 108 |

LIST OF TABLES

| | |
|---|-----|
| Table 1.1. Influenza A virus LAIV amino acid changes | 41 |
| Table 1.2. Targeting sequences are used to direct viral and cellular proteins to the appropriate locations | 42 |
| Table 2.1. Total secreted cytokine | 71 |
| Table A.1. Primer sequences | 130 |

LIST OF ABBREVIATIONS

| | |
|---------|--|
| A/LAIV | live, attenuated influenza A virus vaccine |
| ALI | air-liquid interface |
| att | Attenuation |
| B/LAIV | live, attenuated influenza B virus vaccine |
| ca | cold-adapted |
| CBD | caveolin-1 binding domain |
| CRAC | cholesterol recognition amino acid consensus |
| DMEM | Dulbecco's modified Eagle medium |
| DM | differentiation medium |
| DPI | days post infection |
| E | envelope small membrane protein |
| ELISA | enzyme-linked immunosorbent assay |
| ER | endoplasmic reticulum |
| ERGIC | endoplasmic reticulum-Golgi apparatus intermediate compartment |
| HA | Hemagglutinin |
| HCV | hepatitis C virus |
| HIV-1 | human immunodeficiency virus 1 |
| HMA | hexamethylene amiloride |
| hNEC | human nasal epithelial cells |
| HPI | hours post infection |
| IAV | influenza A virus |
| IBV | influenza B virus |
| ICV | influenza C virus |
| IgA | immunoglobulin A |
| IgG | immunoglobulin G |
| IM | infection media |
| IFN | Interferon |
| LAIV | live, attenuated influenza vaccine |
| LIR | LC3-interacting region |
| M1 | matrix protein 1 |
| M2 | matrix protein 2 |
| M2-Baso | M2 targeted to the basolateral plasma membrane |
| M2e | M2 ectodomain |
| M2-ER | M2 targeted to the endoplasmic reticulum |
| M2-FLAG | M2 with a FLAG tag |
| mAb | monoclonal antibody |
| MDCK | Madin-Darby canine kidney cells |

| | |
|--------------------|---|
| MERS-CoV | Middle East respiratory syndrome coronavirus |
| mTEC | mouse tracheal epithelial cells |
| NA | Neuraminidase |
| NP | Nucleoprotein |
| NS1 | nonstructural protein 1 |
| NS2 | nonstructural protein 2 |
| PA | polymerase acidic protein |
| pAb | polyclonal antibody |
| PB1 | polymerase basic protein 1 |
| PB2 | polymerase basic protein 2 |
| PBCV-1 | Paramecium bursaria chlorella virus 1 |
| RSV | respiratory syncytial virus |
| RT | room temperature |
| rUd | A/Udorn/72(H3N2) |
| rVic | A/Victoria/361/2011(H3N2) |
| SARS-CoV | severe acute respiratory syndrome coronavirus |
| sGP | soluble glycoprotein |
| SH | small hydrophobic protein |
| SRP | signal recognition particle |
| SS | seed stock |
| TCID ₅₀ | 50% tissue culture infectious dose |
| TGEV | transmissible gastroenteritis coronavirus |
| ts | temperature sensitivity |
| Vpu | viral protein U |
| vRNP | viral ribonucleoprotein complex |
| WS | working stock |
| wt | wild type |

CHAPTER 1: INTRODUCTION

BACKGROUND

INFLUENZA A VIRUS GENERAL BIOLOGY

Influenza A viruses (IAV) are members of the *Orthomyxoviridae* family of viruses with negative-sense, single-stranded RNA genomes. Their genomes are comprised of 8 segments encoding 10-14 proteins (1). IAV particles have a complex structure that takes a spherical or filamentous form (Fig. 1.1A). The helically encapsidated segments are contained by a lipid membrane derived from the host plasma membrane. This envelope contains the viral glycoproteins, hemagglutinin (HA) and neuraminidase (NA), and the ion channel protein, matrix protein 2 (M2). IAV matrix protein 1 (M1) lines the interior of the envelope. The core of the virion consists of the viral ribonucleoprotein complexes (vRNP), which each contain one of the 8 genome segments coated with the virus nucleoprotein (NP). Each NP coated segment is associated with a virus polymerase complex consisting of polymerase basic protein 1 (PB1), polymerase basic protein 2 (PB2), and polymerase acid protein (PA). The soluble nonstructural protein 2 (NS2) is also present in purified virus particles (1, 2).

IAV binds to sialic acids on the apical surface of respiratory epithelial cells to initiate infection. The viral glycoprotein HA binds different arrangements of sialic acid depending on its species of origin. HA proteins from human viruses preferentially bind sialic acid connected to the

penultimate sugar residue by an α 2-6 linkage, whereas avian virus HA proteins preferentially bind sialic acid connected by an α 2-3 linkage (3). The invading IAV particle is endocytosed via receptor mediated endocytosis, and the low pH of the maturing endosome triggers the fusion protein, HA, to fuse the viral membrane with the host endosomal membrane (Fig. 1.1B). Efficient uncoating after fusion requires the ion channel activity of M2 which facilitates the flux of H^+ from the endosome to the interior of the particle. This pH change disrupts protein-protein interactions between M1 and the vRNP, freeing the vRNP into the cytoplasm (4, 5). Next, the vRNP are transported into the nucleus. Each protein in the vRNP complex possesses a nuclear localization signal, which allows for the importation of the complexes into the nucleus (1, 6, 7). Once in the nucleus, the viral polymerase complex (PB1, PB2, and PA), transcribes mRNA from the negative sense genome. PB1 is the RNA-dependent RNA polymerase, PB2 binds the 5' cap of the host cellular RNA, and PA cleaves the host cellular RNA to free the cap for priming transcription of viral mRNA. Importantly, the negative sense genomic RNA serves as the template for both viral mRNA and positive sense anti-genome. It is thought that the concentration of newly produced NP controls the switch between mRNA and anti-genome synthesis, that is, as NP concentrations increase, the polymerase complex switches to producing anti-genome (8, 9). Alternatively, the polymerase complex may have no preference for mRNA or anti-genome, but it is not until NP reaches sufficient

concentrations to help stabilize anti-genome that anti-genome begins to accumulate (10, 11). After the viral genome has been replicated and the viral proteins are synthesized by host cell machinery, assembly and budding occur. Briefly, the viral glycoproteins, HA and NA, M2, M1 and the vRNPs accumulate at or adjacent to lipid rafts in the apical plasma membrane. Efficient virus assembly and budding both require M2 (Fig. 1.2, 1.3A, and 1.3B) (12). NA is needed to remove sialic acid residues from the infected host cell (13, 14). This prevents HA from anchoring the nascent particles to the cell and allows the particles to disperse through the airway lumen and infect additional cells. Most mammalian viruses are released with HA in the uncleaved form, HA0. In the airway lumen, host protease cleaves HA0 into HA1 and HA2, which contains the fusion peptide. This cleavage primes HA for inducing the next round of replication (1).

Influenza viruses infect approximately 18% of unvaccinated individuals every year (15), causing around 20,000 deaths in the USA alone (16). The annual economic burden of influenza virus infections in the USA is estimated to be 87 billion dollars (17). IAVs are classified into antigenic subtypes based on their HA (H1-H18) and NA (N1-N11) molecules, although only 3 HA subtypes and 2 NA subtypes typically infect humans (H1-H3 and N1-N2). However other subtypes can replicate in humans and pose pandemic risks (e.g. H5N1 and H7N9). The other subtypes circulate in various animal species, with water fowl being the primary reservoir for IAV genetic and

antigenic diversity. The viruses currently circulating in humans are H1N1 (pandemic 2009 H1N1), H3N2, influenza B virus (IBV), and influenza C virus (ICV). Like IAV, IBV causes seasonal epidemics while ICV generally causes mild disease and does not cause epidemics (18). IBV does not have extensive animal reservoirs like IAV. It only replicates in humans and seals, but it does have two lineages that co-circulate in humans (Victoria and Yamagata) (19). Two classes of anti-influenza drugs are approved for treatment in the USA and Europe: M2 ion channel inhibitors and neuraminidase inhibitors (18).

LIVE-ATTENUATED INFLUENZA VACCINES

At the population level, influenza viruses undergo frequent genetic drifts resulting in new antigenic variants that can escape existing HA and NA specific immunity (20). Antigenic shift, or the emergence of a new antigenic type due to reassortment or zoonosis, can also lead to escape of preexisting population level immunity (21). These phenomena necessitate frequent updating of the influenza vaccine to account for the novel antigens present in new, dominant strains. Vaccines are the current best practice for decreasing the public health burden of influenza viruses. Injectable trivalent inactivated influenza vaccine (formalin inactivated) has been available in the USA since the 1940s and includes one strain of each IAV H1N1, IAV H3N2, and IBV (22). In 2003, the USA FDA approved trivalent LAIV for healthy individuals aged 5-49, and in 2007, an updated LAIV was approved for healthy

individuals aged 2-49 (20). Since there is not cross-protection between IBV lineages, quadrivalent vaccines recently (2013) replaced trivalent vaccines and include one strain of each influenza B strain lineage (in addition to the other strains of the trivalent vaccine) (23).

LAIV is created as a 6:2 reassortment virus containing the HA and NA gene segments from the *wt*, circulating strain for which immunity is desired, and the 6 internal gene segments (PB2, PA, PB1, NP, M, and NS) from the cold-adapted master donor viruses. For IAV (A/LAIV), the donor virus is cold-adapted A/Ann Arbor/6/1960 (H2N2), and for IBV (B/LAIV), the donor virus is cold-adapted B/Ann Arbor/1/1966. Three phenotypes are conferred by the LAIV internal gene segments: *cold-adaptation* (*ca*; the ability to replicate at 25°C), *attenuation* (*att*; decreased replication, especially as measured *in vivo*), and *temperature sensitivity* (*ts*; decreased replication at “high” temperatures like 37°C). Both *wt* A/Ann Arbor/6/1960 and *wt* B/Ann Arbor/1/1966 were extensively passaged at gradually decreasing temperatures in primary chicken kidney cells until they were able to replicate efficiently at 25°C (20, 24).

For A/LAIV, there were 24 nucleotide mutations and 11 amino acid changes that occurred while cold-adapting A/Ann Arbor/6/1960 (H2N2) (Table 1.1) (25). Using immortalized cell lines (MDCK) and embryonated hens’ eggs, the *ts* and *att* phenotypes were mapped to mutations in the PB2 (S265), PB1 (E391, E581, and T661) and NP (G34) genes (26, 27) (Table 1.1). However, *in*

in vivo experiments in ferrets and humans showed that the mutations in the M and PA segments are sufficient to confer *att* (28). Additional *in vivo* work in ferrets, hamsters, and humans revealed that the PB2, PB1, PA, and M segments of LAIV all contribute to the *att* phenotype (29) (Table 1.1). More recently, primary human nasal epithelial cells (hNECs) have been demonstrated to be a useful model for studies involving the LAIV *att* and *ts* phenotypes. (30-33). Using these cells, the M segment A/LAIV mutation (M2-A86S) was confirmed to specifically contribute to the *att* and *ts* phenotypes (33). Other A/LAIV work in hNECs revealed decreased A/LAIV replication compared to WT despite similar numbers of virus particles released into the supernatant fluid (31) and an altered and generally more robust innate immune response associated with A/LAIV (32). For B/LAIV, the *ts* phenotype was mapped to the PA (M431) and NP (A114 and H410) gene segments and the *att* phenotype was mapped to these same mutations and the M segment (Q159 and V183) (20, 34, 35).

Due to problems with decreased LAIV effectiveness, the USA Advisory Committee for Immunization Practices recommended that LAIV not be used in the USA during the 2016-2017 influenza season (36, 37). The low effectiveness has been hypothesized to have been caused by pre-existing immunity in the population preventing sufficient replication of the attenuated vaccine viruses and the biology of the virus strains themselves (37). Specifically, the H1N1 component of the vaccine replicates poorly in

many of the systems in which it has been tested (including tissue culture), making it too attenuated to induce a protective immune response. However, it may be possible to genetically engineer LAIV to replicate optimally such that it can produce a robust immune response, while remaining safe (33, 37).

VIRAL MEMBRANE PROTEIN LOCALIZATION

Viruses are master manipulators of the cells they infect, taking advantage of robust cellular processes to quickly and efficiently replicate without having to “reinvent the wheel”. This includes the process of protein targeting and localization. Membrane proteins, both viral and cellular, must traffic to the location of their function. For many enveloped virus proteins, this is the site of assembly. Flockhouse virus transmembrane proteins target to the mitochondrial membrane (38), coronavirus transmembrane proteins target to the ER-Golgi intermediate compartment (ERGIC) (39), and influenza A virus proteins target to the plasma membrane (12). For proteins targeted through the secretory pathway, when an ER signal sequence emerges from the ribosome, it is co-translationally bound by a signal recognition particle (SRP) that then docks the ribosome/nascent peptide complex to the ER via the SRP receptor (40). The signal peptide is then bound by the protein translocator which feeds the protein into the ER lumen as it is translated. The hydrophobic signal peptide is usually cleaved by a signal peptide peptidase, but the presence of a stop-transfer sequence allows for dissociation from the

protein translocator and the formation of a transmembrane domain that will anchor the protein to the plasma membrane. This process results in a transmembrane protein with the N-terminus in the ER lumen and the C-terminus facing the cytosol. However, multipass transmembrane proteins and proteins with differing topologies are possible depending on if the signal peptide/start transfer sequence is cleaved and the number and order of additional stop and start transfer sequences (40). Depending on any additional targeting sequences, proteins are then processed and trafficked normally to their final destination. This is accomplished through the concerted efforts of Rab proteins and Rab effector proteins that direct vesicles to the correct region, while SNARE proteins mediate fusion in a destination specific manner (40).

In polarized epithelial cells, there are two zones of the plasma membrane divided by the tight junction (Fig. 1.4). Above the tight junction, facing the luminal space, is the apical plasma membrane. Below the tight junction, including the majority of the lateral surfaces of the cell and the side facing the basal lamina, is the basolateral plasma membrane. The default destination for transmembrane cargo in the secretory pathway is the plasma membrane. Apically targeted proteins have diverse features that allow for their targeting. These include GPI-anchors, N-linked glycans, and signals in their transmembrane domains (Table 1.2). It is also thought that proteins without any other targeting signals find their way to the apical plasma

membrane by default (41). This is in contrast to basolateral targeting, which is thought to be dominant to apical targeting because adding a basolateral targeting sequence to an otherwise apically targeted protein will often result in the basolateral targeting of that protein (42). Basolateral targeting sequences include a C-terminal dileucine motif and tyrosine based signals (Fig. 1.4 and Table 1.2) (41). Proteins can also be targeted to the secretory pathway. Targeting proteins to the ER can be done through either ER retention signals (43) or retrieval signals that return the protein to the ER from further along in the secretory pathway (44). Proteins targeted to other cellular compartments and organelles use similar mechanisms, but contain distinct targeting signals (Table 1.2).

VIROPORINS MEDIATE REPLICATION THROUGH ION CHANNEL DEPENDENT AND INDEPENDENT MECHANISMS

The following review is in preparation for submission by Nicholas Wohlgemuth and Andrew Pekosz.

ABSTRACT

Viroporins are small transmembrane proteins that perform numerous, important viral functions. They commonly form homo-oligomers in host cells and display ion channel activity with poor specificity. Viroporins are

primarily considered only for their ion channel activity despite commonly possessing unusually long tail domains for viral membrane proteins. The cytoplasmic tail of IAV M2, the best characterized viroporin, plays critical roles in virus assembly, virus budding, and the regulation of host cell responses. While, the ion-channel activity of viroporins makes a tempting antiviral target, better understating of the non-ion channel functions of viroporins will allow for the better design and targeting of antiviral drugs. Because of their highly conserved nature, viroporins also provide intriguing targets for vaccination, and several vaccine candidates already target viroporin antigens. Future research into the critical, non-ion channel functions of viroporins could lead to better antiviral treatments and prophylactics.

INTRODUCTION

There are over 200 known viruses that readily infect humans (45) with the constant threat of emergence and reemergence adding to this number (46-48). Despite the universal burden of virus infection, there is a dearth of effective treatment options for the vast majority of viral pathogens, necessitating further research into their basic biology and pathophysiology (49). One of the first antiviral drugs to be clinically licensed in the USA was amantadine, an ion channel inhibitor that targets IAV M2 (50-56). M2 is a member of the expanding virus protein class known as viroporins, of which there are now

known members in many clinically important human viruses including human immunodeficiency virus 1 (HIV-1), hepatitis C virus (HCV), and Middle East respiratory syndrome coronavirus (MERS-CoV). Better understanding the biology of these diverse mediators of virus pathogenesis could lead to the development of novel therapeutics targeting both the ion channel activity of these proteins and their many other functions.

GENERAL CHARACTERISTICS

Viroporins are characterized by their small size (60-120 amino acids), homo-oligomerization (commonly 4-6 subunits), transmembrane domains, and ability to create hydrophilic pores through a phospholipid bilayer (57). These virally expressed ion channels are often significantly smaller than their cellular counterparts. The cytoplasmic tails of M2 and other viroporins have been demonstrated to contain other features and domains that interact with virus or cellular proteins and lipids. These domains have diverse functions such as inducing membrane curvature, budding, and assembly.

CLASSIFICATION

Nieva, *et al.* (49) have proposed a classification system for viroporins based on the number of their transmembrane domains and topology. Class I viroporins are oligomers of single-pass transmembrane proteins while class II viroporins are oligomers of helix-turn-helix hairpin transmembrane proteins that span

the membrane with each helix. Subclass IA viroporins have their C-terminus facing the cytosol and their N-terminus facing the organelle lumen. This group includes IAV M2, HIV-1 viral protein U (Vpu), and CoV envelope small membrane protein (E) (49), while subclass IB viroporins have flipped topology and includes human respiratory syncytial virus (RSV) small hydrophobic protein (SH) and poliovirus 3A proteins (49). Subclass IIA viroporins have both their N- and C-termini facing the organelle lumen and includes HCV p7, while subclass IIB viroporins again have flipped topology, with both protein termini facing the cytosol and include the poliovirus 2B protein (49).

ION CHANNEL ACTIVITY

Viroporins rarely act as traditional cellular voltage- or ligand-gated channels, and often lack high ion selectivity (56). This is unsurprising considering the limited coding capacity of viruses and the small size of viroporins compared to their cellular counterparts. However, two of the best characterized viroporins, IAV M2 and *Paramecium bursaria chlorella* virus 1 (PBCV-1) Kcv protein, are highly selective for protons and potassium ions (58, 59) respectively. M2 and Kcv act more similarly to cellular ion channels in this regard. Nevertheless, other viroporins often have some small degree of selectivity. For example, HIV-1 Vpu and HCV p7 have mild cationic selectivity (60, 61).

Importantly, the specificity of many viroporins is context-specific. RSV SH protein is selective for cations at neutral pH and for anions at low pH (62). Additionally, the highly conserved IAV M2 His37 residue has been demonstrated to reside in the pore and, upon protonation at low pH, contribute to both ion channel activation and proton selectivity (63-68). At neutral pH, the nearby Trp41 residues cluster and block proton channel activity (49, 67, 69). However, at acidic pH's, the Trp residues open and allow for the transport of protons (66, 68). Another striking example of viroporin specificity switching is the SARS-CoV E protein, where the charge of the lipid membrane environment affects the ionic specificity of the pore (70-73).

Cells spend a great deal of energy using pores and channels to maintain membrane gradients that are critical for basic house-keeping functions and homeostasis. However, viroporins often thwart these cellular efforts. For example, viroporins can increase the intracellular Ca^{2+} ion concentration by either allowing extracellular Ca^{2+} to enter from outside the cell or by releasing Ca^{2+} from intracellular stores (74-78). This increase in Ca^{2+} concentration can have drastic effects on cellular functions including mediating the activity of enzymes and inducing apoptosis. The ion channel activities of IAV M2 (79-84) and HCV p7 (85, 86) neutralize the pH in the late Golgi compartment, protecting virus particle and glycoprotein structure and disrupting cellular protein trafficking (56). Furthermore, a number of viroporins, including IAV M2 (87), RSV SH (88), and HCV p7 (89), have been

demonstrated to activate the NLRP3 inflammasome, a process generally activated through the disruption of intracellular K^+ concentrations (56, 90, 91).

ION CHANNEL DEPENDENT AND INDEPENDENT EFFECTS ON VIRUS REPLICATION AND CELLULAR FUNCTION

Viroporins have been traditionally studied for their ion channel activity and the effects this activity has on virus replication and cellular activities.

However, due to limits on virus genome size and coding capacity, viral proteins, including viroporins, often assume numerous, diverse functions during replication. Consequently, the non-conductive domains of viroporins, including ectodomains and cytoplasmic tails, perform critical roles in virus replication that would seem out of place for cellular ion channels.

Influenza virus M2

The class IA viroporin IAV M2 has the most well characterized structure of any viroporin. Despite this, the precise structural mechanisms for activity and inhibition are not perfectly understood, due in part to the structural properties of M2 varying depending on experimental conditions (66, 92). The IAV M2 protein is perhaps the most well studied viroporin with regards to both its ion channel activity and ion channel independent activities. The M2 ion channel has been demonstrated to be critical in numerous aspects of the

virus lifecycle. During entry, the influenza virus particle is endocytosed. Following acidification of the endosome, ion channel activity of M2 allows for the acidification of the internal environment of the virus particle. This allows for the release of the vRNPs from the virus M1, which frees the vRNP to enter the nucleus, permitting transcription and replication to begin (1). As mentioned above, M2 ion channel activity also neutralizes the pH in the late Golgi, preventing the premature triggering of the viral fusion protein, HA (79, 82, 83, 93-96).

Despite its well characterized role as an ion channel, IAV M2 is a 97 amino acid protein with 53 of those amino acids (54.6%) present in the cytoplasmic tail (Fig. 1.2). The region of the cytoplasmic tail nearest to the transmembrane domain is required for efficient ion channel activity (97) and has been demonstrated to encode an amphipathic helix. The helix is thought to insert into the plasma membrane, induce membrane curvature, and facilitate ESCRT-independent membrane fusion and virion budding (12, 98, 99). However, the extent of this region's effect on budding and replication is dependent on virus strain and the experimental system used (42, 100-103). IAV budding occurs at lipid rafts in the apical plasma membrane (Fig. 1.3A). M2 is thought to localize to lipid rafts via cholesterol recognition amino acid consensus (CRAC) motifs in the amphipathic helix region of the cytoplasmic tail (98, 104) or through joint targeting with M1, since when expressed alone, M2 does not localize to lipid rafts (12, 105, 106). However, removal of the

CRAC motifs does not result in a significant defect in virus replication *in vitro*, but does decrease virulence *in vivo* (100, 107), raising questions about the CRAC domain's role during *in vitro* particle assembly. Similarly, palmitoylation of a cysteine residue at position 50 in this region is not required for replication *in vitro*, but does contribute to virulence *in vivo* (107, 108). The CRAC motif region of M2 also contains a caveolin-1 binding domain (CBD) that may play a role in the subcellular localization of M2 (Fig. 1.2) (12, 109, 110).

While the membrane proximal region of the M2 cytoplasmic tail has been implicated in the budding and scission processes of virus egress, the C-terminal end of the cytoplasmic tail is critical for virus assembly and the incorporation of vRNPs into budding virus particles (Fig. 1.3C) (111-115). Through systematically truncating the M2 cytoplasmic tail, several groups identified a region of M2 from amino acid position 70 to 77 as critical for virus replication and interaction with M1 (Fig. 1.2) (111, 112, 114, 115). Follow up studies identified a highly conserved tyrosine residue at position 76 that is required for replication, normal NP and M1 incorporation into virus particles, and filament formation on the surface of cells (Fig. 1.2) (113, 116). Together, these studies support a two-step model of IAV assembly coordinated by the viral M2 protein and its interactions with M1 (112) (Fig. 1.3). In the first step, the M2 cytoplasmic tail binds to M1, specifically M1 that is bound to the vRNP complex, ensuring that M1 and the vRNP are properly localized to the

apical plasma membrane (Fig. 1.3A). As multiple vRNP complexes are brought together by M1 in lipid rafts, the combined effects of HA, NA, M1, and M2 cause particle budding to occur. M2 is excluded from the lipid rafts, leaving it concentrated at the neck of budding (Fig. 1.3). Through additional interactions with M1, M2 then drives both scission and normal particle morphology (spherical and filamentous) (Fig. 1.3B). When the M2 cytoplasmic tail is truncated, or critical amino acid residues are mutated, one, or both steps of virus assembly and budding can be disrupted (Fig. 1.3C) (111, 112).

Depending on the virus strain (111, 112, 114, 115), the M2 cytoplasmic tail region from amino acid 82-89 is critical for influenza virus replication (Fig. 1.2). Scanning alanine mutagenesis of the region failed to identify any specific residues that conferred this phenotype (112), but this region contains two highly conserved alanine residues at positions 83 and 86 that were never mutated as part of the original studies. Additionally, M2-86 is the site of a mutation only seen in the A/LAIV backbone virus. The LAIV-associated serine residue at position 86 turns out to be associated with decreased replication in hNECs, but not in immortalized cells, and is also associated with an altered cytokine secretion profile in infected cells (33). Nearer to the distal end of the cytoplasmic tail (Fig. 1.2), is a LC3-interacting region (LIR) capable of binding host LC3, relocalizing it to the plasma membrane, and subverting autophagy (117-120).

While IAV M2 is the best characterized, IBV and ICV also express M2 proteins, BM2 and CM2, respectively. BM2 and CM2 are small proteins (109 and 115 amino acids respectively) with short ectodomains (7 and 23 residues respectively), hydrophobic transmembrane domains (19 and 23 residues respectively), and long cytoplasmic tails (83 and 69 residues respectively) and form homo-tetramers in membranes (121-124). Similar to M2, both BM2 (125) and CM2 (126) are crucial for assembly and genome packaging, and while the transmembrane domains are generally interchangeable among the M2 proteins, the cytoplasmic tails are species specific and not interchangeable (127, 128). Similar to M2, BM2 interacts with cellular factors, promoting virus replication. Specifically, BM2 binds and inhibits the cell cycle regulator and pro-apoptotic protein p53 (129). CM2 is able to alter intracellular pH (127), but unlike M2 and BM2, CM2 is posttranslationally glycosylated (124).

HIV-1 Vpu

The Vpu accessory protein is encoded by HIV-1 and numerous simian immunodeficiency virus strains (130). It is an 81 amino acid integral membrane protein with a 54 amino acid cytoplasmic tail (131). The cytoplasmic tail contains two amphipathic helices joined by a hinge region (132, 133). The cation selective ion channel activity of Vpu is highly evolutionarily conserved with, likely, a robust, as yet undiscovered,

functional significance that is independent of its better characterized roles in host protein inhibition and degradation (134). However, membrane depolarization enhances virus particle release (135) and mutations disrupting ion channel formation reduce pathogenicity (56, 136, 137). Furthermore, substitution of Vpu with IAV M2 results in a virus that remains pathogenic (138). The oligomeric structure of the class IA viroporin HIV Vpu has not been solved to atomic resolution, but monomers of Vpu span membranes from residues 8-25 (49, 139). *In vitro* experiments (140) and *in silico* modelling (141, 142) have demonstrated that Vpu likely exists as a tetramer, pentamer, or larger oligomer (49).

Vpu, in contrast to most viroporins, is known primarily for its non-ion channel activities. One of these activities is its downregulation of the host surface protein CD4. Specifically, Vpu targets nascent CD4 in the ER, leading to proteasomal degradation of CD4 via the ERAD pathway and a 30-fold decrease in half-life (131, 143). Vpu and CD4 have been demonstrated to physically interact in the ER (144) via their cytoplasmic tails (144, 145), and this interaction is critical for CD4 degradation (131). It is thought that two conserved serine residues in the hinge region of the cytoplasmic tail become phosphorylated, recruit beta transducin-repeat containing protein, which in turn recruits ubiquitin proteolysis machinery, leading to the degradation of CD4 (146-150).

Another well characterized function of Vpu is the promotion of virus particle release (151, 152). This is thought to occur primarily through Vpu inhibition of the interferon stimulated gene BST2, a restriction factor that prevents the release of numerous enveloped viruses (153, 154). BST2 is thought to form a “tethered picket fence” around lipid rafts, likely organizing them in ways that are suboptimal for virus budding (155, 156). Additionally, BST2 “tethers” newly released virus particles to the infected cell preventing their release (157-161). As part of its normal localization, BST2 cycles from the plasma membrane through clathrin-coated vesicles to the trans-Golgi network and back (162, 163). Vpu binds BST2 (164-168) and slows down its recycling to the plasma membrane. Vpu also decreases the trafficking of newly synthesized BST2 to the plasma membrane, further decreasing the amount of BST2 available for antiviral activities (156, 169-172). Furthermore, Vpu can enhance BST2 degradation through ESCRT-dependent lysosomal degradation (156, 173-175).

HCV p7

HCV p7 is a small integral membrane protein that is critical for the production and release of infectious HCV virus particles (176). HCV monomers assemble as a homo-hexamer shaped like a large flower with the “petals” protruding towards the lumen and potentially serving as interacting sites with ER resident proteins (49, 176, 177). p7 is a 63 amino acid protein

with two transmembrane regions and both N- and C-terminal ends facing the ER lumen (class IIA) (178, 179). p7 has an 18 amino acid N-terminal end followed by two transmembrane helices (14 and 17 residues) separated by a 7 amino acid basic loop, and a 7 amino acid C-terminal tail (180, 181).

HCV p7 has ion channel activity with a small preference for cations (61, 86, 176, 181-186). As described for M2, its ion channel activity is activated at low pH (187). It can even substitute for M2 by protecting HA throughout the exocytic pathway (85), and M2 can partially restore HCV infectious virus production when expressed *in trans* (86). The ion channel activity of p7 has also been directly linked to its facilitation of the production of infectious HCV particles (180, 188, 189). It is thought that the p7 ion channel might be a regulator of a pH-dependent maturation process of the viral particles, but the precise mechanism has yet to be determined (176). Because intracellular particles are pH-sensitive while mature extracellular particles are not, p7 may help protect intracellular virions before they mature (86, 176). p7 causes changes to intracellular pH that may trigger NLRP3 inflammasome activation and downstream cytokine production (190).

Despite having smaller cytoplasmic and luminal regions than other viroporins, p7 has a number of non-ion channel dependent functions during virus replication. p7 helps modulate assembly through its interactions with viral NS2, independent of its ion channel activity. In this role, p7 is likely recruiting the envelope glycoproteins to the site of assembly, the ER (191-

196). Furthermore, the p7/NS2 interaction facilitates relocalization of core to the ER (197, 198). Independent of its ion channel activity, p7 can also act as a lipid raft adhesion factor, likely helping foment the lipid composition necessary for particle envelopment and budding (199). These interactions may explain the critical role p7 plays in capsid assembly and envelopment (56, 200).

Coronavirus E

Coronavirus E protein is a small (76-109 amino acid) transmembrane protein that plays many roles during coronavirus replication (reviewed by Ruch and Machamer 2012 (201)). It is thought to form homo-pentamers to account for its ion channel activities (202-205). E proteins are relatively diverse among Coronavirus species. They contain a hydrophobic domain near the N-terminal end that inserts into cell membranes such that the N-terminal end extends into the organellar lumen and the C-terminal end extends into the cytoplasm (206, 207). Additionally, there are conserved cysteines that are targets for palmitoylation and also highly conserved proline residues (201, 208-211).

The ion channel activity of some coronavirus E proteins displays preference for monovalent cations, especially Na^+ (212, 213) and is inhibited by hexamethylene amiloride (HMA), a broad spectrum Na^+/H^+ exchanger (56). While the role of E ion channel activity in virus replication is uncertain, HMA does inhibit replication (212). Furthermore, mutations in the

transmembrane domain effect ion channel activity and cause defects in replication (214, 215).

Similar to M2, the cytoplasmic tail of E interacts with a number of viral and cellular proteins to promote virus replication. Coronaviruses assemble and bud at the ERGIC membrane (216, 217). The expression of viral E and M (whose cytoplasmic tails interact (218)) can drive the formation of virus like particles (VLP) indicating that E plays a role in assembly and budding (219-221). Introducing mutations in the E protein cytoplasmic tail can result in unstable virus particles with altered morphology, possibly due to scission defects (222). Mutations in the transmembrane domain do not affect assembly, further implicating the cytoplasmic tail as the region critical for the assembly and budding processes (209, 214). Knocking out the E gene in some Coronaviruses does not totally ablate assembly and budding, although virus particles do assemble less efficiently than during WT infections (223-225). Palmitoylation of the E protein cytoplasmic tail is thought to be important for assembly and the E/M interaction (209-211). The precise mechanism by which E promotes assembly and budding is unknown, but these studies show that it may be an important facilitator of the budding and scission process (201).

Furthermore, SARS-CoV E interacts with the cellular tight junction protein PALS1, potentially promoting disassembly of the tight junctions during infection (226). Specifically, the last four C-terminal residues of E

interact with the PDZ domain of PALS1 (70, 226). PDZ domains are common among cellular proteins that bind C-terminal tails of proteins, hinting at the possibility of more cellular interaction partners of E (70, 227).

One of the most drastic effects on the morphology of cells infected with the coronavirus infectious bronchitis virus is the swelling of the Golgi complex, which is dependent on a single residue in the transmembrane domain of E (214). This swelling is coupled with a rearrangement and displacement of the Golgi complex from its perinuclear location (228, 229). Importantly, some of these changes are seen in normal cells producing large cargo like procollagen (230, 231). When E has been knocked out during transmissible gastroenteritis coronavirus (TGEV) or SARS-CoV infection, there is evidence that particles are properly assembled, but become arrested in the secretory pathway (224, 225). Together, these data suggest that SARS-CoV E protein expression is associated with a swelling of the Golgi complex that can better accommodate the trafficking of coronavirus particles during egress (201).

Other viroporins

While they seem to be more commonly encoded by RNA viruses, several DNA viruses do encode viroporins. *Chloroviruses* are a genus of giant viruses in the *Phycodnaviridae* family which infect freshwater, unicellular, *chlorella*-like green algae (232, 233). Because of the nature of their replication (DNA viruses that replicate in the cytoplasm) and their large genome sizes (greater

than 300,000 nucleotides), *Chloroviruses* encode viral versions of many cellular proteins to facilitate their replication. Likely due to viral genome packaging restrictions, many of their proteins are among the smallest examples of their functional class. PBCV-1 encodes Kcv, a 94 amino acid K⁺ channel protein (58, 234-236). The functional form is a homo-tetramer with complex characteristics including gating, high selectivity, and voltage sensitivity (58, 237). It is hypothesized that the ion channel depolarizes the infected cell's plasma membrane, preventing superinfection, by another *Chlorovirus* (238). In contrast to many of the viroporins of RNA viruses, Kcv appears to function solely as an ion channel, and has only a small cytoplasmic tail (12 amino acids) that is not known to provide any secondary functions for replication. Another DNA virus viroporin-like protein, agnoprotein, is found in some polyomaviruses including JC and BK viruses. Little is known about polyomavirus agnoprotein, but it displays some common features of viroporins and is important for replication (92).

Many other RNA viruses also encode viroporins. Rotavirus nonstructural protein 4 (NSP4) is larger (175 amino acids) than most other identified viroporins, and its viroporin activity was only discovered and characterized recently (75, 239-242). NSP4 is perhaps best known for its role as the first discovered viral enterotoxin (243), and it acts as an enterotoxin in both its secreted form and viroporin form through two distinct pathways (244). Like other viroporins, NSP4 is thought to promote virus budding, and

this activity is likely mediated by its ion channel activity. The structure of NSP4 has not been biochemically determined, but the viroporin domain is thought to be 44 amino acids long starting at amino acid position 47 (75). NSP4 has a preference for cations over anions and is able to conduct Ca^{2+} , an activity linked to its enterotoxic effects and ability to promote assembly and budding (240, 242). Additional research is needed to determine the precise structure of full length NSP4 and mechanistic insights into its other roles during infection, including induction of autophagy to promote replication (245).

The soluble form of Ebolavirus glycoprotein (sGP) is translated as the result of RNA editing of the GP gene, and it matures through a proteolytic cleavage process that releases a small fragment (40 amino acids) known as delta peptide (246). This delta peptide is important during virus entry (247), and is highly conserved among related filoviruses (248). An *in silico* analysis predicted the presence of a lysine-rich amphipathic sequence at the C-terminal end of the protein with high structural relatedness to Rotavirus NSP4 (248). *In vitro* studies have confirmed that the delta peptide increases ion and small molecule permeability across lipid membranes (249). Additional research needs to be done to determine the roles of this newly identified viroporin during infection and if this activity plays a role in the delta peptide's ability to facilitate entry.

Hepatitis E virus ORF3 is a 114 amino acid protein that has recently been shown to be a viroporin (250, 251). Little is known about the structure, but it is purported to form homo-oligomers in the ER of infected cells, and displays ion channel activity (250). Furthermore, ORF3 is essential for particle release from infected cells (250, 252-255), and can inhibit the expression of cytokines and chemokines during infection (256). Future studies are needed to confirm the ion channel activity of ORF3, determine its structure, and which domains of the protein are facilitating virion release and inhibiting the immune response.

The alphavirus 6K protein is about 60 amino acids in length (257) and both increases membrane permeability and forms ion channels in lipid bilayers (258, 259). Similar to other viroporins, 6K is important for virus assembly and budding. Specifically, mutating cysteines in 6K caused a decrease in the release of virus particles, coincident with increased nucleocapsid content in virus particles and aberrant envelope formation (260). Additional work has confirmed that 6K is critical for assembly and budding (261-263), but few structural studies have been performed to validate this role and determine the mechanism (264). Recently, a new alphavirus protein was discovered which is encoded as the result of a frame shifting event during 6K translation. The newly discovered transframe (TF) protein contains a C-terminal extension in the -1 open reading frame, maintains ion channel activity, and may have redundant roles with 6K. TF is

not strictly required for virus propagation in culture, but it does promote the release of virus particles (265).

There are numerous other viroporins and potential viroporins among virus families. Human respiratory syncytial virus encodes a small hydrophobic protein (SH) that exhibits some viroporin-like features but is not critical for replication *in vitro*. However, deleting SH does lead to attenuation *in vivo* (266-268) and inhibits the induction of apoptosis (269, 270). Protein 2B is an approximately 100 amino acid long protein encoded by enteroviruses of the *Picornaviridae* family (271). It has two transmembrane domains, and in most species, both its C- and N-terminal ends face the lumen of the endomembrane system (272, 273). Precise structural studies have not been done, but 2B increases cytosolic Ca²⁺, alters membrane trafficking, and promotes viral replication, all activities commonly associated with viroporins (74, 92, 274). Avian reovirus p10 (a fusion-associated small transmembrane protein) is thought to be a viroporin, inhibit apoptosis, and promote syncytia formation and virus release (275-278).

VIROPORIN TARGETED TREATMENTS AND VACCINES

Inhibitors of viroporins

Viroporins make excellent targets for antiviral therapy because they are essential to many aspects of virus replication. Many viroporins are critical for

the release of infectious particles, while others have effects on cellular membranes that promote replication, and still others are important mediators of host immune responses. Because viroporins are so much smaller and less complex than most host ion channels, it is possible to specifically inhibit their activity with minimal side effects. Amantadine and its derivatives are well documented inhibitors of M2 ion channel activity (279). Similarly, long alkyl-chain iminosugar derivatives block HCV p7 ion channel activity and the release of infectious virus particles (184, 280, 281). Amiloride derivatives (like HMA) inhibit the channel activity of HIV-1 Vpu and SARS-CoV E proteins (212, 282). Other inhibitors have also been used to target viroporins, with varying degrees of success (56). However, targeting antiviral therapy towards the non-ion channel functions of viroporins could have substantial benefits. Dual and combination therapies have the advantage of decreasing the probability of resistance developing *de novo*. Furthermore, using multiple drugs to target different activities of a viroporin could decrease the likelihood of resistance due to malleability constraints on such small, polyfunctional proteins. Mutations that provide resistance to the drug may negatively affect one of the viroporin's other functions, preventing evolutionary selection.

Vaccines targeted against viroporins

Because they are highly conserved viral proteins, viroporins make attractive vaccine targets for viruses that escape host immune responses via antigenic diversity. As described above for IAV, vaccines targeting the more immunogenic glycoproteins (HA and NA) require annual vaccination due to antigenic shift and drift. Decisions about which strains to incorporate into the vaccine are made too far in advance to consistently match the strains that are prevalent during the upcoming season, decreasing vaccine effectiveness. However, IAV M2 is more highly conserved than HA and NA, and therefore vaccines targeting M2 may have greater cross reactivity across IAV strains and subtypes, even against novel and pandemic strains. One promising vaccine target is the ectodomain of M2 (M2e) (reviewed in Kolpe, *et al.* 2017 and Schotsaert, *et al.* 2009 (283, 284)). The earliest evidence that anti-M2 immunity might be effective is that a mouse monoclonal antibody specific for the M2 ectodomain (14C2) demonstrated negative effects on the replication of several IAV strains *in vitro* (285). Furthermore, passive transfer of 14C2 to infected mice results in decreased amounts of virus detected in the lungs (286). One of the first reported M2e vaccines has the M2e domain fused to the Hepatitis B core protein and provides protection from lethal challenge in the mouse model (287). Other M2e-fusion and whole M2 vaccines have been developed, but so far, none have advanced to human trials.

Alterations to the IAV M2 cytoplasmic tail have also led to several vaccine candidates. Extending the M2 cytoplasmic tail by adding a myc epitope to the end leads to decreased virus replication *in vivo*, but not *in vitro*, and immunization with this mutant virus protects mice from subsequent lethal challenge (288). Furthermore, as discussed above, large truncations of the M2 cytoplasmic tail result in decreased replication *in vitro* (111, 112, 114, 115), but shorter truncations have minimal effects on replication *in vitro*, yet still decrease virus replication in mice and induce heterotypic immunity (289, 290). Additionally, IAV with defective M2 ion channel activity (291) or M2 deleted entirely (292, 293) have been proposed as vaccine candidates. The M2 deletion vaccine also provides effective heterosubtypic protection in both mice and ferrets (293, 294). One downside to the M2 truncation and deletion vaccines is that M2 contains several cytotoxic T-cell epitopes and can induce T cell based immunity (295-298). In addition to these promising IAV vaccine candidates, mutating the M2 cytoplasmic tail to target M2 away from the site of budding and assembly results in decreased replication in primary respiratory epithelial cells and could yield a promising vaccine candidate (42). Furthermore, currently licensed vaccines like the LAIV (discussed above) could be optimized through mutations in M2 that optimize virus replication to a level that provides robust immunity but remains safe (33, 37).

In addition to IAV M2, viroporin-based vaccines could potentially be used to protect against any of the viruses discussed above. Deleting E from the SARS-CoV genome or SH from the RSV genome results in attenuated viruses that could potentially be developed as live, attenuated vaccines (224, 268). However, because of this vulnerability, viruses seem to have evolved other immunodominant epitopes that prevent robust, natural immune responses to viroporins. For example, while IAV M2 contains T cell epitopes, the immunodominant T cell responses are against the M1 and NP proteins (299, 300). Further development of vaccine candidates and delivery systems may overcome these challenges.

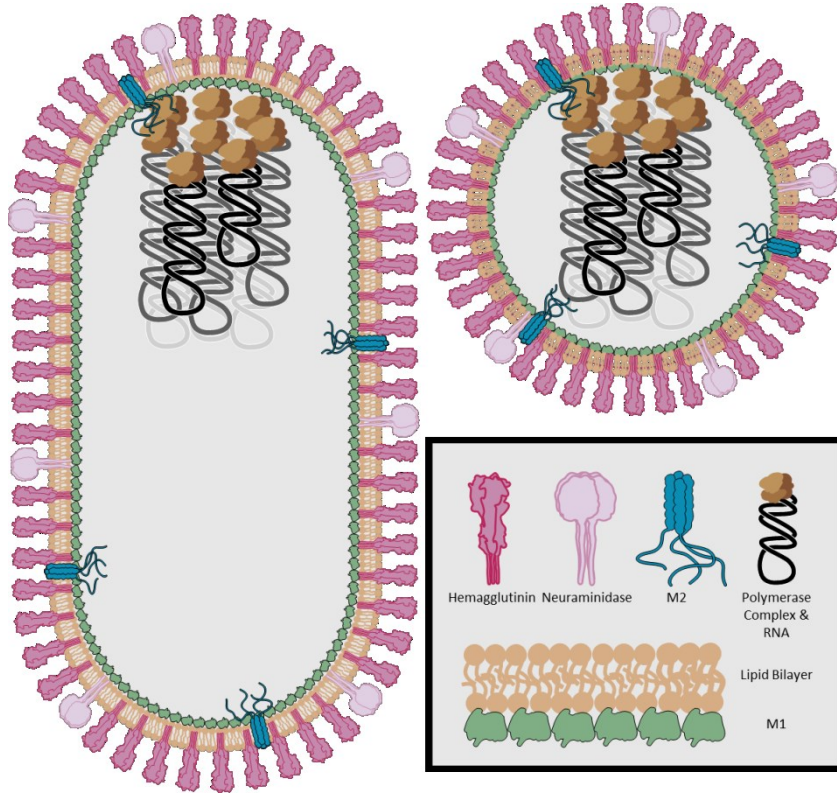
CONCLUSIONS AND FUTURE PERSPECTIVES

This review focuses on the sometimes secondarily considered, non-ion channel activities of viroporins. Viroporins are an emerging target for both clinical intervention with drugs and prevention via vaccination. Viruses are infamous for ‘doing more with less’, with regard to genome size, compared to other pathogens. To think of viroporins as just ion channels is to discount decades of research into the polyfunctionality of viral proteins and genome-coding capacity restrictions placed on viruses. For many viroporins there is a scarcity of mechanistic studies attributing the various known functions to the different regions of the protein. Regulating host processes including membrane trafficking and apoptosis could be via non-ion channel domains

interacting with cellular proteins, via ion channel activity disrupting cellular homeostasis, or via other mechanisms. While ion channel activity is likely conserved due to its necessity for replication, assessing the role of non-ion channel domains in virus replication could provide valuable information for drug and prophylactic discovery efforts.

FIGURES AND TABLES

A



B

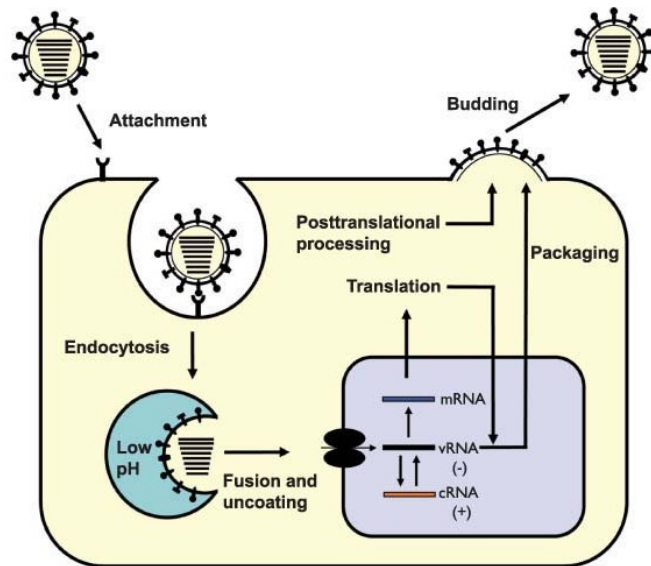


Figure 1.1. Influenza A virus biology. A) Influenza A virus particle with “spherical” (right) and filamentous (left) morphology. Image adapted from Noda, et al. 2012 (301). Artwork generated by Katherine J. Fenstermacher. Both virus particles have the 8 vRNPs surrounded by an envelope coated with HA and NA. M2 is present in low concentrations in the envelope. B) Influenza A virus replication cycle. Image from Shaw and Palese 2013 (1). Upon binding the surface of the cell, the virus particle is endocytosed and the low pH of the endosome triggers both fusion and the release of vRNP into the cytoplasm. The vRNPs are then imported into the nucleus where the viral RNA is replicated and viral mRNA transcribed. Viral proteins and vRNPs concentrate at the apical plasma membrane for assembly and budding (1).

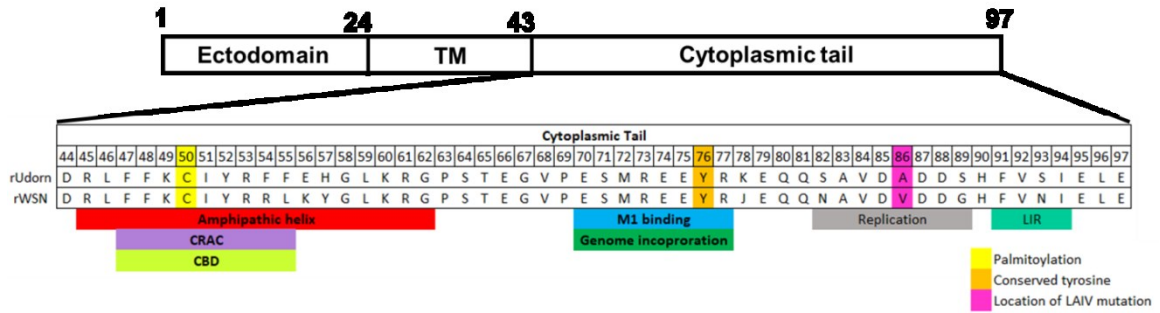


Figure 1.2. M2 schematic. M2 is a 97 amino acid protein encoded as a splice variant of the virus M gene segment. The 53 amino acid cytoplasmic tail contains numerous functional domains important for replication. CRAC – cholesterol recognition amino acid consensus domain. CBD – caveolin-1 binding domain. LIR – LC3 interacting region.

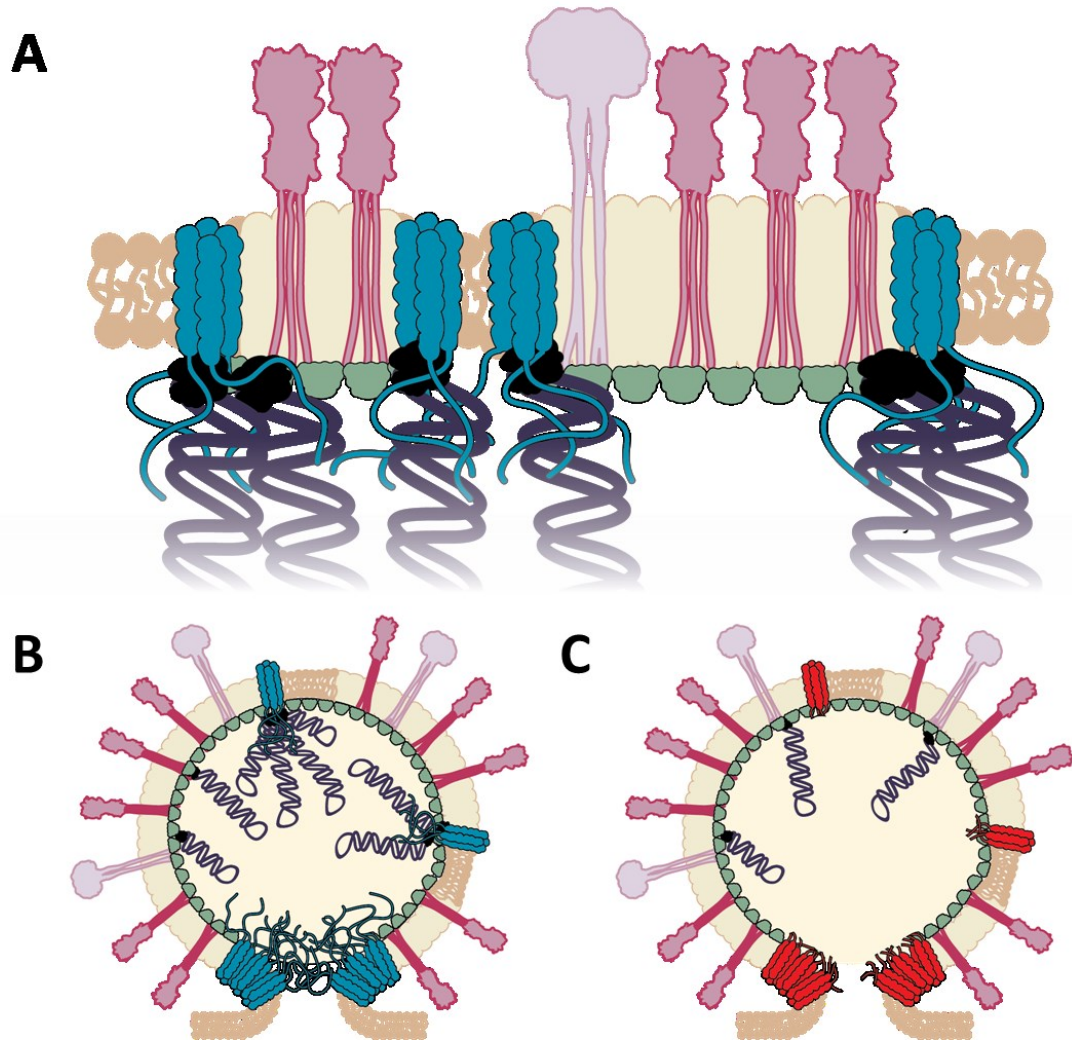


Figure 1.3. The two-step process of influenza A virus assembly and budding. A) Step 1: aggregation of virus particle components at the apical plasma membrane. The M2/M1/vRNP tripartite interaction is critical for the efficient recruitment and packaging of vRNP. B) Step 2 with full length M2: M2 and M1 mediate virion particle morphology and the efficient packing of vRNP and M2 at the budding “neck” facilitates particle scission and budding. C) Step 2 with truncated M2: the M1/M2 interaction is disrupted, altering particle morphology and decreasing the incorporation of vRNP into the

budding particle. Key: dark pink protein – HA, light pink protein – NA, purple hairpin with black polymerase complex- vRNP, green protein – M1, teal protein – full-length M2, red protein – truncated M2. Artwork generated by Katherine J. Fenstermacher.

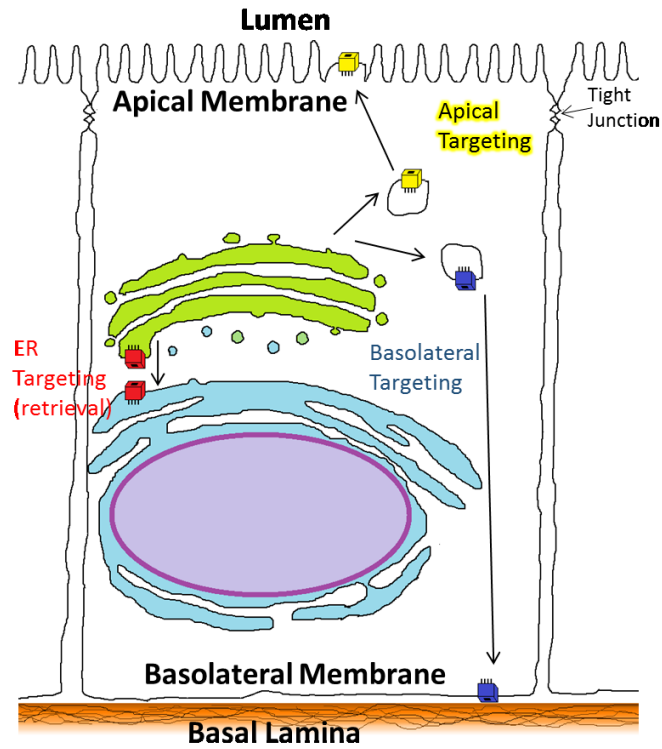


Figure 1.4. Targeting of proteins to the plasma membrane or ER in polarized epithelial cells. Targeting sequences are required to target viral and cellular proteins to different regions of the cell.

| Segment | Amino acid | Phenotype |
|---------|---|---------------|
| PB2 | S265 | <i>ts/att</i> |
| PB1 | E391 D457 E581 T661 | <i>ts/att</i> |
| PA | E613 P715 | <i>att</i> |
| NP | N23 G34 | <i>ts/att</i> |
| M2 | S86 | <i>ts/att</i> |
| NS1 | T153 | |

Table 1.1. Influenza A virus LAIV amino acid changes. During the cold-adaptation process, A/Ann Arbor/6/1960 (H2N2) accumulated 11 amino acid changes in its internal gene segments. It is generally considered that five of those changes (bolded) confer the *attenuation (att)* and *temperature sensitivity (ts)* phenotypes. However, additional work has demonstrated that the PA segment and M2 mutation contribute to the *ts* and *att* phenotypes. Adapted from Jin and Subbarao 2015 (20).

| Subcellular location | Targeting sequence |
|-----------------------------|---|
| Nucleus | Short sequence of positively charged residues |
| Mitochondria | Positively charged amphipathic helix |
| Peroxisome | C-terminal –SKL |
| ER | C-terminal -KDEL or –KKXX |
| Apical plasma membrane | N-linked glycans, GPI anchors |
| Basolateral plasma membrane | C-terminal -LL, C-terminal AASLLAP, C-terminal YXXL |

Table 1.2. Targeting sequences are used to direct viral and cellular proteins to the appropriate locations (40). Apical and basolateral targeted sequences reviewed in Stoops and Caplan, 2014 (41).

**CHAPTER 2: THE M2 PROTEIN OF LIVE,
ATTENUATED INFLUENZA VACCINE
ENCODES A MUTATION THAT REDUCES
REPLICATION IN HUMAN NASAL
EPITHELIAL CELLS**

Nicholas Wohlgemuth, Yang Ye, Katherine J. Fenstermacher, Hsuan Liu,
Andrew P. Lane, Andrew Pekosz

Vaccine. 2017. Epub 2017 Oct 25. PMID: 29079099.

ABSTRACT

The influenza A virus components of the live, attenuated influenza vaccine (LAIV) encode the HA and NA gene segments from a circulating virus strain and the remaining gene segments from the cold-adapted master donor virus, A/Ann Arbor/6/1960 (H2N2). The master donor virus imparts at least three phenotypes: *temperature-sensitivity (ts)*, *attenuation (att)*, and *cold-adaption (ca)*. The genetic loci responsible for the *att* and *ts* phenotypes of LAIV were mapped to PB1, PB2, and NP by reverse genetics experiments using immortalized cell lines. However, several *in vivo* studies have demonstrated that the M segment, which acquired an alanine (Ala) to serine (Ser) mutation at M2 position 86 during cold-adaption – a mutation found in no other influenza A virus strain – contributes to the *att* phenotype. Prior studies have shown this region of the M2 cytoplasmic tail to be critical for influenza virus replication. Using reverse genetics, we demonstrate that certain amino acid substitutions at M2 positions 83 and 86 alter the replication of influenza A/Udorn/307/72 (H3N2). Importantly, substitution of a Ser at M2 position 86 reduces A/Udorn/307/72 replication in differentiated primary human nasal epithelial cell (hNECs) cultures, but does not substantially affect replication in MDCK cells. When a Ser was substituted for Ala at M2 86 in LAIV, the virus replicated to higher titers and with faster kinetics in hNEC cultures, implicating that this amino acid change contributes to LAIV attenuation. Increased replication also resulted in

increased production of IFN- λ . These data indicate the LAIV associated Ser mutation at M2 position 86 contributes to the *att* phenotype and is associated with a differential regulation of interferon in LAIV infection.

INTRODUCTION

Influenza A virus (IAV) is a member of the *Orthomyxoviridae* family and contains an 8-segment, negative-sense RNA genome encoding 10 to 14 proteins (1). The live attenuated influenza vaccine (LAIV) is a 6:2 reassortant vaccine virus containing the PB2, PB1, PA, NP, M, and NS genome segments of a live-attenuated donor virus that was selected for its attenuated (*att*) and temperature-sensitivity (*ts*; replication at $\leq 32^{\circ}\text{C}$ but not $\geq 39^{\circ}\text{C}$) phenotypes. There are 11 amino acid differences between the LAIV strain and the IAV strain from which it was derived (25). The *att* and *ts* LAIV phenotypes have been mapped to the PB1 (E391, G581, T661), PB2 (S265), and NP (G34) genes by experiments in immortalized cell lines (20, 26, 27, 29, 302). These experiments did not demonstrate a contribution of the M2-A86S mutation to temperature dependent LAIV replication. However, *in vivo* experiments in hamsters, ferrets and even humans have implicated the LAIV mutation M2-A86S as important for the *att* phenotype (20, 28, 29, 303). Few studies have been performed to understand the molecular mechanisms conferring these phenotypes. During single-step replication in Madin-Darby canine kidney (MDCK) cells at 39°C , viral RNA synthesis and vRNP export from the

nucleus are reduced. Furthermore, incorporation of the viral matrix protein M1 into virus particles was reduced, causing heterogeneous and irregular virion morphology (20, 302). LAIV replication is restricted within physiological ranges of temperature (32 to 37°C) during infection of primary, differentiated human nasal epithelial cell (hNEC) cultures (30, 31), suggesting that other mutations in the LAIV genome may contribute to reduced virus replication in primary respiratory epithelial cell cultures.

The M2 protein is a 97 amino acid integral membrane protein with a 54 amino acid cytoplasmic tail (304). It is a highly conserved protein required for virus entry (305), membrane scission (99) and the production of infectious virus particles (111-115). M2 forms disulfide-linked homo-tetramers with pH-gated, proton-selective ion channel activity (101, 306). The ion channel activity is critical for virus uncoating – by allowing protons to enter the virion interior, and thus permitting the vRNP to dissociate from M1 (1, 59, 307, 308) – and preventing the premature cleavage of HA by neutralizing the pH in the late Golgi (93). M2 has also been shown to be important for inhibition of autophagy and preventing autophagosome fusion with lysosomes (117, 119, 120).

The distal region of the M2 cytoplasmic tail is essential for IAV replication and is involved in vRNP incorporation into progeny virions (111-115). When the M2 cytoplasmic tail is truncated by deleting the last 16 amino acids there is decreased release of infectious virus particles, which is not

observed when only the last 8 amino acids are deleted (112). When the region (M2 82-89) was mutated to alanine residues, infectious particle production was not altered. However, the original alanine residues at M2 positions 83 and 86 were never mutated and their contribution to the M2 protein functions never investigated. The A83 residue is conserved across a wide range of IAV strains while A86 is highly conserved except for pandemic 2009 H1N1 viruses (Val) and LAIV (Ser).

To investigate the role amino acids at positions 83 and 86 of M2 may play in IAV replication and attenuation, we generated recombinant viruses with substitutions at these amino acids. This allowed us to show that both amino acid positions contributed to efficient virus replication. Both glutamic acid and serine substitutions at position 86 caused an approximately 2-log decrease in virus replication in primary human nasal epithelial cells (hNEC) but not MDCK cells. The magnitude of decrease was dependent on the temperature (greater reduction at 37°C than at the permissive temperature of 32°C) of the cells during infection. Introducing an M2-S86A substitution increased LAIV replication and altered interferon lambda (IFN-λ) production in hNEC cultures, indicating a role for the M2-86S amino acid change in both the *att* and *ts* phenotypes of LAIV.

MATERIALS AND METHODS

Plasmids

The plasmid pHH21 expressing full length influenza virus gene segments was used to generate recombinant viruses (111) as described below. All mutations were introduced using the QuikChange Lightning site-directed mutagenesis kit (Agilent). All inserts and mutations were confirmed by sequencing. Primer sequences are in Table A.1 in the appendix.

Cell culture

MDCK cells and HEK 293T (293T) cells were cultured in Dulbecco's modified Eagle medium (DMEM) supplemented with 10% fetal bovine serum (FBS), 100 U/mL penicillin, 100 µg/mL streptomycin, and 2 mM GlutaMAX (Gibco). Human nasal epithelial cell (hNEC) cultures were isolated from non-diseased tissue after endoscopic sinus surgery for non-infection related conditions and grown at air-liquid interface (ALI) as previously described (31, 309-311). hNEC differentiation medium (DM) and culture conditions have previously been described in detail (31). The donors for the hNEC cultures were females ages 57 and 61 (Fig. 2.2), males ages 47 and 67 (Fig. 2.3) and males ages 72 and 67 (Fig. 2.4, Fig. 2.5 and Table 2.1).

Viruses

Recombinant A/Udorn/307/72 (H3N2) (rUd) has been described previously (108, 112, 305, 312). A recombinant LAIV consisting of the internal gene segments of A/Ann Arbor/6/1960 (H2N2) and the HA and NA segments from A/Victoria/361/2011(H3N2) (rVic-LAIV) was generated using sequences available in Genbank and the NIAID Influenza Research Database (25, 313, 314). Recombinant viruses were rescued using the 12-plasmid reverse genetics system (108, 305, 312, 315). Briefly, 293T cells were transfected with pHH21 plasmids encoding all 8 influenza A virus gene segments along with protein expression plasmids encoding NP, PA, PB1, and PB2. Transfected cells were then co-cultured with MDCK cells, and sampled every 24 hours for the presence of infectious virus. Viruses were then plaque purified and confirmed by sequencing. The entire M segment open reading frame was sequenced in all recombinant viruses to ensure the absence of any second site mutations. All rVic-LAIV rescues were performed at 32°C. Stocks of virus were generated by infecting MDCK cells at a low multiplicity of infection (MOI) as described below.

Plaque assays

Plaque assays were performed in 6-well plates of confluent MDCK cells. Serial 10-fold dilutions of the virus inoculum were generated in infection media (IM; DMEM supplemented with 0.3% BSA [Sigma], 100 U/mL

penicillin, 100 µg/mL streptomycin, 2 mM GlutaMAX [Gibco], and 4 µg/mL N-acetyl tryptsin [NAT; Sigma]). Cells were washed twice with PBS containing calcium and magnesium (PBS+) and 250 µL of inoculum was added. The cells were incubated for 1 hour at RT with rocking. The inoculum was removed and replaced with IM containing 1% agarose. Cells were then incubated at 32°C for 4-5 days, fixed in 2% formaldehyde, and stained in a Naphthol Blue Black solution. Individual plaque diameters were determined by ImageJ. For synthetic virus generation, the agar above individual plaques was removed with a sterile pipette, aspirated into 1 mL of IM, and stored at -80°C.

50% Tissue culture infectious dose (TCID₅₀) assay

MDCK cells were plated in 96-well plates, grown to confluence, and washed twice with PBS+. Tenfold serial dilutions of the virus inoculum were made and 200 µL of dilution was added to each of 6 wells in the plate, followed by incubation for 7 days at 32°C. Cells were then fixed by adding 100 µL of 4% formaldehyde in PBS per well, followed by staining with a Naphthol Blue Black solution. Endpoint calculations were determined by the Reed-Muench method (316).

Low MOI infection

Before all low MOI infections, cells are washed twice with PBS+. Seed stocks (SS) were generated by incubating 250 μ L of the plaque pick solution on fully confluent MDCK cells for 1 hour at room temperature. The inoculum was removed, cells were washed twice with PBS+, and then 1 mL of IM was added before returning the cells to the incubator at 32°C. Virus supernatant was harvested when 50% of the cells displayed cytopathic effect upon inspection with light microscopy, usually 24-48 hours post-infection (HPI). Seed stocks were then titrated by TCID₅₀ assay, and used to generate working stocks. Working stocks were generated as described for seed stocks, except infections were performed in 75 or 150 cm² flasks and the inoculum used was SS diluted to an MOI of 0.01 in IM.

Multistep virus growth curves were performed at a MOI of 0.001 in MDCK cells and 0.1 in hNECs. For MDCK cell infections, the inoculum was diluted in IM, added to cells, and allowed to incubate at 32 or 37°C for 1 hour. Cells were then washed 3 times with PBS+ and incubated with fresh IM at 32 or 37°C. At the indicated HPI, all media were removed and replaced with fresh IM. The amount of infectious virus in each sample was determined by TCID₅₀ assay on MDCK cells. For hNECs, the apical surface was washed with IM without NAT and the basolateral DM was replaced immediately before infection. Inoculum diluted in IM without NAT was then added and allowed to incubate on cells at the growth curve temperature for 1 hour. The

inoculum was then removed, the cells were washed three times with PBS+, left at ALI, and returned to 32°C or 37°C. At the indicated times post-infection, IM without NAT was added to the apical chamber of the wells and allowed to incubate on cells at 32°C for 10 minutes, removed, and then the cells were returned to the incubator at ALI. Basolateral DM was removed and replaced every 48 hours for the duration of the growth curves. All samples were stored at -80°C.

Interferon, cytokine and chemokine measurements

Secreted interferons, cytokines, and chemokines were quantified from the apical and basolateral samples from the 48 and 96 hour post-infection samples from the hNEC multistep virus growth curves. Measurements were performed using the V-PLEX Human Chemokine Panel 1 (CCL2, CCL3, CCL4, CCL11, CCL13, CCL17, CCL22, CCL26, CXCL10, and IL-8), V-PLEX Human IL-6 kit (Meso Scale Discovery), and the DIY Human IFN Lambda 1/2/3 (IL-29/28A/28B) ELISA (PBL Assay Science) according to manufacturers' instructions. Of the 12 analytes tested, 10 (CCL2, CCL3, CCL4, CCL11, CCL17, CCL22, CXCL10, IL-8, IL-6, and IFN- λ) were specifically induced in virus-infected cultures. The amount secreted was adjusted by sample volume (either 100 or 150 μ l for the apical washes, 500 μ l for the basolateral supernatants) to show total pg secreted.

Statistical analyses

Multistep growth curves were analyzed by two-way ANOVA with a Dunnett's posttest performed for all viruses when significant differences from WT virus were present. Plaque diameters and cytokine and chemokine measurements were analyzed by ANOVA. All statistical analyses were performed in GraphPad Prism 7.0.

RESULTS

Rescue of recombinant viruses with mutations in the M2 cytoplasmic tail

Previous work showed that the region of M2 containing amino acids 82-89 was important for virus replication and efficient genome packaging, but scanning alanine mutagenesis failed to identify any single residue responsible for the phenotype (111). However, substitutions at M2 amino acid positions 83 and 86 were not made. Since an Ala residue is present at M2 position 83 in nearly 100% of North American human influenza virus isolates, we replaced Ala83 with a number of amino acids to assess the overall tolerance of that position to mutations (Fig. 2.1). Approximately 63.5% of IAV strains contain Ala at position 86 (Fig. 2.1), and Ala is the residue found in most H3N2 influenza A virus isolates. The M2-86Val mutation is present in 36.4% of sequences in the database and is encoded primarily by H1N1 viruses. The A/Ann Arbor/6/1960 (H2N2) LAIV M2

protein contains an Ala to Ser mutation at position 86 of the M2 cytoplasmic tail (25) which was acquired during the cold-adaption of the virus. Given this natural variation in amino acid sequences at M2 position 86, we focused on a limited number of substitutions at this position (Fig. 2.1). These substitutions were initially introduced into the A/Udorn/307/72 infectious clone, which is an H3N2 virus with highly conserved Ala residues at M2 amino acid positions 83 and 86.

Replication of rUd M2-83 mutants in MDCK cells and hNEC cultures

In order to mimic the temperature of the upper respiratory tract, all experiments with the rUd M2-83 viruses were performed at 32°C, the temperature of the upper respiratory tract. Plaque assays performed on MDCK cells showed no difference in plaque size between rUd M2-WT, A83V, A83P, A83M, A83E, and A83K (Fig. 2.2A and 2B). On MDCK cells, rUd M2-WT, A83V, A83P, A83M, and A83K all replicated with similar kinetics and produced a comparable amount of infectious virus after low MOI infection (Fig. 2.2C). The rUd M2-A83E showed a modest increase in replication compared to rUd M2-WT (Fig. 2.2C). In hNEC cultures, rUd M2-WT, A83V, A83P, and A83E all replicated with similar kinetics while rUd M2-A83K replicated slightly faster than rUd M2-WT (Fig 2.2D). The rUd M2-A83M replicated with significantly worse compared to WT (approximately 100-fold lower infectious virus production). The data indicate that rUd M2 position 83

does not have a large effect on virus replication, except in the case of rUd M2-A83M on hNECs, indicating the site is relatively amenable to mutation, despite being highly conserved in natural influenza isolates.

Replication of rUd M2-86 mutants in MDCK cells and hNEC cultures

Plaque assays performed on MDCK cells showed no difference in plaque size between the rUd M2-WT, A86V, A86S, and A86E (Fig. 2.3A and 3B). In MDCK cells at 32°C, rUd M2-WT, A86S, and A86E all replicated with similar kinetics and produced a comparable amount of infectious virus (Fig 3C). rUd M2-A86V showed a small, but statistically significant, increase in replication compared to rUd M2-WT. Because the M2-86S mutation is associated with LAIV – a virus known to have restricted replication at higher temperatures – the growth curves were also performed at 37°C. All of the viruses replicated with similar kinetics and titers compared to rUd M2-WT (Fig. 2.3D) at this temperature in MDCK. Virus replication was then assessed at both temperatures in hNEC cultures. At 32°C on hNECs, rUd M2-WT and A86V replicated similarly, while A86S and A86E replicated with decreased kinetics compared to rUd M2-WT (Fig. 2.3E). Strikingly, on hNECs at 37°C, rUd M2-A86V, A86S, and A86E all replicated with significantly decreased kinetics and to a lower peak titer compared to rUd M2WT (Fig. 2.3F). Taken together, the data suggest that mutations at rUd M2 position 86 are detrimental to virus replication, and this effect is most evident in hNECs at 37°C.

Replication of rVic-LAIV M2-86 mutants in MDCK cells and hNEC cultures

Because the M2-A86S mutation arose during LAIV cold-adaption and this mutation altered rUd replication in hNEC cultures, we chose to study the effect of this mutation in the LAIV genetic background. Recombinant LAIV expressing the HA and NA proteins from A/Victoria/361/2011 (rVic-LAIV) was rescued along with an rVic-LAIV M2-S86A containing virus. Plaque assays performed on MDCK cells showed no difference in plaque size between rVic-LAIV and rVic-LAIV M2-S86A (Fig. 2.4A and 4B). Multi-step growth curves performed in MDCK cells at 32 and 37°C (Fig. 2.4C and 4D) showed consistent virus replication with rVic-LAIV M2-S86A virus having slightly reduced virus replication kinetics at 37°C. In hNEC cultures, the viruses replicated with identical kinetics at 32°C, but rVic-LAIV M2-S86A replicated to significantly higher titers at 37°C (Fig. 2.4E and 4F). Together, the data indicate that the LAIV-associated mutation, M2-A86S, contributes to the *att* and *ts* phenotypes on hNEC cultures, but not MDCK cells.

Induction of chemokines, cytokines, and IFN- λ by rVic-LAIV M2-A86S in hNEC cultures

Because LAIV induces a significantly different epithelial cell innate immune response compared to seasonal influenza (30, 32), the effect of the M2-S86A

mutation on interferon and chemokine secretion in hNEC cultures was determined at 48 and 96 HPI. Expression of ten of the 12 analytes increased with temperature and time in response to infection, irrespective of the infecting virus (Fig. 2.5 and Table 2.1). Secretion of the induced factors was directional, with higher amounts detected in the basolateral media (Fig. 2.5). While IFN- λ secretion was similar between the two viruses at 32°C, differences emerged during infections at a higher temperature. At 37°C, IFN- λ secretion was significantly greater for rVic-LAIV than rVic-LAIV M2-S86A at 48 HPI, but significantly less at 96 HPI (Table 2.1). Together these data indicate that an M2-S86A mutation increases LAIV virus replication and alters innate immune responses in hNEC cultures at 37°C, identifying it as another mutation responsible for attenuating LAIV replication in a temperature-dependent manner.

DISCUSSION

The LAIV-associated M segment contributes, in part, to LAIV's attenuation phenotype (20, 29, 303). The only M segment mutation between the WT and cold-adapted strains of A/Ann Arbor/6/1960 is a missense mutation at M2 position 86 from an alanine in the WT strain to a serine in the cold-adapted vaccine strain (25). Our data indicate that the M2-A86S mutation acquired during LAIV cold-adaptation contributes to reduced virus replication in hNEC cultures but not MDCK cells, in a temperature-dependent manner and can

alter the production of IFN- λ . This suggests that LAIV attenuation in hNEC cultures is not solely driven by the *ts* and *ca* mutations identified in the polymerase complex proteins. In addition to being the location of an LAIV-associated mutation, M2 amino acid position 86 is also present in a region of M2 previously identified as critical for IAV replication and budding (112, 115). Scanning alanine mutagenesis of these regions was unable to fully recapitulate the replication defect associated with the M2 truncations used to identify the regions. This could be because alanine is ubiquitous at M2 amino acid position 83 in circulating strains of influenza and common at position 86 (Fig. 2.1). Mutating the alanine at M2 position 83 did not have a consistent effect on the replication of virus in either MDCK cells or hNECs (Fig. 2.2C and 2D). However, substituting a methionine at this position led to a defect in replication, indicating that the presence of an alanine at this position is not critical for replication, though the position is not fully malleable.

Because most of the previous studies of LAIV *in vitro* replication were performed in immortalized cell lines including MDCK cells or embryonated hen's eggs, it is perhaps not surprising that the contribution of the M2 mutation was not recognized previously, as the replication differences we observed were specific to infection of hNEC cultures and not in MDCK cells. Primary, differentiated epithelial cell cultures provide greater clinical relevance and phenotype penetrance than immortalized cell lines (30, 31, 113, 317-322). This is particularly true for studying LAIV (30, 31). These

cultures can contain multiple epithelial cell types including ciliated cells, basal cells, goblet cells and club cells (323, 324). Additionally, immortalized cell lines and embryonated chickens' eggs both lack elements of the epithelial cell innate immune system and virus restriction factors. There is a greater replication restriction of LAIV at both 32 and 37°C in primary, differentiated epithelial cell cultures compared to MDCK cells (31, 320). This difference in replication on primary human respiratory epithelial cells has been associated with a robust, unique innate immune response (30) and an increased ratio of non-infectious to infectious virus particles (31, 32). The M2-A86S mutation attenuated rUdorn virus replication on hNECs at 32 and 37°C (Fig. 2.3E and 3F). Consistent with this, introducing the M2-S86A mutation into the LAIV background increased virus replication at 37°C (Fig. 2.4F) in hNEC cultures. This increase in LAIV replication on hNECs was associated with altered induction of IFN- λ production at 48 HPI (Table 2.1). IFN- λ receptor expression is restricted to epithelial cells and IFN- λ is critical to protecting epithelial tissues during virus challenge (325, 326). These results are consistent with the robust innate immune response seen with LAIV infections compared to WT viruses (30, 32). The significance of the changes in the kinetics and magnitude of IFN- λ secretion in response to virus infection are not clear at this time, but it will be interesting to investigate the effect of these mutations on LAIV infection in an animal model. Every cytokine and chemokine tested was secreted preferentially into the basolateral media (Fig.

2.5). This agrees with previous reports of a basolateral bias in cytokine secretion during influenza virus infection of primary respiratory epithelial cells (319). A M2-A86V substitution did show reduced replication in the rUdorn virus background despite it being present in some natural isolates of IAV. This may be due to the fact that rUdorn is a H3N2 virus while the A86V substitution is only found in H1N1 subtype viruses, indicating a strain-specific role for this position. Strain specific effects of mutations in the M2 protein have been documented previously (108, 111-113).

Previous work has shown that at the non-permissive temperatures of 38.5 to 40°C, the M1 protein of LAIV viruses is not efficiently packaged into budding particles (327) and particles exhibited a more heterogeneous, enlarged morphology (302). However, there is no decrease in M1 incorporation into virus particles at the physiologically relevant temperatures of 32 and 37°C (31). We therefore chose these temperatures to better model the effects of these mutations at the temperatures of the human respiratory tract, 32°C (upper) and 37°C (lower). For the M2-83 mutation experiments, we used 32°C to accurately model infections of the upper respiratory tract. However, because the M2-86 mutation is associated with the temperature-sensitive LAIV vaccine, we used both 32 and 37°C.

Annual influenza vaccination is the primary means of preventing seasonal influenza and decreasing its sociologic and economic impacts. LAIV has been shown to be more efficacious than inactivated influenza in children

aged 6-69 months (20, 328) and adults (20, 329, 330). However, LAIV is not being recommended for use during the 2016-2017 influenza season due to low effectiveness (36). Few studies have been performed to understand the LAIV *att* phenotypes at the molecular level, and it remains to be determined if all of the LAIV associated mutations are relevant and necessary for the production of a safe and efficacious vaccine. Our studies show that one can obtain a better understanding of the LAIV attenuation through the use of hNEC cultures and suggest that LAIV attenuation is not solely due to polymerase complex mutations. This implies that LAIV can be re-engineered to replicate either more or less efficiently through the manipulation of the M2 protein sequences including, but not limited to positions 83 and 86. The decreased replication on hNECs and altered innate immune induction associated with the LAIV M2-A86S mutation demonstrate the merit of this strategy and justifies the investigation of the other LAIV-associated mutations with these methods.

Acknowledgements

We thank the members of the Pekosz laboratory, Sabra Klein, and members of the Klein laboratory for useful and critical discussions of the data. The work was supported by the Shikani/El Hibri Prize for Discovery and Innovation (AP), R01 AI097417 (AP), HHSN272201400007C (AP), R01 AI072502 (APL) and T32 AI007417 (NW).

FIGURES AND TABLES

M2 Cytoplasmic Tail

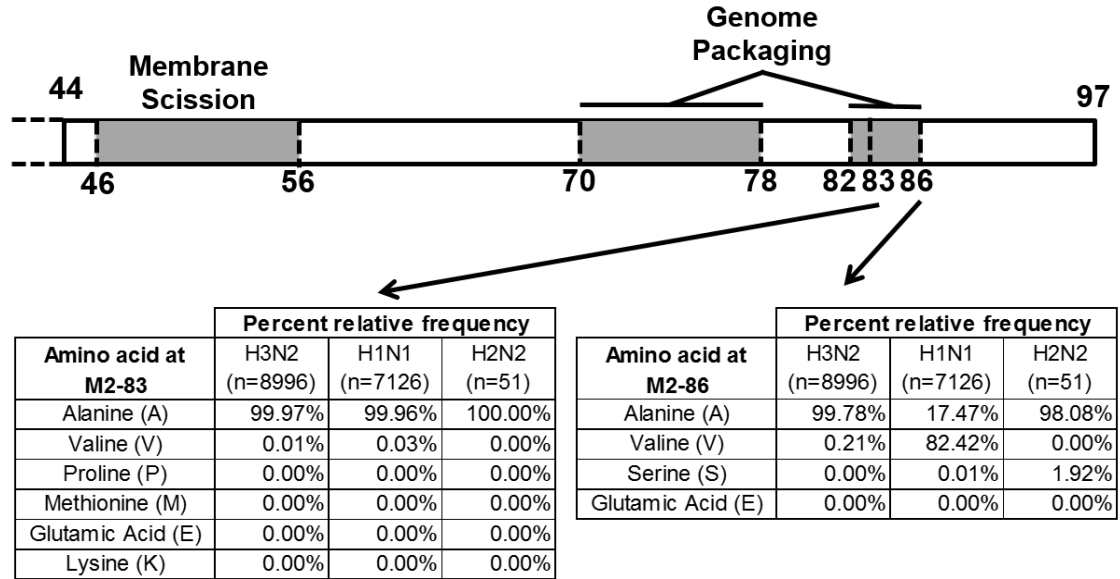


Figure 2.1. M2 cytoplasmic tail. M2 cytoplasmic tail schematic depicting amino acid frequency in all H3N2, H1N1, and H2N2 human isolate sequences from North America (complete genomes only) available in the Influenza Research Database. Search was performed 7/2/2017.

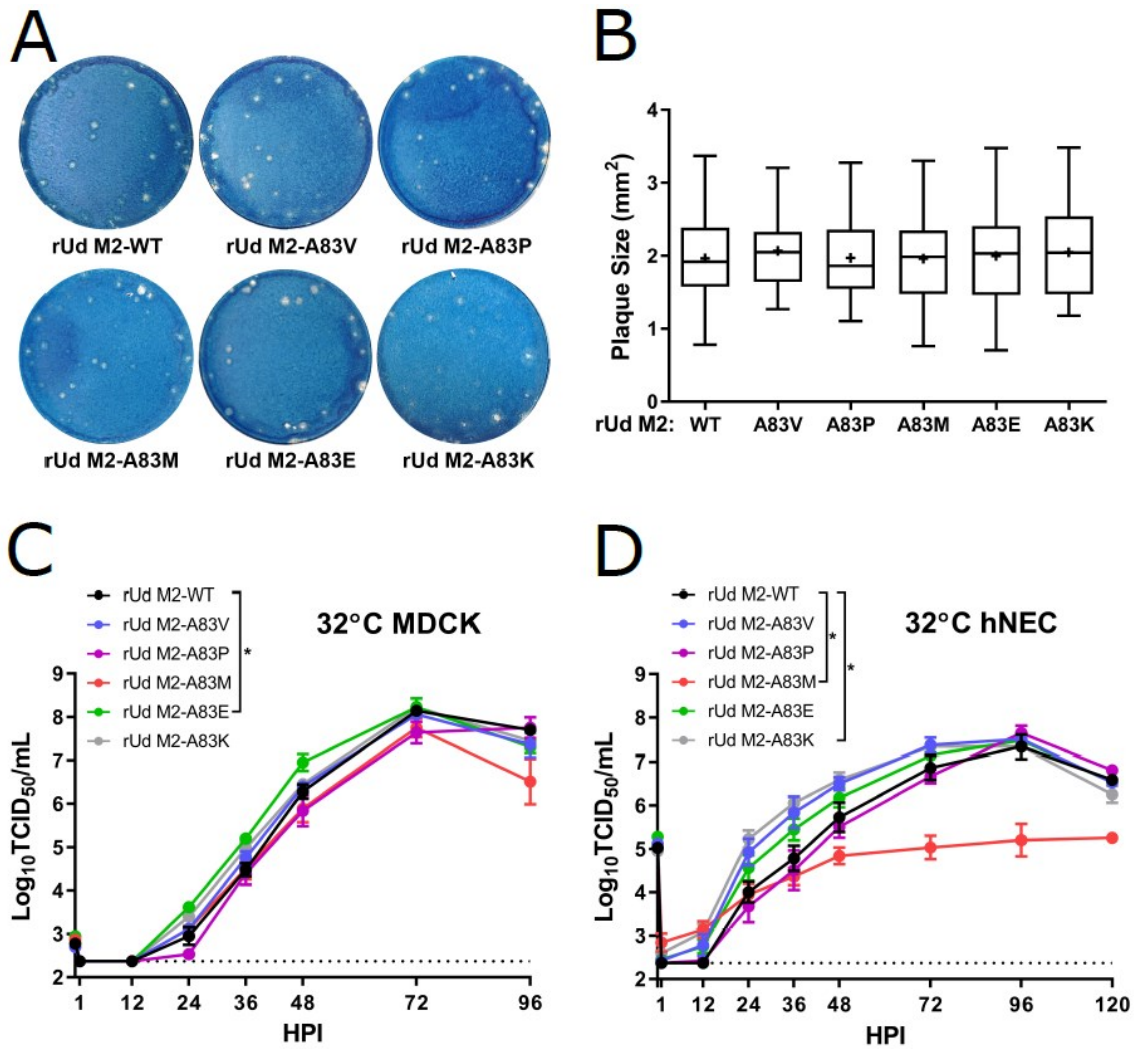


Figure 2.2. Replication of M2-83 mutants on MDCK cells. (A) Plaque assays performed with the indicated viruses on MDCK cells. (B) Quantification of plaque diameter from 34-64 individual plaques per virus identified from 2-3 independent experiments. * $p < 0.05$. No mutations had statistically significant differences compared to rUd M2-WT. Low MOI multistep growth curves performed on (C) MDCK cells or (D) hNECs with the indicated viruses at 32^o C. Data are pooled from two independent replicates

each with $n = 3$ wells per virus (total $n = 6$ wells per virus). $*p < 0.05$ compared to rUd M2-WT (two-way ANOVA with Dunnett's posttest). In (C) no time points were significantly different while in (D) rUd M2-A83M (48, 72, 96, and 120 HPI), rUd M2-A83K (24, 36, and 48 HPI) showed differences. Dotted line indicates limit of detection.

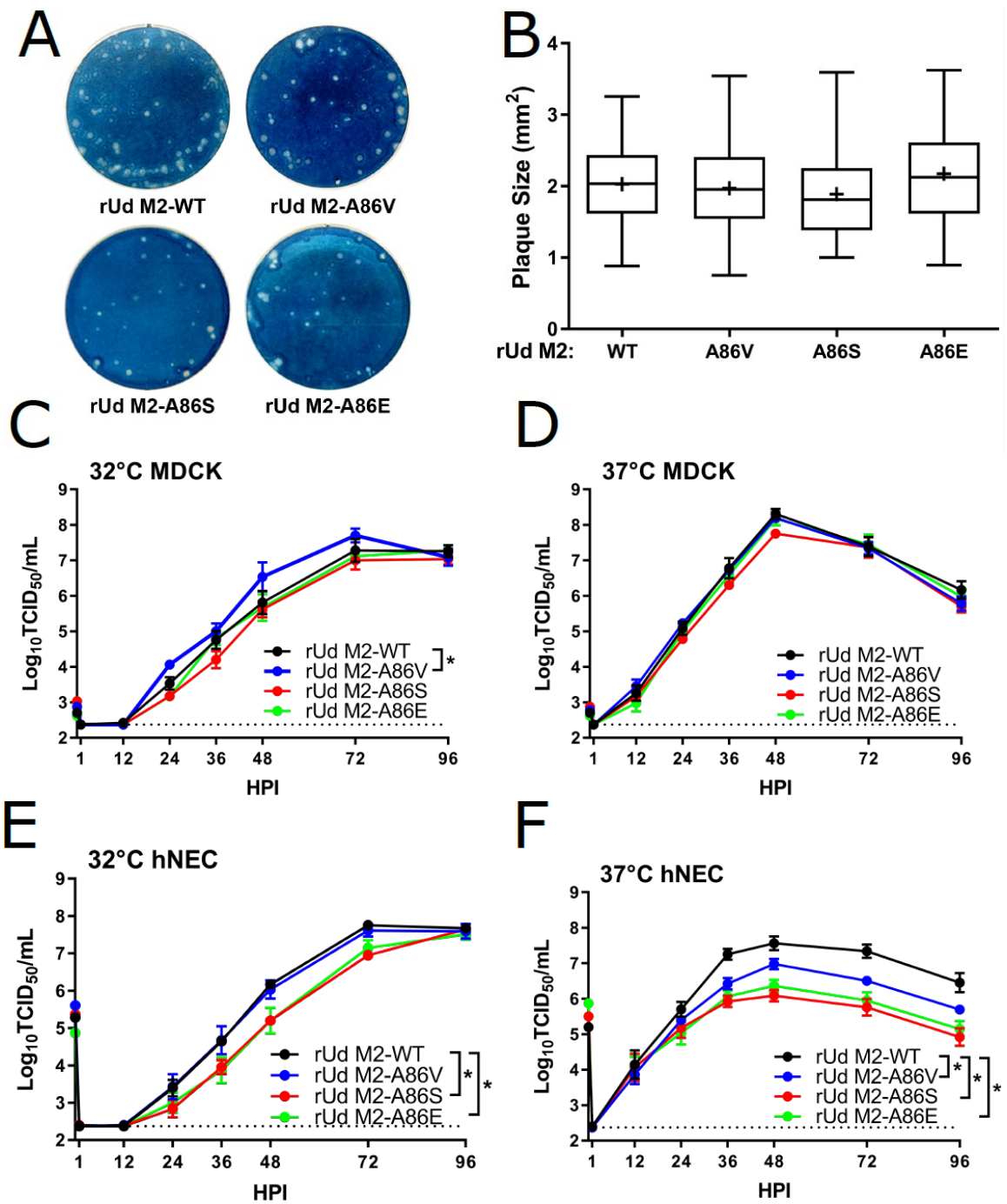


Figure 2.3. Replication of M2-86 mutants in the rUd background on MDCK cells and hNECs. (A) Plaque assays performed with the indicated viruses on MDCK cells. (B) Quantification of plaque diameter from 84-137

individual plaques per virus identified from 2-3 independent experiments. * $p < 0.05$. No conditions were statistically significant compared to rUd M2-WT. Low MOI multistep growth curves performed on (C and D) MDCK cells or (E and F) hNECs with the indicated viruses at 32⁰ C (C and E) or 37⁰ C (D and F). Data are pooled from two independent replicates each with $n = 3$ wells per virus (total $n = 6$ wells per virus). * $p < 0.05$ compared to rUd M2-WT (two-way ANOVA with Dunnett's posttest) significant differences ($p < 0.05$) compared to rUd M2-WT: In (C) no time points were significantly different while in (E) rUd M2-A86S (48 and 72 HPI), rUd M2-A86E (36 and 48 HPI) and (F) rUd M2-A86V (36 and 72 HPI), rUd M2-A86S (36, 48, 72, 96 HPI), rUd M2-A86E (36, 48, 72, 96 HPI) showed differences. Dotted line indicates limit of detection.

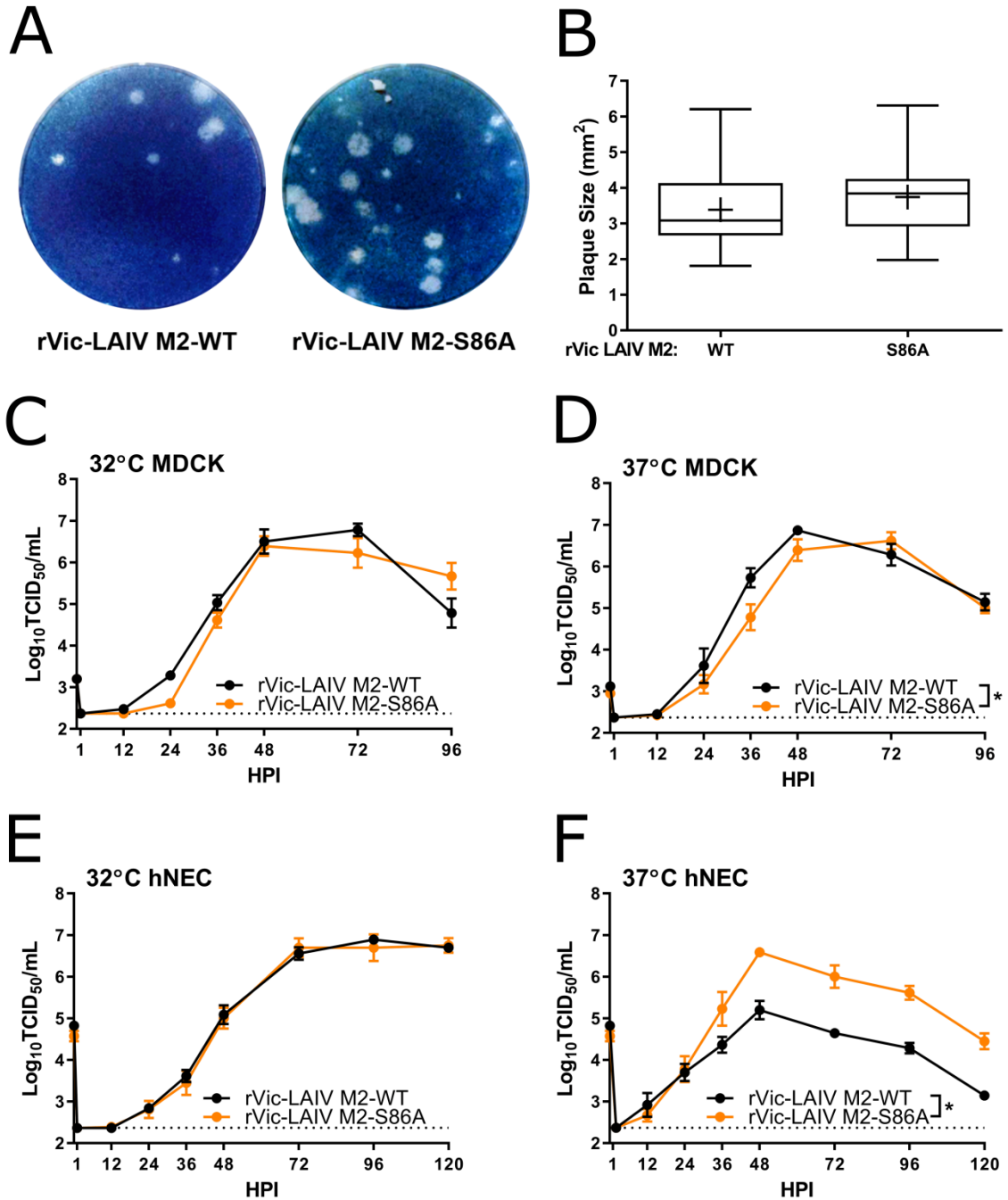


Figure 2.4. Replication of M2-86 mutants in the rVic-LAIV

background in MDCK cells. (A) Plaque assays performed with the

indicated viruses on MDCK cells. (B) Quantification of plaque diameter from

24-47 individual plaques per virus identified from 2-3 independent experiments. *p < 0.05. No mutations had statistically significant differences compared to rVic-LAIV. Low MOI multistep growth curves performed on (C and D) MDCK cells or (E and F) hNECs with the indicated viruses at 32⁰ C (C and E) or 37⁰ C (D and F). Data are pooled from two independent replicates each with n = 3 wells per virus (total n = 6 wells per virus). *p < 0.05 compared to rVic-LAIV (two-way ANOVA with Dunnett's posttest). In (D) rVic-LAIV M2-S86A (36 HPI) and (F) rVic-LAIV M2-S86A (36, 48, 72, 96, and 120 HPI) showed differences. Dotted line indicates limit of detection.

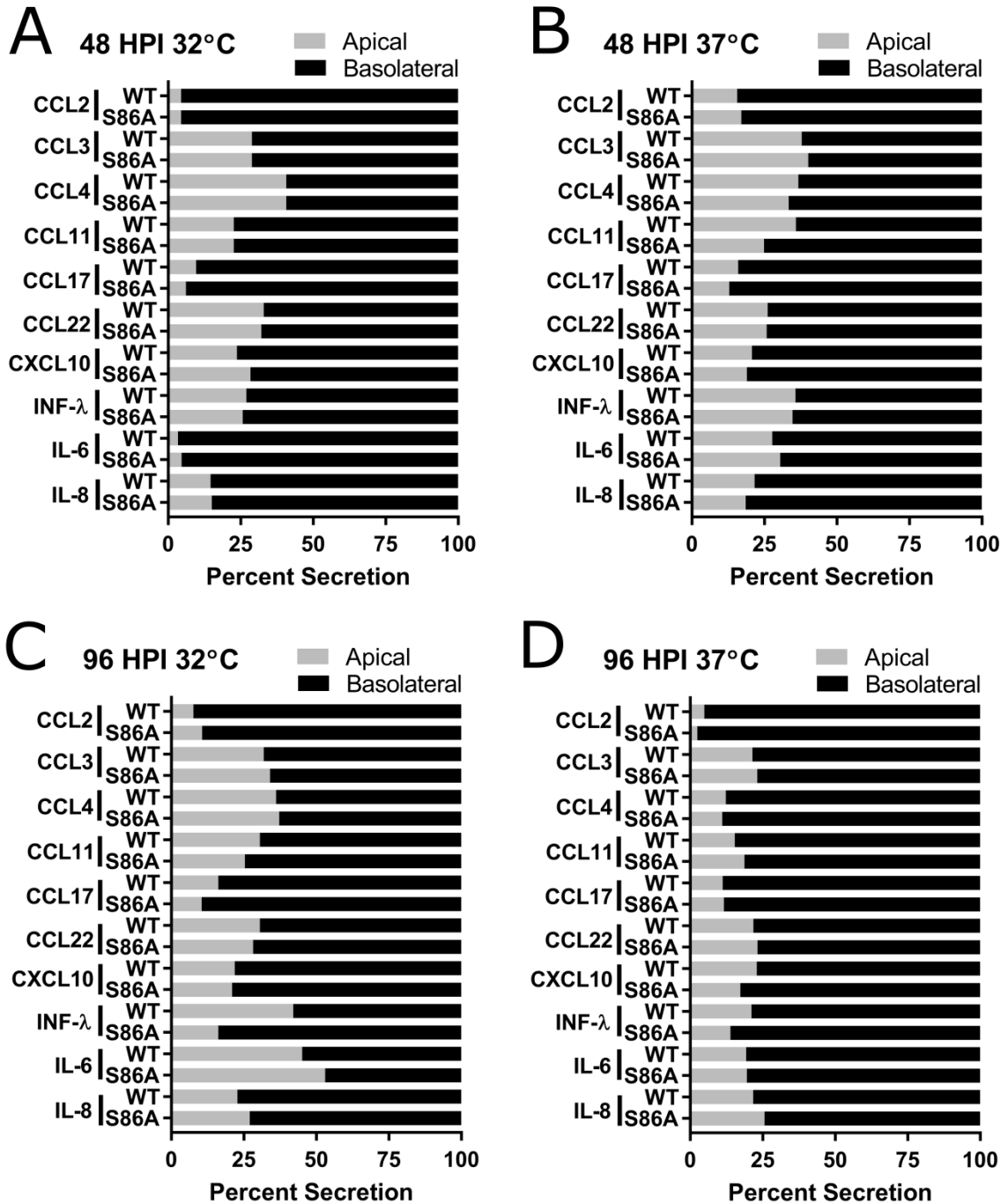


Figure 2.5. Comparison of apical versus basolateral secretion of cytokines and chemokines. Samples collected 48 (A and B) and 96 (C and D) HPI during low MOI multistep growth curve experiment (Fig. 2.4E and 4F, Table 2.1)

performed at 32⁰C (A and C) and 37⁰C (B and D). WT =rVic LAIV M2-WT; S86A =
rVic LAIV M2-S86A. Data are pooled from two independent replicates each with n = 3
wells per virus.

| | 32°C | | | | 37°C | | | |
|--------|----------------|----------------|-----------------|----------------|--------------------|-----------------------|----------------------|------------------------|
| | 48 HPI | | 96 HPI | | 48 HPI | | 96 HPI | |
| | M2-86A | M2-86S | M2-86A | M2-86S | M2-86A | M2-86S | M2-86A | M2-86S |
| CCL2 | 3.2 ± 0.5 | 2.9 ± 0.2 | 4.1 ± 1.5 | 3 ± 0.2 | 7.5 ± 0.5 | 8.5 ± 1.2 | 39.3 ± 15 | 26.5 ± 10.1 |
| CCL3 | N.D. | N.D. | 15.5 ± 1.9 | 13.8 ± 0.4 | 16.5 ± 1.8 | 19.9 ± 2.6 | 45.7 ± 9.4 | 48.9 ± 8.3 |
| CCL4 | N.D. | N.D. | 5.8 ± 0.7 | 5.1 ± 0.5 | 7 ± 1.6 | 8.6 ± 2 | 37.7 ± 11.2 | 34.1 ± 6.3 |
| CCL11 | N.D. | N.D. | 13.9 ± 1.5 | 14.9 ± 1.9 | 14.8 ± 2.7 | 20.1 ± 5.3 | 39.5 ± 7.9 | 54.8 ± 11.1 |
| CCL13 | 9.8 ± 0.3 | 9.9 ± 0.3 | 9.8 ± 0.3 | 9.9 ± 0.3 | 9.8 ± 0.3 | 9.8 ± 0.3 | 9.8 ± 0.3 | 9.9 ± 0.3 |
| CCL17 | 3.2 ± 0.2 | 2.4 ± 0.2 | 8.4 ± 0.3 | 6.1 ± 1.1 | 14.4 ± 0.5 | 15.4 ± 2.6 | 24 ± 1.4 | 23 ± 4.9 |
| CCL22 | 13.3 ± 0.6 | 12.9 ± 0.5 | 22.6 ± 1.7 | 26 ± 2.6 | 35 ± 2.8* | 54.4 ± 4* | 110 ± 12.3 | 112.5 ± 3.6 |
| CCL26 | 10.4 ± 0.7 | 10.8 ± 0.7 | 10.4 ± 0.7 | 10.3 ± 0.8 | 10.6 ± 0.7 | 10.4 ± 0.7 | 10.4 ± 0.7 | 10.4 ± 0.7 |
| CXCL10 | 22.3 ± 8.8 | 15.1 ± 5.1 | 2139.2 ± 1027.1 | 1000.4 ± 457.3 | 2509.2 ± 1250.9 | 3127.3 ± 1287.1 | 5804.8 ± 195.2 | 5234.8 ± 543.3 |
| IFN-λ | 184.5 ± 12.3 | 179.4 ± 7.6 | 288.5 ± 53.9 | 269.9 ± 44.3 | 424.6 ± 55* | 920.4 ± 132.9* | 5888.3 ± 130* | 3658.8 ± 390.1* |
| IL-6 | 6.5 ± 2.6 | 8.1 ± 3.3 | 9.6 ± 2.9 | 7.7 ± 1.3 | 20.4 ± 4.4 | 36.1 ± 6.2 | 528.7 ± 85 | 430.7 ± 83.1 |
| IL-8 | 1655.1 ± 385.8 | 1702.7 ± 374.9 | 1323.2 ± 116.5 | 1503.6 ± 87.8 | 3412.1 ± 620.4 | 4557.2 ± 433.1 | 25820.9 ± 3920.1 | 27445.7 ± 2865.3 |

Table 2.1. Total secreted cytokine (pg/μL). Samples collected during low MOI multistep growth curve experiment (2.4E and 4F). Data are pooled from two independent replicates each with n = 3 wells per virus. None detected (N.D.) means that levels were below the lower limit of detection. *p < 0.05 virus specific difference at the indicated time post infection (two-way ANOVA).

**CHAPTER 3: INFLUENZA A VIRUS M2 PROTEIN
APICAL TARGETING IS REQUIRED FOR
EFFICIENT VIRUS BUDDING AND REPLICATION**

Nicholas Wohlgemuth, Andrew P. Lane, and Andrew Pekosz

ABSTRACT

The influenza A virus (IAV) M2 protein is a multifunction protein with critical roles in virion assembly and budding. M2 is targeted to the apical plasma membrane of polarized epithelial cells, and the interaction of the viral proteins M2, M1, HA, and NA near glycolipid rafts in the apical plasma membrane is hypothesized to coordinate the assembly of infectious virus particles. To determine the role of M2 protein apical targeting in IAV replication, assembly, and budding a panel of M2 proteins with basolateral plasma membrane (M2-Baso) or endoplasmic reticulum (M2-ER) targeting sequences was generated. MDCK II cells stably expressing M2-Baso, but not M2-ER, complemented the replication of M2-stop viruses. However, in primary human nasal epithelial cell (hNEC) cultures, viruses encoding M2-Baso and M2-ER replicated to negligible titers compared to WT virus. M2-Baso replication was negatively correlated with cell polarization. These results demonstrate that M2 apical targeting is essential for IAV replication, targeting M2 to the ER results in a strong, cell type independent inhibition of virus replication, and targeting M2 to the basolateral membrane has greater effects in hNECs than in MDCK cells.

IMPORTANCE

Influenza A virus assembly and particle release occurs at the apical membrane of polarized epithelial cells. The integral membrane proteins

encoded by the virus – HA, NA and M2 – are all targeted to the apical membrane and believed to recruit the other structural proteins to sites of virus assembly. By targeting M2 to the basolateral or ER membranes, influenza A virus replication was significantly reduced. Basolateral targeting of M2 reduced the infectious virus titers with minimal effects on virus particle release while targeting to the ER resulted in reduced infectious and total virus particle release. Therefore, altering the expression and the intracellular targeting of M2 has major effects on virus replication through different mechanisms.

INTRODUCTION

Virus infections frequently target the polarized epithelial cells lining the respiratory tract, digestive tract, or mucosal surfaces. Efficient production of progeny viruses requires directional coordination among virion components to traffic to either the apical or basolateral plasma membrane. Some viruses target their proteins to the apical plasma membrane and then bud into the lumen and can primarily only spread among epithelial cells. Other viruses target their proteins to the basolateral plasma membrane where they assemble and are more prone to progress to systemic and disseminated infections (331, 332).

Influenza A virus (IAV) is in the family *Orthomyxoviridae* and has a genome consisting of eight negative-sense, single-stranded RNA segments

encoding 10 to 14 proteins (1). All three integral membrane proteins, HA (333, 334), NA (335-337), and M2 (338), are targeted to the apical plasma membrane. M2 apical targeting is not dependent on its acylation or cholesterol-binding residues (107). The viral matrix protein, M1, and the viral ribonucleoprotein (vRNP) complex traffic to the apical plasma membrane as well, and must interact with the apically targeted viral surface proteins (12, 339-341) for efficient virion assembly (112-114). M1 and vRNP traffic to the apical plasma membrane through interactions with the cytoskeleton (342), and NP has been shown to be intrinsically targeted to the apical plasma membrane (1, 343).

The influenza virus M2 protein is a 97 amino acid integral membrane protein that forms disulfide-linked tetramers. M2 is predominantly associated with its well characterized proton channel activity. During the virus entry process, this activity allows for the acidification of the virion interior, which permits vRNP release from M1 (1, 59, 307, 308). The C-terminal 54 amino acids of M2 form the highly conserved cytoplasmic tail, which is important for both the assembly and budding processes of viral egress, but have little effect on the M2 proton channel activity (97). The membrane distal region of the cytoplasmic tail is critical for the incorporation of vRNPs into budding particles (111-115). The membrane proximal region of M2 can induce membrane curvature and has been implicated in ESCRT-independent membrane scission and budding of IAV particles (12, 99), though

the extent to which this activity is needed appears to vary between virus strains and experimental systems (100-103).

To investigate the role M2 apical targeting plays in IAV replication, assembly, and budding, we generated M2 constructs targeted away from the apical plasma membrane, the site of virus budding and assembly. When M2 was targeted to the ER with a dilysine retrieval signal (43, 44, 82), virus particles were not released due to a defect in budding. When M2 was targeted to the basolateral plasma membrane, the effect on virus particle production was dependent on the polarization of the cell model being used. The data indicate that both the level of expression as well as the intracellular localization of M2 impact infectious virus production.

MATERIALS AND METHODS

Plasmids

The plasmid pCAGGS (pC) (344) expressing the cDNA for the M2 protein from A/Udorn/72(H3N2) (rUdorn) has been previously described (111, 345). The pHH21 plasmids expressing full length influenza virus gene segments were used to generate recombinant viruses (111) as described below. pHH21 plasmids encoding the A/Victoria/361/2011(H3N2) (rVic) virus RNA segments were generated using sequences available in Genbank and the NIAID Influenza Research Database (25, 313, 314). The plasmid pBABE, which expresses puromycin N-acetyltransferase, was used for puromycin resistance

in stably transfected cells. All mutations were introduced using the QuikChange Lightning site-directed mutagenesis kit (Agilent). All inserts and mutations were confirmed by sequencing. Primer sequences are in Table A.1 in the appendix.

Cells

Madin-Darby canine kidney (MDCK) cells and HEK 293T (293T) cells were cultured in Dulbecco's modified Eagle medium (DMEM) supplemented with 10% fetal bovine serum (FBS), 100 U/mL penicillin, 100 µg/mL streptomycin, and 2 mM GlutaMAX (Gibco). M2-MDCK cells stably transfected with the pCAGGS plasmid expressing the M2 protein from A/Udorn/72(H3N2) were cultured as described for MDCK cells except the media was supplemented with 5 µM amantadine hydrochloride and 7.5 µg/mL puromycin dihydrochloride (111). MDCK type II cells (MDCK II) (a gift from Dr. Ann Hubbard) were cultured in Minimum Essential Medium (MEM) supplemented with 10% FBS, 100 U/mL penicillin, 100 µg/mL streptomycin, and 2 mM GlutaMAX. Human nasal epithelial cell (hNEC) cultures were derived from epithelial cells isolated from non-diseased tissue after endoscopic sinus surgery for non-infection related conditions and grown at air-liquid interface (ALI) as previously described (31, 309-311). hNEC differentiation medium (DM), infection media (IM), and culture conditions have previously been described in detail (31). hNEC polarization was

monitored by measuring transepithelial resistance with a Millicell-ERS after adding 250 μ L of warm IM without NAT to the apical chamber.

Antibodies

M2 was detected with an anti-M2 rabbit polyclonal antibody (pAb) (GeneTex GTX125951) or the anti-M2 monoclonal antibody (mAb) 14C2 which recognizes the extracellular domain of M2. HA was detected with a pAb anti-H3 (goat) serum derived from A/Aichi/2/1968 (BEI V314-591-157). The antibody that recognizes calnexin is a rabbit pAb (Genscript A01240-40) and the ZO-1A12 mAb (ThermoFisher 33-9100) recognizes ZO-1. β -actin was detected by a mouse mAb (Abcam ab6276). The antibody that recognizes NP is a rabbit pAb (GeneTex GTX125989). All secondary antibodies used are ThermoFisher Scientific Alexa Fluor (AF) fluorescent antibodies conjugated to AF488, AF555, or AF647.

Stable cell line production and culture

Stable MDCK II cell lines expressing rUdorn M2, rUdorn M2-ER, rUdorn M2-Baso, rUdorn M2-FLAG, and eGFP were established by cotransfecting pBABE (0.5 μ g/well) with pC plasmids encoding the cDNA of interest (1.0 μ g/well) and Lipofectamine 2000 (9 μ L/well). Transfections were performed in suspension. At 20 h post transfection the transfection mixture was removed and replaced with culture media supplemented with 5 μ M amantadine

hydrochloride (Sigma). At 48 h post transfection cells were detached with trypsin and plated at low densities onto 96-well plates with culture media supplemented with amantadine hydrochloride and 3.75 µg/mL puromycin dihydrochloride (Sigma). The puromycin-resistant cells were screened for clonality (wells containing a single colony) and M2 expression by plate reader or fluorescence-activated cell sorting (FACS). Live cells were stained on ice with 14C2 (1:500 dilution) followed by AF488 conjugated goat anti-mouse antibody (1:500 dilution). Fluorescence was measured with a FilterMax F5 Multi-Mode Microplate reader (Molecular Devices). Because M2-ER and M2-Baso are not expressed on the apical surface, 18-24 clonal wells were expanded and analyzed by FACS as described below. Stably transfected cells were then grown in media supplemented with 5 µM amantadine hydrochloride and 3.75 µg/mL puromycin dihydrochloride for MDCK II cells and 7.5 µg/mL puromycin dihydrochloride for MDCK cells.

Flow cytometry

Cells were detached with trypsin, fixed for 15 minutes at room temperature (RT) with 2% paraformaldehyde (PFA) in PBS, permeabilized with 0.2% Triton X-100 (Sigma) in PBS, blocked for 1 h in PBS with 3% donkey serum and 0.5% bovine serum albumin (BSA; Sigma), and stained for 1 h with 14C2 (1:500 diluted in blocking solution) followed by staining for 1 h with AF labeled donkey anti-mouse antibodies (1:500 diluted in blocking solution).

Cells were washed between each step with PBS. Surface M2 staining was performed as above, except without permeabilization. The cells were analyzed by flow cytometry on a BD FACSCalibur and the data was processed and analyzed using FlowJo software.

Viruses

Recombinant A/Udorn/72/(H3N2) (rUdorn) and recombinant A/WSN/33 (H1N1) (rWSN) have been described previously (108, 111, 112, 305, 312).

Recombinant A/Victoria/361/2011(H3N2) (rVic) virus was rescued using the 12-plasmid reverse genetics system (108, 305, 312, 315). Briefly, 293T cells were transfected with pHH21 plasmids encoding all 8 influenza A virus gene segments along with protein expression plasmids encoding the NP, PA, PB1, and PB2 cDNAs. Transfected cells were then co-cultured with M2-MDCK cells, and sampled every 24 hours for the release of virus particles. Viruses were plaque-purified and confirmed by sequencing. Stocks of virus were generated by infecting MDCK cells at a low multiplicity of infection (MOI) as described below.

Plaque assays

Plaque assays were performed in 6-well plates of confluent M2-MDCK cells. Serial 10-fold dilutions of the virus inoculum were generated in infection media (IM; DMEM supplemented with 0.3% BSA [Sigma], 100 U/mL

penicillin, 100 µg/mL streptomycin, 2 mM GlutaMAX [Gibco], and 4 µg/mL N-acetyl tryptin [NAT; Sigma]). Cells were washed twice with PBS containing calcium (100 mg/mL CaCl₂) and magnesium (100 mg/mL MgCl₂•6H₂O) (PBS+) and 250 µL of inoculum was added. The cells were incubated for 1 hour at RT with rocking. The inoculum was removed and replaced with IM containing 1% agarose. Cells were then incubated at 37°C for 2-5 days, fixed in 2% formaldehyde, and stained in a naphthol blue black solution. For synthetic virus generation, before fixing, the agar above individual plaques was removed with a sterile pipette, aspirated into 1 mL of IM, and stored at -80°C.

50% tissue culture infectious dose (TCID₅₀) assay

MDCK or M2-MDCK cells were plated in 96-well plates, grown to confluence, and washed twice with PBS+. Ten-fold serial dilutions of the virus inoculum were made and 200 µL of each dilution was added to each of 6 wells in the plate, followed by incubation for 5 days at 37°C. Cells were then fixed by adding 100 µL of 4% formaldehyde in PBS per well, followed by staining with a naphthol blue black solution.

Low MOI infection

Before all infections, cells are first washed twice with PBS+. Seed stocks (SS) were generated by incubating 250 µL of the plaque picks generated above on

fully confluent MDCK cells for 1 hour at RT. Inoculum was removed, cells were washed twice with PBS+, and then 1 mL of IM was added before returning the cells to the incubator at 37°C. Virus supernatant was harvested when 50% of the cells displayed cytopathic effect upon inspection with light microscopy (usually 24-48 hours post infection (HPI)). The infectious virus titer of the SS was then determined by TCID₅₀ assay, and used to generate working stocks (WS). The WS was generated as for seed stocks, except infections were performed in 75 or 150 cm² flasks and the inoculum used was SS diluted to an MOI of 0.01 in IM.

Multistep virus growth curves were performed at a MOI of 0.001 in MDCK cells and 0.1 in hNECs. For MDCK cell infections, the inoculum was diluted in IM, added to cells, and allowed to incubate at RT with rocking for 1 hour. Cells were then washed 3 times with PBS+ and incubated with fresh IM at 37°C. At the indicated HPI, all media were removed and replaced with fresh IM. The amount of infectious virus in each sample was determined by TCID₅₀ assay on M2-MDCK cells. For hNECs, the apical surface was washed with IM without NAT and the basolateral DM was replaced immediately before infection. Inoculum diluted in IM without NAT was then added and allowed to incubate on cells at 32°C for 1-2 hours. The inoculum was then removed, the cells were washed three times with PBS+, left at ALI, and returned to 32°C. At the indicated times post infection, IM without NAT was added to the apical chamber of the wells and allowed to incubate at 32°C for 5

minutes, removed, and the cells were returned to the incubator at ALI.

Basolateral DM was removed and replaced every 48 hours for the duration of the growth curves. All samples were stored at -80°C.

High MOI infection

High MOI (1 or 2 TCID₅₀ per cell) infections were performed as low MOI infections except, at the indicated time post infection, in addition to collecting virus supernatant, cells were lysed in 1% SDS in PBS, collected, and stored at -20°C. Infection supernatant was cleared of cell debris by centrifugation at 1400 x g for 10 minutes and infectious virus titers determined by TCID₅₀.

For hNECs, prior to the first time point, the apical surface was washed with an acidic PBS wash (PBS+ adjusted to a pH of 5.2 with citric acid) (346).

Microscopy

MDCK II cells stably transfected with the indicated constructs were grown for six days on collagen-coated polystyrene Transwell inserts (Costar). Cells were then fixed with 2% PFA at RT for 15 minutes or ice cold methanol for 10 minutes at -20°C. Cells were then washed and stored in PBS at 4°C. PFA fixed cells (but not methanol-fixed cells) were permeabilized with 0.2% Triton-X 100 (Sigma) in PBS for 15 minutes at RT before blocking. PFA-fixed cells were then blocked in PBS with 2% donkey serum and 0.5% BSA (blocking solution), stained with polyclonal rabbit anti-M2 antibody (1:400 in

blocking solution) and ZO-1A12 (1:50 in blocking solution) followed by secondary AF488-linked donkey anti-rabbit antibody and AF555-linked donkey anti-mouse antibody (both 1:500 in blocking solution). Methanol-fixed cells were stained the same way except with 14C2 and rabbit anti-calnexin antibody as primary antibodies and AF488-linked donkey anti-rabbit and AF555-linked donkey anti-mouse as secondary antibodies (all 1:500 in blocking solution). Cells were washed after each step by dipping membranes in PBS with 0.2% Tween-20 (PBST) 12 times. Cells were washed one final time in MilliQ water before mounting in Prolong gold antifade with DAPI (ThermoFisher). Cells were imaged using a Zeiss LSM 700 microscope with Zen software for image acquisition. Images were taken with a 63x objective in Z-stack mode with 0.25 or 0.5 μm spacing between stacks. Images were analyzed and processed with Volocity and FIJI.

SDS-PAGE and western blotting

Virus supernatant from high MOI infections was concentrated through a 35% sucrose cushion at 118,000 x g for 1 hour in an Optima Max-TL Beckman Ultracentrifuge. Alternatively, concentrating viral supernatants with Amicon Ultra – 0.5 ML Centrifugal Units (Ultracel – 100K; Millipore) or using non-concentrated infection supernatant yielded comparable results. All samples were mixed with 4X SDS-PAGE sample buffer containing dithiothreitol (DTT; Thermo) before heating for 5 min at 100°C. Samples were loaded

alongside Precision Plus Protein Standards All Blue protein ladder (Biorad) into a 4-15% Mini-PROTEAN TGX Gel (Biorad) and run at 100 V. Proteins were transferred onto an Immobilon – FL polyvinyl difluoride membrane at 100 V for 1 hour. Afterwards, membranes were blocked in PBS containing 0.2% Tween 20 and 5% blotting-grade blocker (Biorad). The membrane was then stained with primary antibodies (1:1000 goat anti Aichi, 1:1000 rabbit anti NP, or 1:10,000 mouse anti- β -actin), then stained with the appropriate AF conjugated secondary antibodies (1:1000). Between each step, the membrane was washed 3 times with PBS containing 0.2% Tween 20. Protein was detected using a FluorChem Q system (Proteinsimple). Cellular expression of viral proteins was normalized by β -actin expression, had mock subtracted, and then was normalized to average WT values. Levels of viral protein in the supernatant had mock subtracted and then were normalized to average WT values.

Statistical analyses

Multistep growth curves were analyzed by two-way ANOVA. FACS, M2-Baso mislocalization, endpoint dilution assays, high MOI infection virus replication and protein expression, and transepithelial resistance (TER) dependence on titer were analyzed by ANOVA. M2-ER localization and M2-ER and M2-Stop high MOI infections were analyzed with unpaired t-tests. All statistical analyses were performed in GraphPad Prism 7.0.

RESULTS

Expression of mistargeted M2 constructs

To investigate the role of M2 apical targeting on virus assembly and budding, amino acid sequences were mutated (C-terminal KKXX motif) to target it to the ER (43, 44, 82) or added (C-terminal AAASLLAP) to target M2 to the basolateral plasma membrane (347) (Fig. 3.1A). Additionally, a FLAG-tagged M2 construct was created to control for the addition of C-terminal amino acid residues at the end of the M2-Baso protein. Stable cell lines expressing the M2 cDNAs in MDCK II cells were generated and characterized for surface and total M2 expression by flow cytometry using the anti-M2 monoclonal antibody 14C2 either before, or after permeabilization (Fig. 3.1B). WT M2, M2-FLAG, M2-Baso, and M2-ER all express approximately the same amount of total M2. However, M2-ER is not present on the cell surface while WT M2, M2-FLAG, and M2-Baso all express similar amounts of cell surface M2.

Confocal immunofluorescence microscopy was then used to assess the subcellular localization of these constructs. For determining the extent of basolateral targeting of M2-Baso, ZO-1 was used to stain the tight junctions and demarcate the border between the apical and basolateral plasma membrane (Fig. 3.1C). WT M2 and M2-FLAG primarily stain at or above the level of the tight junction, indicating apical plasma membrane localization. Alternatively, M2-Baso has increased staining below the tight junction, and

has significantly less apical staining than either WT M2 or M2-FLAG (Fig. 3.1D). To determine the localization of the M2-ER construct, the ER was stained with an anti-calnexin antibody (Fig. 3.1E), and then colocalization of M2 and calnexin was determined (Fig. 3.1F). M2-ER exhibits a significant increase in ER localization compared to WT M2.

Complementation of viruses that do not express M2

Infectious virus production requires small amounts of M2 and M2 expressed *in trans* can complement the replication of recombinant viruses that do not encode the M2 protein (111). Accordingly, MDCK II cells stably transfected with WT M2 or M2-FLAG allowed for the replication of rUdorn M2-Stop virus (Fig. 3.2A). M2-Baso expressing cells allowed for a significantly lower production of infectious virus particles, while M2-ER and eGFP expressing cells did not support virus replication above the limit of detection (234 TCID₅₀/mL). Similarly, when rWSN M2-Stop virus was used, WT M2, M2-FLAG, and M2-Baso expressing cells, all detected similar quantities of infectious virus particles, while M2-ER and eGFP expressing cells detected significantly fewer viral particles, indicating that the inhibitory effect of M2-Baso is not as prominent in rWSN M2-Stop infected cells (Fig. 3.2C). In contrast, all cell lines supported similar levels of both rUdorn WT and rWSN WT infectious virus production, demonstrating that there are no nonspecific, detrimental effects associated with expressing M2 on the ER or basolateral

plasma membrane (Fig. 3.2B and 2D). For a more sensitive measure of the ability of the M2 constructs to complement IAV infection, low MOI growth curves were performed. MDCK II cells expressing WT M2, M2-FLAG, and M2-Baso were all able to replicate rUdorn M2-Stop to approximately 1×10^8 TCID₅₀/mL by 24 to 36 HPI (Fig. 3.2E). The M2-Baso expressing cells showed slightly slower kinetics of virus production and a later time of peak virus production, but these differences did not reach statistical significance. Neither M2-ER nor eGFP expressing cells were able to support rUdorn M2-Stop infectious virus production to appreciable levels. Additionally, WT M2, M2-FLAG, M2-Baso, M2-ER, and eGFP expressing MDCK II cells were all able to replicate WT rUdorn to the same approximate peak titer with similar kinetics, indicating that there are no non-specific, detrimental replication defects associated with expressing M2 on the ER or basolateral plasma membrane (Fig. 3.2F).

Replication of recombinant viruses expressing mistargeted M2

Recombinant IAV encoding the mistargeted M2 proteins were generated in the rVic background to further study the effects of M2 localization on virus infection and to better model recent seasonal IAV strains. The rVic M2-ER was unable to replicate to detectable levels in MDCK cells (Fig. 3.3A), but was able to replicate to similar levels as both rVic WT and rVic M2-FLAG in M2-MDCK cells (Fig. 3.3B), indicating that the rVic M2-ER mutation can be

complemented by M2-WT protein. The rVic M2-Baso replicated to lower peak titers and with slower kinetics in MDCK cells (Fig. 3.3A) but was indistinguishable from rVic WT and rVic M2-FLAG after infection of MDCK-M2 cells (Fig. 3.3B), indicating that the effect of targeting M2 to the basolateral membrane was not as detrimental to virus replication as targeting it to the ER.

To utilize a more relevant cell culture model for studying the rVic viruses, primary, differentiated human nasal epithelial cell (hNEC) cultures were used. In hNECs, both rVic M2-ER and rVic M2-Baso were unable to replicate to appreciable levels while rVic M2-FLAG replicates with significantly decreased kinetics compared to rVic WT (Fig. 3.3C). Taken together, the data indicate that targeting M2 to the ER has a clear detrimental effect on influenza virus replication while targeting it to the basolateral membrane results in a more variable, cell type specific inhibition of virus replication.

High MOI infection and protein analysis of rVic M2-Baso in hNECs

Following high MOI infection, rVic M2-Baso replicates to significantly lower titers than rVic WT on hNECs (Fig. 3.4A), consistent with the low MOI growth curve results. In contrast to the low MOI data, rVic M2-FLAG replicates to a higher titer than rVic WT during high MOI infections on hNECs (Fig. 3.4A). Infectious particles and viral proteins were never detected

in the basolateral chamber of hNECs infected with rVic WT, rVic M2-FLAG, or rVic M2-Baso (Fig. 3.4B and 4C). Cells infected with rVic M2-FLAG and M2-Baso express similar levels of HA2, but had higher levels of cell associated NP than rVic WT (Fig. 3.4C, 4D, and 4E). In the apical supernatant, all three viruses had similar levels of HA2 and NP, suggesting virus particle release was consistent despite the differences in infectious virus titers. Taken together, the data indicate that the reduced amount of infectious virus particles in the rVic M2-Baso infected hNECs is not due to reduced virus budding, but a decrease in the infectivity of the released virus particles.

rVic M2-baso replication and cell polarization

High MOI infections on hNEC cultures with different degrees of polarization, as determined by TER, were performed to assess the degree to which the reduced replication of rVic M2-Baso was dependent upon the polarization state of the hNEC cultures. Both rVic WT and rVic M2-FLAG replicated to equivalent levels in hNEC cultures with low or high TER levels as indicated by linear regression slopes that do not significantly deviate from 0 (Fig. 3.5A) and similar amounts of infectious virus detected in cells with a TER reading greater than $650 \Omega \cdot \text{cm}^2$ or cells with a TER reading less than $650 \Omega \cdot \text{cm}^2$ (Fig. 3.5B). This indicated that the polarization of the cultures did not affect infectious virus production. However, rVic M2-Baso replicates less efficiently

in hNEC cultures with high TER readings compared to cultures with low TER readings, as evident by the negative correlation between virus replication and hNEC polarity (Fig. 3.5A). The slope is statistically different from both 0 and the slope of the rVic WT and rVic M2-FLAG lines. Consistent with these results, rVic M2-Baso replicates to a higher titer in cells with a TER reading of less than $650 \Omega \cdot \text{cm}^2$ than in cells with a TER reading of $650 \Omega \cdot \text{cm}^2$ or greater (Fig. 3.5B).

High MOI infection and protein analysis of rVic M2-ER and rUdorn M2-Stop in MDCK cells

Consistent with the low MOI growth curve results, rVic M2-ER replicates to a significantly decreased titer compared to rVic WT during high MOI infections of MDCK cells (Fig. 3.6A). Cells infected with either rVic WT or rVic M2-ER express similar levels of both HA2 and NP (Fig. 3.6B, 6C, and 6D). However, there is no detectable HA2 or NP in the supernatant of cells infected with M2-ER, indicating that despite cells being infected, no virus particles were released (Fig. 3.6B, 6E, and 6F). Like rVic M2-ER, rUdorn M2-Stop replicates to a significantly lower titer than rUdorn WT virus in MDCK cells (Fig. 3.7A). While cells infected with rUdorn M2-Stop express similar quantities of viral proteins HA2 and NP as cells infected with rUdorn WT (Fig. 3.7B, 7C, and 7D), rUdorn M2-Stop infected cell supernatant has detectable, albeit slightly lower amounts of HA2 and NP compared to rUdorn

WT (Fig. 3.7B, 7E, and 7F). Together, the data indicate that rVic M2-ER has significantly lower release of viral proteins when compared to rUdorn M2-stop, suggesting mislocalizing M2 to the ER has a stronger effect on virus particle release than deleting the protein completely.

DISCUSSION

IAV infects and buds primarily from the apical plasma membrane during infection of polarized epithelial cells. All three viral integral membrane proteins are targeted to the apical plasma membrane (333-338). Because of this, it would be expected that critical egress processes like scission and genome packaging may be disrupted if viral proteins critical for these roles were targeted to other locations in the cell. When a basolateral localization signal is added to the HA cytoplasmic tail, HA loses its strict apical targeting, but virus budding still occurs at the apical plasma membrane without a drastic decrease in virus replication (348-350). This has been seen with other viral glycoproteins as well. When vesicular stomatitis virus glycoprotein loses its strict targeting to the basolateral plasma membrane, virus was still predominantly released at the basolateral plasma membrane (351). During measles virus infection of polarized epithelial cells, the glycoproteins H (apical and basolateral) and F (basolateral) are not strictly targeted to the apical plasma membrane, but virus is preferentially released apically (352). However, when basolateral targeting signals in these proteins were

disrupted, virus was unable to spread by syncytia formation and had decreased lateral spread *in vivo*, indicating a role for basolateral glycoprotein targeting in measles virus cell-to-cell spread (353). Furthermore, measles virus matrix protein interacts with the cytoplasmic tails of the glycoproteins, permitting M-glycoprotein co-targeting to the apical plasma membrane and allowing for virus airway shedding (354). Similarly, the data described here indicate that M2 apical targeting is required for IAV replication and budding.

In contrast to HA (348, 349), M2 targeted to the basolateral plasma membrane (Fig. 3.1A, 1C, and 1D) or the ER (Fig. 3.1A, 1E, and 1F) resulted in substantial replication defects (Fig. 3.3). This was demonstrated for rVic M2-ER virus in MDCK cells (Fig. 3.3A) and hNECs (Fig. 3.3C) and with rUdorn M2-ER in the transcomplementation system (Fig. 3.2E). For M2-Baso, the replication defect was apparent on MDCK cells infected with rVic M2-Baso (Fig. 3.3A) and hNECs (Fig. 3.3C), but not in the transcomplementation system (Fig. 3.2E). The phenotype penetrates more strongly when M2-Baso is expressed by the recombinant virus (Fig. 3.3A) rather than the cells being infected (Fig. 3.2E). This is potentially due to the ability of stably transfected cells to express more M2 than infected cells, making them more likely to have spillover of M2 into the apical compartment. Only a small amount of M2 is required to complement infection of an M2-stop virus (111), so even a small amount of spillover to the apical compartment could rescue replication to near WT levels. However, the MDCK

cells used in the recombinant virus studies are highly polarized (as determined by TER; data not shown), and the difference in phenotype penetrance may be due to the cell strain used in each study. When rUdorn expressing WT M2 infects MDCK II cells stably transfected with M2-ER, M2-Baso, or WT M2, it replicates to similar levels with similar kinetics (Fig. 3.2F), indicating that expressing M2 at these membranes does not disrupt the ability of the cell to sustain virus replication. This is consistent with a prior report showing that M2-ER does not inhibit the transport of HA to the cell surface (82). Furthermore, MDCK cells stably transfected with WT M2 support the replication of rVic WT, rVic M2-ER, and rVic M2-Baso to the same levels (Fig. 3.3B), demonstrating that there are no detrimental effects associated with encoding the mutations in the virus genome.

Both rVic M2-Baso and rVic M2-ER are unable to replicate in hNEC cultures. Moreover, rVic M2-ER replication is barely detectable on MDCK cells while rVic M2-Baso does produce some infectious virus particles. MDCK cells and hNECs differ in numerous characteristics, but critically for these results, hNECs, as *ex vivo* nasal epithelial cells, are more highly polarized than MDCK cells, an immortalized cell line derived from canine kidney cells. Accordingly, rVic M2-Baso replicates to significantly lower titers on highly polarized hNEC cultures than poorly polarized hNEC cultures (Fig. 3.5A and 5B), indicating that the M2-Baso replication phenotype is cell polarization-dependent.

M2 plays several roles during IAV replication that could account for the emergence of a replication defect when targeting M2 away from the apical plasma membrane. The C-terminal end of the M2 cytoplasmic tail is essential for incorporation of vRNPs into budding particles (111-113). The membrane proximal region of the M2 cytoplasmic tail contributes to virus membrane scission and budding in an ESCRT-independent manner in some studies (12, 98, 99). However, other studies have shown that many of the individual amino acids in this region of M2 are either dispensable or have a modest phenotype, suggesting the virus strain or the cell culture system utilized may play an important role in phenotype penetration (100-103). During infection of hNECs, rVic M2-Baso and rVic WT secrete similar amounts of virus protein into the apical supernatant (Fig. 3.4B, 4F, and 4G) despite rVic M2-Baso having significantly reduced production of infectious virus (Fig. 3.4A). *In vivo* epithelial cells and hNECs produce mucus that can interact with IAV particles. After removing the inoculum during high MOI infections of hNECs, the apical surface was washed with an HA-inactivating acidic PBS wash (PBS+ titrated to a pH of 5.2 with citric acid (346)) to prevent infectious virus left over from the inoculum from being detected at subsequent time points. However, this inactivated virus may still be present at these time points and detected as either “cell-associated” or “secreted” into the supernatant, confounding the hNEC protein results.

High MOI infection with rVic M2-ER on MDCK cells resulted in a significant decrease in virus replication (Fig. 3.6A) associated with a near complete absence of virus particle release (Fig. 3.6B, 6E, and 6F). Similarly, when M2 was not expressed (M2-stop virus), virus replication was reduced (Fig. 3.7A) but detectable amounts of viral proteins were present in the apical supernatant (Fig. 3.7B, 7E, and 7F). Taken together, the data indicate that targeting M2 to the ER results in a greater reduction of virus particle budding than deleting the protein completely. This may indicate that M2-ER is bringing other viral or cellular factors needed for virus budding away from the apical membrane, thus sequestering them away from the sites of virus budding. M2 has a well characterized interaction with M1 (112-114) and targeting M2 away from the apical plasma membrane may result in the relocalization of M1 and/or the vRNP. The putative cellular ubiquitin ligase UBR4 associates with M2 and promotes plasma membrane localization of not only M2, but also HA and NA (355). Furthermore, M2 relocates the essential autophagy protein LC3 to the plasma membrane, resulting in viral subversion of autophagy (117). Annexin A6 interacts with the M2 protein and alters virus budding (356). Finally, M2 and both cellular Rab11 and the β subunit of the F1Fo-ATPase are important for IAV filament budding (357, 358). Therefore, targeting M2 away from the apical plasma membrane may disrupt any number of viral and cellular protein interactions critical for influenza virus assembly, budding, and replication.

Membrane targeting by viral proteins is a critical determinant of tropism and pathogenesis (332). Sendai virus is a pneumotropic mouse virus and buds predominantly from the apical plasma membrane. However, a mutant that buds nonspecifically, from the apical and basolateral plasma membranes, was isolated and determined to expand tropism and alter pathogenesis (359-362). Similarly, for coronaviruses, apical release is associated with local spread and transmission, while basolateral release is associated with systemic infection (363, 364). In human airway epithelial cells, IAV is released from the apical surface of infected cells (365, 366). IAV principally causes acute respiratory illness. However, systemic infections and complications are often associated with poor prognosis. The mechanisms of IAV systemic dissemination are poorly understood, but may involve the depolarization of epithelial cells during infection and subsequent infection of endothelial cells (366), in addition to the well characterized addition of an HA multibasic cleavage site (367-371). The data described here indicate that targeting M2 to the ER causes a defect in budding and replication, but relocalizing it to the basolateral membrane has more modest effects on the apical budding of IAV. The contribution of M2 mislocalization and the mislocalization of viral/cellular factors associated with M2 on altered virus budding and infectious virus production needs to be determined.

ACKNOWLEDGEMENTS

We thank the members of the Pekosz laboratory, Sabra Klein, and members of the Klein laboratory for useful and critical discussions of the data. We also thank and acknowledge Cailin Deal, Jean-Marc Guedon, Melanie Simpson, Theodore Oliphant and Matthew McCown for technical assistance. The work was supported by the Shikani/El Hibri Prize for Discovery and Innovation (AP), R01 AI097417 (AP), HHSN272201400007C (AP), R01 AI072502 (APL), T32 AI007417 (NW), S10OD016374 (Zeiss LSM 700 Confocal; S.C. Kuo).

FIGURES

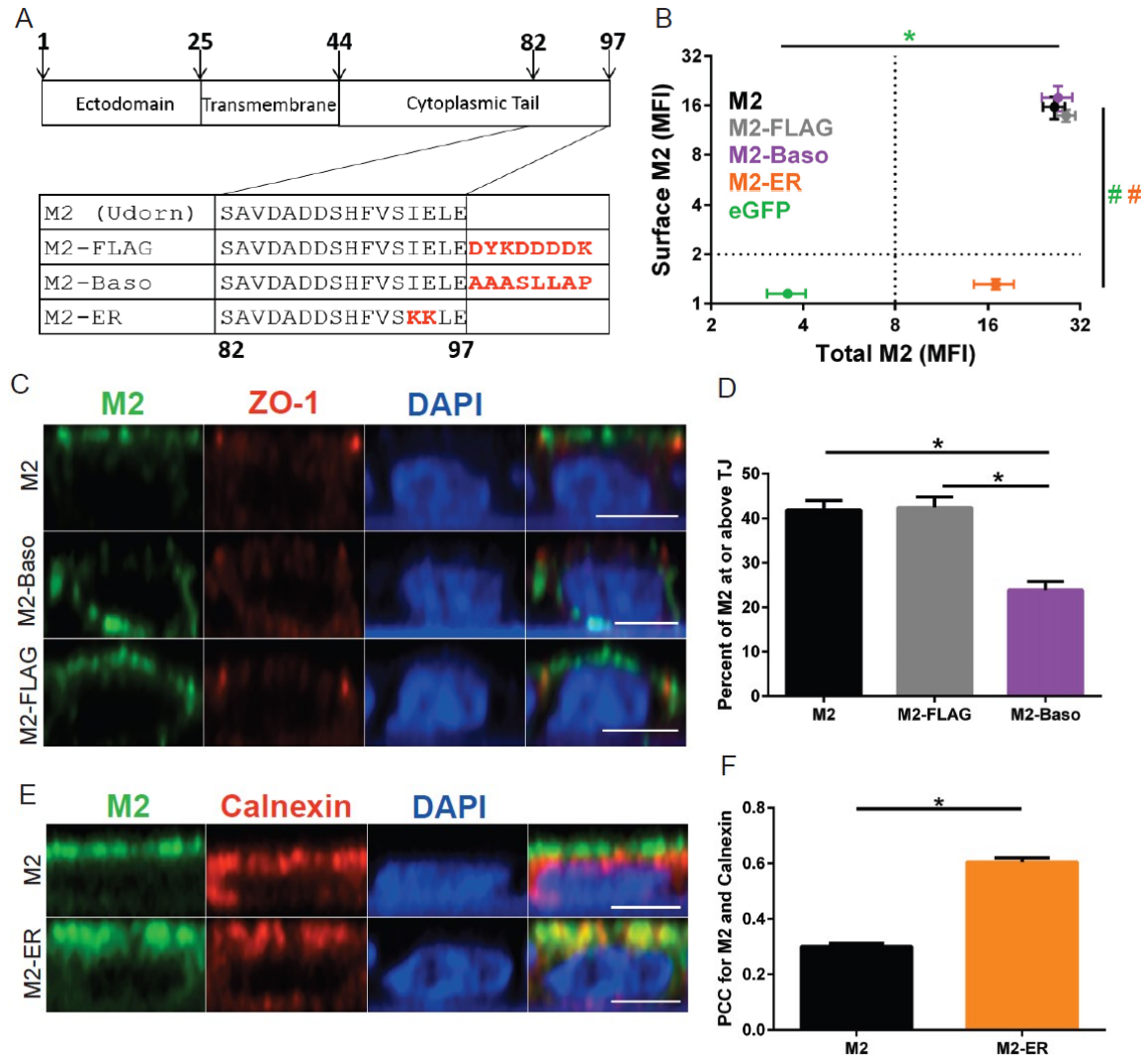


Figure 3.1. Localization of M2 proteins. (A) Schematic of Udorn M2 proteins with mutations made to the cytoplasmic tail to alter intracellular membrane targeting. (B) Surface and total M2 staining of MDCK II cells stably expressing the indicated protein. Error bars indicate SEM. * $p < 0.01$ (total) and # $p < 0.01$ (surface) M2 compared to WT M2 (ANOVA with Bonferroni multiple comparison posttest). Color of significance indicator

matches image legend. n = 4-7 stably transfected cell lines (C and E)

Immunofluorescence confocal microscopy images of MDCK II cells stably expressing the indicated M2 construct and immunostained for the indicated proteins. Scale bar is 5 μ m. (D) Quantification of apical targeting by percent of M2 staining at or above the tight junctions. n = 40 total cells from 2-3 stably transfected cell lines. *p < 0.01 (ANOVA with Bonferroni multiple comparison posttest). (E) Quantification of M2 and calnexin colocalization (Pearson's correlation coefficient). n = 100 total cells from 2-3 stably transfected cell lines. *p < 0.01 (unpaired t test).

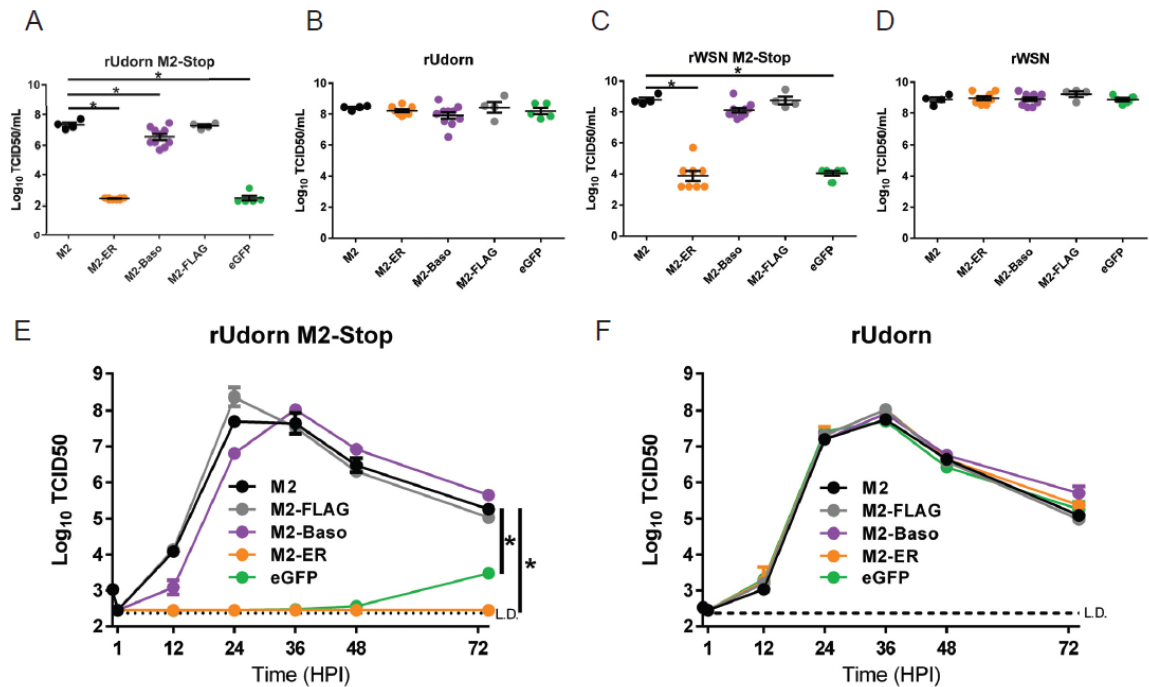


Figure 3.2. Replication of IAV on MDCK II cells stably expressing different M2 proteins. (A) rUdorn M2-Stop, (B) rUdorn, (C) rWSN M2-stop, and (D) rWSN endpoint dilution results on the indicated MDCK II cell lines. Stably transfected proteins are indicated on the x-axis. Virus was incubated on cells for 5 days. * $p < 0.01$ compared to WT M2 (one-way ANOVA). Data are pooled from two independent experiments. (E) rUdorn M2-Stop and (F) rUdorn multistep growth curves performed on MDCK II cells stably expressing the indicated proteins. Infectious virus titers were determined on MDCK-M2 cells. Data are representative of two independent replicates. $n = 3$ wells. * $p < 0.01$ compared to rUd WT (two-way ANOVA).

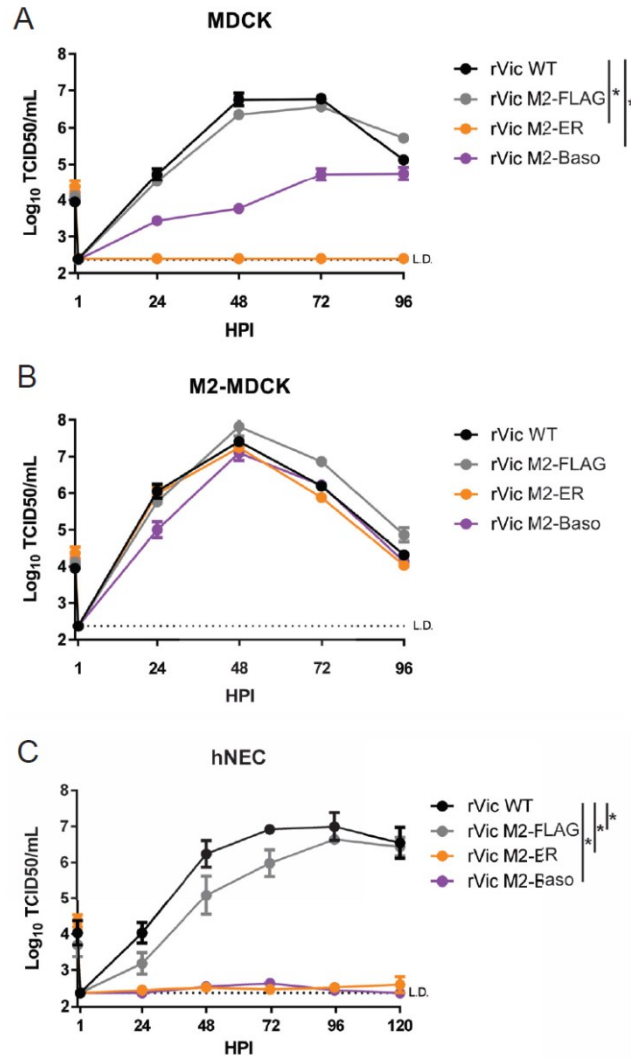


Figure 3.3. Replication of recombinant viruses expressing different M2 constructs. Multistep growth curves performed on (A) MDCK cells, (B) M2-MDCK cells, and (C) hNECs. Data are pooled from two independent replicates for total n = 6-7 wells. *p < 0.01 compared to rVic WT (two-way ANOVA with Bonferroni multiple comparison posttest).

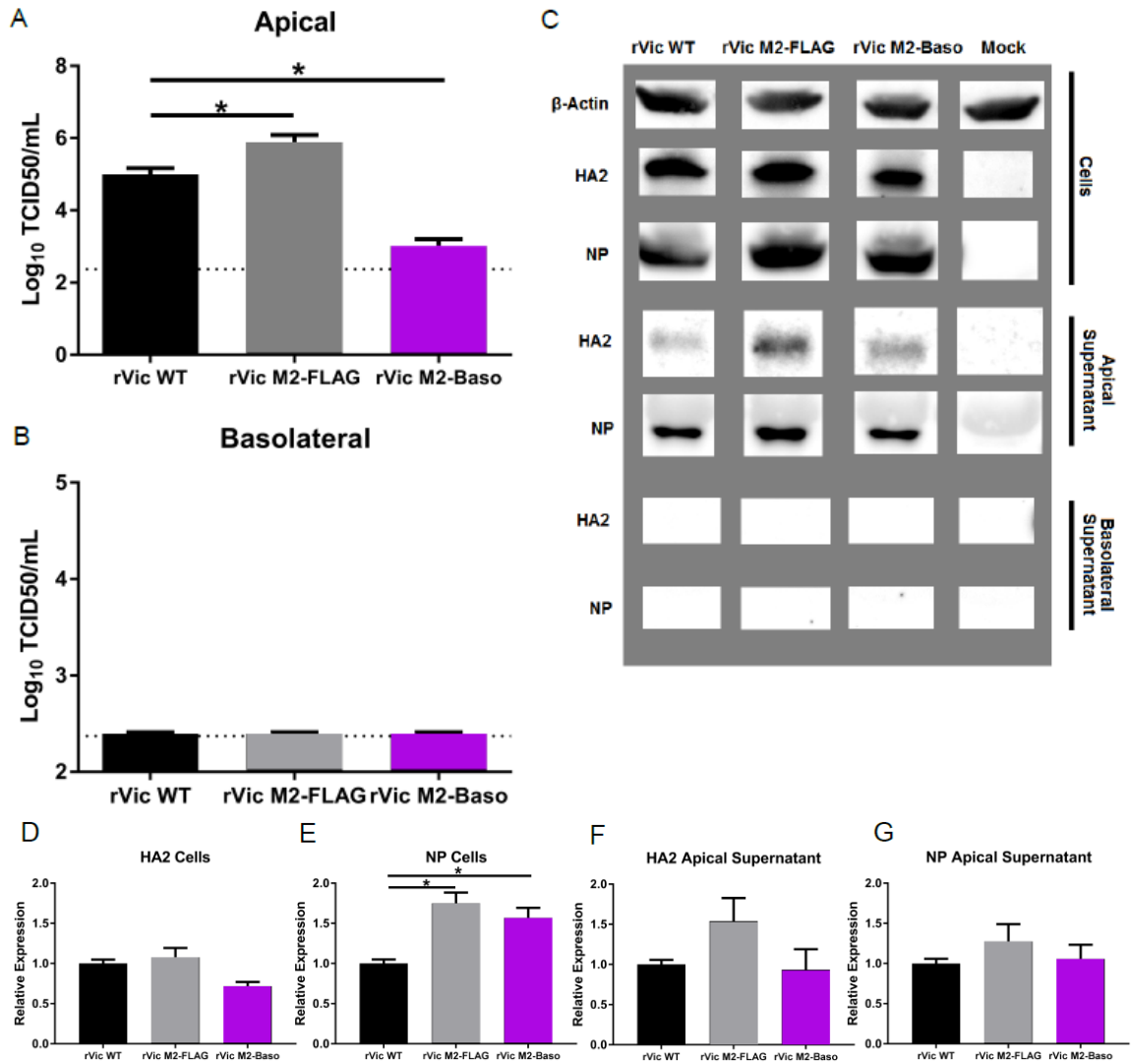


Figure 3.4. Replication and protein expression of rVic M2-Baso and rVic M2-FLAG on hNECs. High MOI infections were performed with the indicated viruses and 24 HPI virus titers in the apical (A) and basolateral (B) chambers were determined. Data are pooled from three independent replicates. $n = 3$ wells in each replicate. $*p < 0.01$ (one-way ANOVA). (C) Infected cell supernatants and cell lysates were analyzed by western blotting with antibodies against HA2 and NP. HA2 quantification for (D) cells and (F)

apical supernatant. NP quantification for (F) cells and (G) apical supernatant. Data are pooled from three independent replicates. n = 3 wells in each replicate. *p < 0.01 (one-way ANOVA).

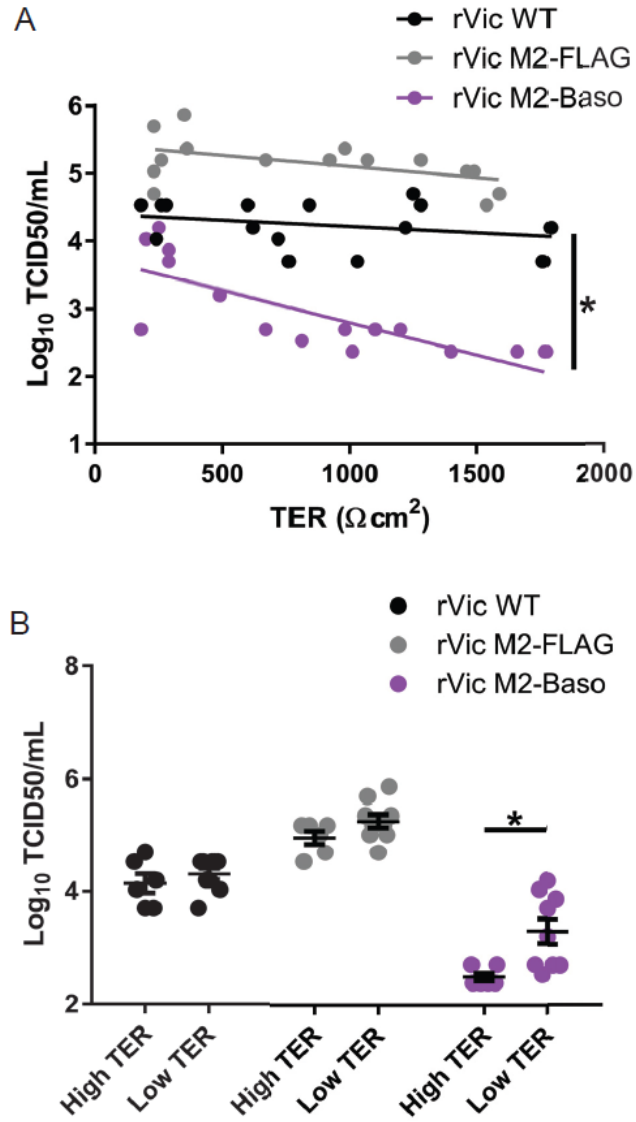


Figure 3.5. The M2-Baso replication defect is dependent on the polarization of the hNEC culture. High MOI infections performed with the indicated viruses for 24 hours. TER was measured before infection. (A) The correlation between hNEC polarization ($\Omega\cdot\text{cm}^2$) and virus titer at 24 HPI (MOI of 1) was quantified using a linear regression model. $n = 15$ per virus pooled from two independent experiments. $*p < 0.05$. (B) Virus replication at

24h on hNEC stratified by TER level (low TER < 650 $\Omega\cdot\text{cm}^2$ < high TER). *p < 0.01 Wilcoxon rank-sum test. n = 15 per virus pooled from two independent experiments.

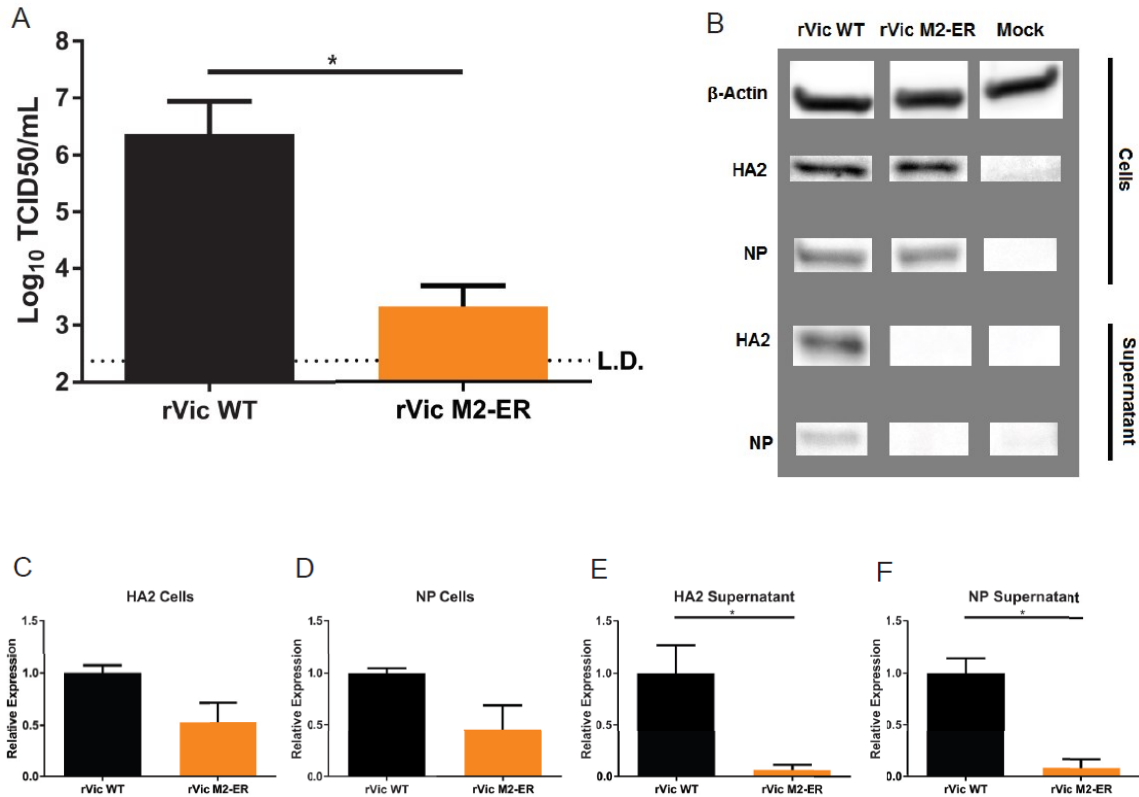


Figure 3.6. Replication and protein expression of rVic M2-ER on MDCK cells. High MOI infections were performed with the indicated viruses for 15-24 hours. (A) Virus titer at endpoint. Data are representative of three independent experiments. $n = 3$ wells per experiment. $*p < 0.01$ (unpaired t test). (B) Infected cell supernatants and cells were lysed and analyzed by western blotting with antibodies against HA2 and NP. HA2 quantification for (C) cells and (E) supernatant and NP quantification for (D) cells and (F) supernatant. Independent replicates were performed in triplicate and average data from each replicate was used. $*p < 0.01$ (unpaired t test).

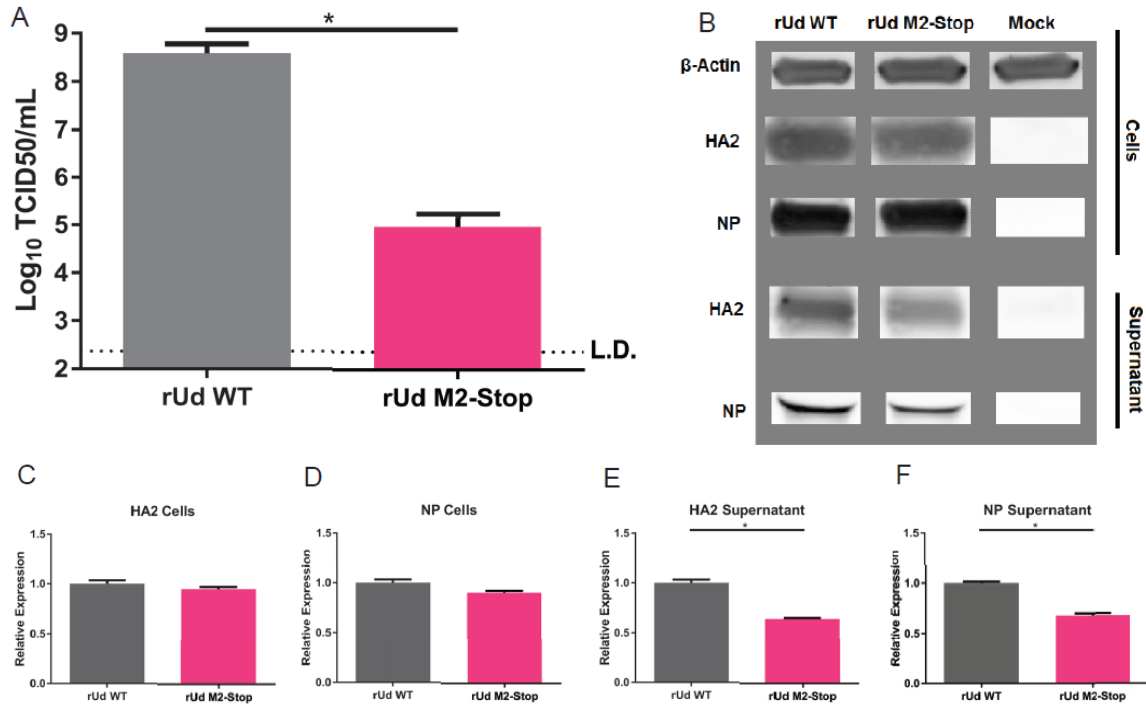


Figure 3.7. Replication and protein expression of rUdorn M2-Stop on MDCK cells. High MOI infections were performed with the indicated viruses for 24 hours. (A) Virus titer at endpoint. Data are representative of three independent experiments. $n = 3$ wells per experiment. $*p < 0.01$ (unpaired t test). (B) Infected cell supernatants and cells were lysed and analyzed by western blotting with antibodies against HA2 and NP. HA2 quantification for (C) cells and (E) supernatant and NP quantification for (D) cells and (F) supernatant. Data are pooled from three independent experiments ($n = 3$). $*p < 0.01$ (unpaired t test).

CHAPTER 4: GENERAL DISCUSSION

The research within this dissertation improves our understanding of the role that M2 plays in IAV replication, assembly, and budding. By adding unique sequences to the IAV M2 protein, I created a virus that failed to replicate efficiently and which could serve as a potential vaccine candidate. By introducing another set of specific mutations into M2, I was able to alter influenza virus vaccine replication to potentially increase its effectiveness in some populations. Together this work has progressed our understanding of both the basic biology of the IAV M2 protein and influenza vaccination strategies.

LAIV is no longer recommended in the USA due to problems with low effectiveness

As described in Chapter 1, the LAIV contains a mixture of three or four different viruses depending on the formulation (quadrivalent: A/H1N1, A/H3N2, B/Victoria, B/Yamagata; trivalent: A/H1N1, A/H3N2, B). The specific strains used in the vaccine are reviewed and updated twice a year by the WHO. A meta-analysis by strain showed efficacy from 85% for the H1N1 component, 76% for the H3N2 component, and 73% for the B component (372). However, in 2009, a novel pandemic H1N1 (pH1N1) emerged and replaced the existing seasonal H1N1 strain. Because the vaccine was updated to include pH1N1 (now the seasonal strain), there have been consistent problems with low effectiveness of the H1N1 component (37, 373). This

ultimately led to the recommendation by the USA Advisory Committee for Immunization Practices to not use the LAIV vaccine beginning with the 2016-2017 influenza season (36). Interestingly, in the UK, Canada, and Finland, the effectiveness problem was not as robust, leading these countries to continue recommending LAIV (37, 374, 375).

Several hypotheses have emerged to explain the decrease in effectiveness seen in LAIV since 2009 (Reviewed by Singanayagam *et al.* 2017 (37)). One hypothesis is that there is bias and heterogeneity in the studies used to assess LAIV effectiveness. Most influenza virus vaccine effectiveness studies are done with a test-negative study design in which patients with influenza-like illness are tested for influenza, then vaccination rates are compared between those who test positive and those who test negative (376). Small sample sizes often lead to inadequate statistical power and large confidence intervals that need to be taken into account when interpreting such vaccine efficacy data. Furthermore, standardizing study parameters such as inclusion criteria, sampling method, and sampling quality could further decrease the heterogeneity and bias seen in some vaccine effectiveness studies (37, 376-378).

Another hypothesis is that previous vaccination and natural immunity can have negative effects on LAIV effectiveness. During LAIV clinical testing, efficacy was not demonstrated in individuals over 50, and efficacy in individuals 18-49 was lower than what was observed in children, supporting

the hypothesis that previous exposure to natural infection or vaccination can, by eliciting a partially protective immune response, prevent robust replication of LAIV and decrease LAIV efficacy (379, 380). Repeated vaccinations with LAIV may have the same cumulative effect in children as adults who have had a lifetime of exposure to natural infections and vaccination, potentially decreasing the effectiveness in children towards what was seen in adults (37). While studies conducted following LAIV vaccination for two consecutive years showed no drop in efficacy (381), the consequence of repeated LAIV vaccination for several years (a decade or more) has not been investigated (37). However, such a study could be performed and used to test this hypothesis.

By its very nature, LAIV is supposed to be attenuated. Egg-adaptation mutations required for efficient replication and eggs (critical for mass production of the vaccine) can further attenuate LAIV strains. As a live vaccine, LAIV is thought to need to replicate in order to induce effective immunity. Consequently, the drop in LAIV effectiveness could be due to the biological characteristics of the pH1N1 virus itself. It has been shown in numerous model systems that pH1N1 replicates poorly. While pH1N1 is antigenically (HA) similar to the 1918 human influenza virus (382), it reemerged as a zoonotic, triple-reassortant virus from swine (383, 384). Numerous mutations are required for the efficient replication of a swine virus in humans. These mutations confer optimal receptor specificity, polymerase

activity, immune system inhibition, and various other functions for better infection of the new host (385, 386). Together, these observations lead to the hypothesis that because pH1N1 is a newly emerged virus, it has not had time to sufficiently adapt for high levels of replication in humans. Pandemic viruses such as pH1N1 can potentially overcome this through its novel antigenicity in younger populations and thus a more susceptible population.

It is known that under optimal conditions LAIV H1N1 can produce effective immunity (387), but this does not seem to be the case in of real-world human effectiveness. Additionally, the thermostability of the pH1N1 strain used in the US vaccine may have been suboptimal and, combined with problems with vaccine handling, may have contributed to the low effectiveness seen for the pH1N1 component of LAIV in the USA, but not in other countries (388-390). As described in Chapter 1, LAIV was derived through the blind passage of WT influenza virus strains at progressively colder temperatures (24). This resulted in 11 amino acid changes in the internal gene segments that confer *att* and cause decreased replications in humans vaccinated with LAIV (20, 25). Since pH1N1 already replicates poorly, the combined effects of its replication deficiencies with the LAIV internal gene segments may cross a threshold below which virus replication is no longer able to induce effective immunity. Further study of the effects that the LAIV mutations have on virus replication could lead to the design of vaccines that are able to replicate optimally despite replication defects in

their immunogenic components (HA and NA) (37). Furthermore, comparative shedding studies in ferrets and humans with various strains of LAIV including pH1N1, could confirm if the replication defects discussed have effects on *in vivo* replication and immunogenicity (390).

Identification of novel determinants of LAIV replication

The Pekosz lab has developed a robust model for studying the LAIV associated phenotypes in primary human nasal epithelial cells (hNECs) (31-33). Using this model, I was able to show that the previously discounted LAIV mutation M2-A86S (20, 26, 27, 302), contributes to both the *ts* and *att* phenotypes (33). These results were not detectable in MDCK cells, confirming the previous results while also demonstrating the superiority of our hNEC model. Furthermore, because the M2-A86S mutation had such drastic effects on virus replication (approximately 100-fold) (33), it is reasonable to assume that this same mutation causes a large decrease in replication *in vivo* (29). In turn, this mutation may be contributing to the inefficient replication of the pH1N1 component of LAIV and decreased vaccine efficacy. Another student under my mentorship in the Pekosz Laboratory demonstrated that the NS gene segment of LAIV (which contains a mutation at NS1 amino acid position 153 – Table 1.1) contributes to increased replication in both the LAIV and WT backbones (391). By further investigating the LAIV-associated mutations

we may be able to develop a rational vaccine strategy through optimizing vaccine virus replication.

Identification of the mechanism behind the M2-86 mutation's role in *attenuation*

In Chapter 2, I was able to show that the LAIV associated M2-A86S mutation is associated with an altered cytokine secretion profile. Specifically, M2-A86S was associated with a greater, early IFN- λ response. Additional evidence has shown that LAIV infections induce robust IFN- λ responses in hNECs (32), which is likely important for virus clearance and attenuation. IFN- λ s (IFNL1-4) are a class of antimicrobial immune regulators critical for protecting epithelial cells during viral infection (392).

To determine if IFN- λ induction is the mechanism by which the M2-A86S mutation confers *att*, a series of high MOI (1-10 infectious units per cell) infections could be performed to confirm the IFN- λ response under these conditions and at earlier times post infection. I hypothesize that the IFN- λ response will be greater at early times post infection, and this response is what controls virus replication at later times post infection. To complement our work, qRT-PCR should be performed on RNA extracted from infected cells to confirm the protein results from Chapter 2. Microarray and pathway analyses (cytokine and metabolic) could then be performed to further clarify the mechanism.

Furthermore, I hypothesize that blocking or knocking out the IFN- λ pathway (e.g. using mouse tracheal epithelial cell [mTEC] cultures from mice with the IFN- λ receptor knocked out) would rescue the replication seen in influenza viruses encoding a serine residue at M2-86. I also predict that adding recombinant IFN- λ to cells infected with WT IAV virus would decrease replication to a greater extent than adding it to M2-86S virus infected cells, because M2-86S has already induced such a robust IFN- λ response. Accordingly, I expect that the downstream effects of IFN- λ , including the induction of the known influenza restriction factor Mx1 (393, 394), would be significantly upregulated during LAIV infection compared to WT infection.

Optimizing LAIV replication and vaccine efficacy for diverse viruses and populations

Other members of the Pekosz laboratory (391, 395) and I (33), have demonstrated that by adding and subtracting the LAIV-associated mutations, we can generate LAIV viruses with variable degrees of replication. For example, by reversing the LAIV-associated M2-A86S mutation, we can increase LAIV virus replication. I hypothesize that a LAIV pH1N1 strain can be produced with the ability to replicate better, both *in vitro* and *in vivo*, allowing it to induce an effective immune response, while remaining safe. Increasing replication creates the potential to increase reactogenicity, which

would have to be carefully monitored and controlled for in these studies. To accomplish this, a more comprehensive panel of viruses containing the individual LAIV-associated mutations (Table 1.1) would need to be generated with both LAIV- and WT-associated residues in both LAIV and WT virus backbones of each H1N1 and H3N2. While a 44 (11 mutations x 2 backbones x 2 subtypes) virus panel may seem unwieldy, triaging the mutations for redundancy (similar effects in both background and subtypes or similar effects with each mutations in same gene) in hNECs would drastically decrease the number of viruses that need to be analyzed further. Assuming all of the mutations cause similar effects regardless of virus backbone and subtype, a panel of 11 viruses could be used for the preliminary animal studies. This number is likely still high as some mutations are unlikely to have significant effects on replication.

For preliminary studies, the individual mutations should be tested for their ability to affect virus replication in age and sex matched mice. Once the effect of individual mutations is established, combinations of mutations can be created to produce vaccine candidate viruses with an array of replication proficiencies. However, humans exist as outbred populations with heterogeneous immune responses and unique virus exposure histories. Performing preliminary vaccine candidate studies in naïve, inbred mice does not adequately model the complex interactions that led to the decreased effectiveness of LAIV (37). A model of outbred mice or, preferably ferrets,

immunized and boosted with quadrivalent LAIV or inactivated vaccine may be sufficient to begin modelling these phenomena. Alternatively, “natural” infection history could be modeled by using mice that have been exposed to sublethal doses of heterologous influenza strains. Furthermore, both age and sex must be analyzed to better predict vaccine effectiveness in diverse ranges of human populations (396, 397). Assessing the effects on replication of the individual LAIV mutations in these diverse populations will better inform the rational design of a novel LAIV utilizing a subset of the current LAIV mutations (and perhaps additional mutations) to fine tune replication. Generally, as exposure (vaccination and natural infection) increases, greater LAIV replication would be required. It is tempting to speculate that in the future, physicians will be able to prescribe an array of LAIV vaccines with different replication efficiencies depending on the patient’s age, sex, and vaccination and exposure history.

Targeting M2 away from the apical plasma membrane decreases virus replication

As described in Chapter 1 and Chapter 3, IAVs attach, enter, assemble, and bud from the apical plasma membrane. To assemble and bud, the virus transmembrane proteins, HA, NA, and M2, all target to the apical plasma membrane using cellular transport machinery (12). Previous work has shown that when HA loses its strict apical targeting there is not a substantial effect

on virus replication (348, 349). In contrast, in Chapter 3 of this dissertation I show that targeting M2 away from the apical plasma membrane to either the basolateral plasma membrane or the ER, results in significantly decreased virus replication (42). While deleting M2 significantly decreases budding, targeting M2 to the ER decreases budding to an even greater extent. This could occur because M2 is binding or interacting with another virus or cellular factor that is important for budding and subsequently bringing that factor with it to the ER. Furthermore, the replication defect associated with targeting M2 to the basolateral plasma membrane is dependent on the polarization of the cell model. In highly polarized hNECs, virus with M2 targeted to the basolateral plasma membrane is functionally dead, while in less polarized MDCKs the virus is still able to replicate.

Identification of the mechanism underlying the decrease in replication from mistargeting M2

Following my work described in Chapter 3, the next step to advance the field is to determine the mechanism underlying the decrease in replication associated with targeting M2 away from the apical plasma membrane.

Identification of the M2 apical targeting sequence

Identifying the apical targeting sequence of M2 could aid in the mistargeting of M2. As shown in Fig. 3.1, the mistargeting of both M2-Baso and M2-ER is

not 100%. This could be due to partial penetrance of the yet-unidentified apical targeting sequence. While basolateral targeting sequences are generally dominant to apical targeting sequences, deleting or mutating the apical targeting sequence may allow for more efficient relocalization of the protein, making follow-up, mechanistic studies easier. Apical targeting sequences can be diverse, and while M2 has both a CRAC domain and a palmitoylated cysteine residue (both of which could contribute to the distribution of M2 in the host cell), mutation of both these features does not drastically affect influenza virus replication (100, 108). Nevertheless, while not statistically significant, there is a slight decrease in replication of M2 virus in primary cells (mTECs) when the palmitoylation site is mutated (108). In light of our recent work on M2 localization, this palmitoylation mutation warrants further investigation into the role it may play in apical targeting. While palmitoylation may contribute to M2 localization, it is unlikely to be the only factor. Apical targeting sequences are often located near the transmembrane domain or at the C-terminal end of the protein (398). The Pekosz lab has previously published analyses of mutations at both the transmembrane proximal region (100) and the C-terminal end (111, 112) but never analyzed these mutants for subcellular localization. Analyzing these mutants (M2-Stop70, M2-Stop82, M2-Stop90, and M2-delCRAC) for their membrane targeting could reveal a region required for apical targeting. Subsequent mutagenesis within an identified region, would pinpoint the

apical targeting sequence. It should be noted that the deletion of the apical targeting sequence would be particularly useful for M2-Baso. While M2-ER has strong effects on virus replication in every model used, M2-Baso only exhibits complete ablation of replication in the highly polarized hNEC system, which is not as amenable to manipulation and biochemical studies. Greater mislocalization in less polarized cells like MDCK cells would make mechanistic studies easier.

Determine if mistargeting M2 has effects on early stages of virus gene expression

At late times post infection, there are not major differences in viral gene expression when M2 is mistargeted (Chapter 3). However, early differences in virus gene expression could delay virus assembly and budding. To rule out this possibility, a series of high MOI infections at earlier times post infection (1, 3, 6, 9 and 12 h) and subsequent western blotting of the resulting samples would reveal the presence of any early blocks in virus replication. WT M2 has been shown to delay the trafficking of HA to the plasma membrane (82). The proposed experiment would assess the levels of HA, NP, M1 and M2 expressed in cells at these early times post infections and ensure there are no significant temporal changes in protein expression compared to WT. I hypothesize, that M2-Baso will traffic normally through the ER and not disrupt the expression of other viral proteins, and M2-ER, depending on if it

is activated at the relatively high pH of the ER and early Golgi compartment, may or may also not disrupt virus protein production kinetics. Although a previous report indicates it will not (82).

Assessing the effects of mistargeting M2 on IAV assembly, budding, and cellular function

In Chapter 3, I demonstrated that targeting M2 away from the apical plasma membrane significantly decreases virus replication, and for M2-ER, this is associated with a decrease in budding. To confirm these findings and expand them to the M2-Baso construct, a series of high MOI confocal immunofluorescence microscopy experiments looking at the localization of several viral and cellular proteins could be performed. As discussed in Chapter 1, M2 is known to interact with M1 and NP (most likely through its interactions with M1). Using similar localization techniques as applied in Chapter 3, one could determine the localization of both M1 and NP and if these proteins are relocalized along with M2. Furthermore, assessing the activation and localization of cellular proteins known to interact with M2 could determine if other functions of M2 are affected by its relocalization. IAV infections normally increase the accumulation of lipidated LC3, a marker of autophagosome formation, in an M2 dependent manner (119). The M2-mistargeting constructs could be co-transfected with GFP-LC3 to determine if the M2-mistargeting mutant viruses are still able to induce LC3 lipidation

during infection, and if there are any changes to the subcellular localization of LC3. Other cellular factors to consider are Annexin A6, which has been shown to interact with M2 and alter virus budding (356), and Rab 11 and the β subunit of the F₁F_o-ATPase, both of which have been shown to be important for proper targeting of viral components to the apical plasma membrane during assembly and budding (99, 357, 358). I hypothesize that M2 is partially relocating both M1 and NP away from the apical plasma membrane, and that this will be detectable by confocal immunofluorescence microscopy under the appropriate conditions.

Systemic influenza virus model

Systemic complications from influenza virus infections are rare but can be dangerous. Most systemic complications are associated with highly pathogenic avian influenza virus infections, which can only be studied only BSL-3 conditions, making studies expensive and time-consuming. Infections can lead to severe central nervous system (CNS) disease and infection including encephalopathy and encephalitis (399-402). However, the mechanisms of such neurocomplications and systemic dissemination are poorly understood. It may involve the depolarization of airway epithelial cells and infection of endothelial cells (366). Additionally, there is a well characterized HA polybasic cleavage site mutation that is required for HA to be primed outside of the airway lumen (367-371).

Despite the severity of influenza systemic complications, there are no systems that accurately model the course of systemic infection. An H1N1 virus from 1933, A/Wilson Smith Neurovirulent/1933 (WSN), is a neurovirulent strain of influenza derived from “throat washings” from a patient (403) and subsequent laboratory adapted through extensive passaging in mice (via intracranial administration) and tissue culture (404, 405). However, it can only cause neurological symptoms following intracranial injection or intranasal infection at unnaturally high doses (406, 407). WSN is able to do this despite lacking a polybasic cleavage site. Thus, WSN is likely utilizing different mechanisms or pathways than natural viruses to induce systemic infection and neurological effects.

The basolateral targeting of critical viral proteins is a well-established route to systemic infection (332, 359-362). In Chapter 3 I describe a M2 protein construct targeted to the basolateral plasma membrane. An HA protein targeted to the basolateral plasma membrane has already been described (348, 349). If an NA protein can be created that is targeted to the basolateral plasma membrane, then there will be constructs of all three virus transmembrane proteins targeted to the basolateral plasma membrane. I hypothesize that adding the C-terminal tag used for M2-Baso (-AAASLLAP) to the end the end of the NA cytoplasmic tail would result in significant basolateral localization of that protein. Furthermore, I hypothesize that a virus with basolaterally targeted HA, NA, and M2, in addition to an HA

polybasic cleavage site, would be able to spread systemically in an animal model, and provide a platform for investigating systemic complications (such as CNS infection) of influenza infection. Importantly, an animal adapted backbone virus would mitigate biosafety risk, and the addition of human specific micro RNA targets would further decrease risk (408). The virus's basolateral directionality would severely restrict its ability to transmit, decreasing biosafety concern further.

Development of a mistargeted M2 vaccine

As discussed in Chapter 1, several vaccine strategies are being developed that utilize M2. Extending the M2 cytoplasmic tail by adding a Myc-tag to the end results in a highly attenuated virus that can induce protective immunity (288). In Chapter 3, I demonstrate that extending the cytoplasmic tail with a basolateral targeting sequence results in a virus that is highly attenuated in hNECs. Furthermore, simply mutating the cytoplasmic tail to contain an ER retrieval signal also attenuated virus replication in hNECs and MDCK cells. Extending the cytoplasmic tail with a FLAG-tag significantly decreased virus replication in hNECs under low MOI infection conditions, but not to the same extent as M2-ER or M2-Baso. I hypothesize that both M2-Baso and M2-ER would make ideal vaccine candidates, proving safe to administer as live viruses, and capable of inducing strong immunity.

To begin testing these constructs for their ability to serve as vaccine platforms, morbidity and mortality would need to be assessed in a small animal model, most likely mice. While ferrets are better models of influenza pathogenesis, mice remain a much cheaper and still relevant model. As a control, the M2-FLAG construct I used in Chapter 3 should be included to create a panel of viruses: mistargeted M2 only (M2-ER), extended M2 only (M2-FLAG), and mistargeted and extended M2 (M2-Baso). First the 50% mouse lethal dose would need to be determined to assess relative safety. I hypothesize that M2-ER and M2-Baso will both require high virus titers (as measured by TCID₅₀) to kill 50% of mice. During these studies, morbidity can also be measured (weight and temperature) and a subset of mice sacrificed to determine if virus is able to replicate in the respiratory tract. Afterwards, these studies should be repeated with the more clinically relevant nonhuman primate models to better assess and predict safety and attenuation in humans.

To determine if infection with M2-ER, M2-Baso, or M2-FLAG can induce protective immune responses, the humoral immune response to the M2-mistargeting viruses could be assessed. Mice could be infected with a sublethal dose of each virus, and then bled at several times post infection (e.g. 7, 14, 21, and 28 dpi) to quantify systemic antiviral antibody titers and subtypes by ELISA and microneutralization. Bronchoalveolar lavages should also be performed to assess mucosal IgA and IgG levels and virus replication.

One benefit to this strategy of immunization would be the inclusion of all potential T cell antigenic sites (discussed in Chapter 1). Current vaccine strategies rely on the use of egg-adapted or attenuated internal gene segments (PB1, PB2, PA, NP, M, and NS). If attenuation can be attained by simply adding sequences to M2, and not mutating or subtracting, then all potential T cell epitopes will be conserved, potentially improving cellular immunity to the vaccine. To assess this, T cells in the blood, lungs, and mesenteric lymph nodes should be quantified for the amount, type, polarization, functionality, and specificity for influenza antigens, particularly those against the internal gene segments (e.g. M1 and NP).

Finally, the mistargeting mutants can be assessed for their ability to generate homo- and heterotypic, protective immune responses. Following immunization with the mutants (a month or more post immunization), lethal or sublethal challenges could be administered with the same or different subtype of virus. Mice could then be monitored for morbidity and mortality. I hypothesize that mice receiving the M2-ER, M2-Baso, and M2-FLAG mutations would all be protected to approximately the same level. However, M2-ER and M2-Baso, because of their inability to replicate in hNECs, could be “safer” and more attenuated than M2-FLAG (Chapter 3). Additionally M2-ER and M2-Baso, by the nature of their poor replication and mistargeted M2, would likely be safer in the population than the existing LAIV vaccine, which has the potential to shed and transmit to unvaccinated individuals (409, 410).

Conclusion

Most live vaccines currently on the market were created through the serendipitous process of blind passaging in suboptimal model systems which resulted in virus attenuation in humans. The work presented in this dissertation transcends this historic strategy, and will help inform the rational design of improved influenza vaccines. Current influenza virus vaccination strategies are not consistently effective and are insufficient to respond quickly to emergent strains. The director of the U.S. National Institute of Allergy and Infectious Diseases of the National Institutes of Health, has repeatedly stressed the need for improved influenza vaccines and the creation of a universal influenza vaccine (411-413). While the work in this dissertation is unlikely to lead to a universal flu vaccine on its own, its findings will help drive the rational design of the next generation influenza vaccines. The idea that M segment point mutations in LAIV can significantly alter virus replication could have substantial impacts on the redesign of LAIV in diverse populations. Furthermore, this idea, that attenuation can be achieved through addition to the M2 cytoplasmic tail, could lead to a novel live, attenuated vaccine strategy. First put forth by Wu and Pekosz (288), this concept was expanded in this dissertation to include additions that alter M2 localization. Such a vaccine could produce broader immune responses than current vaccines due to the inclusion of all WT epitopes. A universal

influenza vaccine is unlikely to become reality for many years, but improvements like those discussed in this dissertation could increase vaccination effectiveness and longevity and help abolish the need for annual vaccination.

APPENDIX

| Primer name | Primer sequence (5' to 3') |
|----------------|--|
| Ud_M2-A83V_1 | GAA CAG CAG AGT GTT GTG GAT GCT GAC G |
| Ud_M2-A83V_2 | C GTC AGC ATC CAC AAC ACT CTG CTG TTC |
| Ud_M2-A83P_1 | GAA CAG CAG AGT CCT GTG GAT GCT GAC G |
| Ud_M2-A83P_2 | C GTC AGC ATC CAC AGG ACT CTG CTG TTC |
| Ud_M2-A83M_1 | GAA CAG CAG AGT ATG GTG GAT GCT GAC G |
| Ud_M2-A83M_2 | C GTC AGC ATC CAC CAT ACT CTG CTG TTC |
| Ud_M2-A83E_1 | GAA CAG CAG AGT GAA GTG GAT GCT GAC G |
| Ud_M2-A83E_2 | C GTC AGC ATC CAC TTC ACT CTG CTG TTC |
| Ud_M2-A83K_1 | GAA CAG CAG AGT AAG GTG GAT GCT GAC G |
| Ud_M2-A83K_2 | C GTC AGC ATC CAC CTT ACT CTG CTG TTC |
| Ud_M2-A86V_1 | CAA AAT GAC TGT CGT CAA CAT CCA CAG C |
| Ud_M2-A86V_2 | GAA CAG CAG AGT GCT GTG GAT GTT GAC G |
| Ud_M2-A86S_1 | CAA AAT GAC TGT CGT CAG AAT CCA CAG C |
| Ud_M2-A86S_2 | GAA CAG CAG AAT GCT GTG GAT TCT GAC G |
| Ud_M2-A86M_1 | CAA AAT GAC TGT CGT CCA TAT CCA CAG C |
| Ud_M2-A86M_2 | GAA CAG CAG AGT GCT GTG GAT ATG GAC G |
| Ud_M2-A86E_1 | CAA AAT GAC TGT CGT CTT CAT CCA CAG CA |
| Ud_M2-A86E_2 | GAA CAG CAG AGT GCT GTG GAT GAA GAC G |
| LAIV_M2-S86A_1 | AAA ATG ACT ATC GTC AGC ATC CAC AGC ACT CTG CTG |
| LAIV_M2-S86A_2 | CAG CAG AGT GCT GTG GAT GCT GAC GAT AGT CAT TTT |
| Ud_M2-FLAG_1 | GTC AGC ATA GAG CTG GAG GAC TAC AAG GAT GAT GAT GAC TAC TAA AAA ACT ACC TTG |
| Ud_M2-FLAG_2 | CAA GGT AGT TTT TTA GTA GTC ATC ATC ATC CTT GTA GTC CTC CAG CTC TAT GCT GAC |
| Vic_M2-FLAG_1 | GTC AGC ATA GAG TTG GAG GAC TAC AAG GAT GAT GAT GAC TAC TAA AAA ACT ACC TTG |
| Vic_M2-FLAG_2 | CAA GGT AGT TTT TTA GTA GTC ATC ATC ATC CTT GTA GTC CTC CAA CTC TAT GCT GAC |
| Ud_M2-Baso_1 | GC ATA GAG CTG GAG GCA GCC GCA AGC CTG CTG GCA CCA TAA AAA ACT ACC TTG |
| Ud_M2-Baso_2 | CAA GGT AGT TTT TTA TGG TGC CAG CAG GCT TGC GGC TGC CTC CAG CTC TAT GC |
| Vic_M2-Baso_1 | GC ATA GAG TTG GAG GCA GCC GCA AGC CTG CTG GCA CCA TAA AAA ACT ACC TTG |
| Vic_M2-Baso_2 | CAA GGT AGT TTT TTA TGG TGC CAG CAG GCT TGC GGC TGC CTC CAA CTC TAT GC |
| M2-ER_1 | G GAT GCT GAC GAC AGT CAT TTT GTC AGC AAA AAG CTG GAG TAA |
| M2-ER_2 | TTA CTC CAG CTT TTT GCT GAC AAA ATG ACT GTC GTC AGC ATC C |

Table A.1. Primer sequences.

REFERENCES

1. Shaw MLP, Peter. Orthomyxoviridae. In: Knipe DM, Howley, Peter M., editor. Fields Virology. 6th ed. Philadelphia: Lippincott Williams & Wilkins; 2013. p. 1151-85.
2. Fraser C, Donnelly CA, Cauchemez S, Hanage WP, Van Kerkhove MD, Hollingsworth TD, Griffin J, Baggaley RF, Jenkins HE, Lyons EJ, Jombart T, Hinsley WR, Grassly NC, Balloux F, Ghani AC, Ferguson NM, Rambaut A, Pybus OG, Lopez-Gatell H, Alpuche-Aranda CM, Chapela IB, Zavala EP, Guevara DM, Checchi F, Garcia E, Hugonnet S, Roth C. Pandemic potential of a strain of influenza A (H1N1): early findings. *Science (New York, NY)*. 2009;324(5934):1557-61. Epub 2009/05/13. PubMed PMID: 19433588 PMCID: PMC3735127.
3. Connor RJ, Kawaoka Y, Webster RG, Paulson JC. Receptor specificity in human, avian, and equine H2 and H3 influenza virus isolates. *Virology*. 1994;205(1):17-23. Epub 1994/11/15. PubMed PMID: 7975212.
4. Matlin KS, Reggio H, Helenius A, Simons K. Infectious entry pathway of influenza virus in a canine kidney cell line. *The Journal of cell biology*. 1981;91(3 Pt 1):601-13. Epub 1981/12/01. PubMed PMID: 7328111 PMCID: PMC2112819.
5. Zhirnov OP, Grigoriev VB. Disassembly of influenza C viruses, distinct from that of influenza A and B viruses requires neutral-alkaline pH. *Virology*. 1994;200(1):284-91. Epub 1994/04/01. PubMed PMID: 8128628.

6. Neumann G, Castrucci MR, Kawaoka Y. Nuclear import and export of influenza virus nucleoprotein. *Journal of virology*. 1997;71(12):9690-700. Epub 1997/11/26. PubMed PMID: 9371635 PMCID: PMCPMC230279.
7. Bullido R, Gomez-Puertas P, Albo C, Portela A. Several protein regions contribute to determine the nuclear and cytoplasmic localization of the influenza A virus nucleoprotein. *The Journal of general virology*. 2000;81(Pt 1):135-42. Epub 2000/01/21. PubMed PMID: 10640551.
8. Beaton AR, Krug RM. Transcription antitermination during influenza viral template RNA synthesis requires the nucleocapsid protein and the absence of a 5' capped end. *Proceedings of the National Academy of Sciences of the United States of America*. 1986;83(17):6282-6. Epub 1986/09/01. PubMed PMID: 3462695 PMCID: PMCPMC386487.
9. Hay AJ, Lomniczi B, Bellamy AR, Skehel JJ. Transcription of the influenza virus genome. *Virology*. 1977;83(2):337-55.
10. Vreede FT, Brownlee GG. Influenza virion-derived viral ribonucleoproteins synthesize both mRNA and cRNA in vitro. *Journal of virology*. 2007;81(5):2196-204. Epub 2006/12/15. PubMed PMID: 17166911 PMCID: PMCPMC1865950.
11. Vreede FT, Jung TE, Brownlee GG. Model suggesting that replication of influenza virus is regulated by stabilization of replicative intermediates. *Journal of virology*. 2004;78(17):9568-72. Epub 2004/08/17. PubMed PMID: 15308750 PMCID: PMCPMC506943.

12. Rossman JS, Lamb RA. Influenza virus assembly and budding. *Virology*. 2011;411(2):229-36. Epub 2011/01/18. PubMed PMID: 21237476
PMCID: PMC3086653.
13. Palese P, Compans RW. Inhibition of influenza virus replication in tissue culture by 2-deoxy-2,3-dehydro-N-trifluoroacetylneuraminic acid (FANA): mechanism of action. *The Journal of general virology*. 1976;33(1):159-63. Epub 1976/10/01. PubMed PMID: 978183.
14. Liu C, Eichelberger MC, Compans RW, Air GM. Influenza type A virus neuraminidase does not play a role in viral entry, replication, assembly, or budding. *Journal of virology*. 1995;69(2):1099-106. Epub 1995/02/01. PubMed PMID: 7815489 PMCID: PMC188682.
15. Hayward AC, Fragaszy EB, Bermingham A, Wang L, Copas A, Edmunds WJ, Ferguson N, Goonetilleke N, Harvey G, Kovar J, Lim MSC, McMichael A, Millett ERC, Nguyen-Van-Tam JS, Nazareth I, Pebody R, Tabassum F, Watson JM, Wurie FB, Johnson AM, Zambon M. Comparative community burden and severity of seasonal and pandemic influenza: results of the Flu Watch cohort study. *The Lancet Respiratory Medicine*. 2014;2(6):445-54.
16. Thompson WW, Weintraub E, Dhankhar P, Cheng PY, Brammer L, Meltzer MI, Bresee JS, Shay DK. Estimates of US influenza-associated deaths made using four different methods. *Influenza Other Respir Viruses*.

2009;3(1):37-49. Epub 2009/05/21. PubMed PMID: 19453440 PMCID:
PMCPMC4986622.

17. Molinari N-AM, Ortega-Sanchez IR, Messonnier ML, Thompson WW, Wortley PM, Weintraub E, Bridges CB. The annual impact of seasonal influenza in the US: Measuring disease burden and costs. *Vaccine*. 2007;25(27):5086-96.

18. Paules C, Subbarao K. Influenza. *Lancet* (London, England). 2017;390(10095):697-708. Epub 2017/03/18. PubMed PMID: 28302313.

19. Bennett J, Dolin R, Blaser M. Mandell, Douglas, and Bennett's principles and practices of infectious diseases. 8 ed. Philadelphia, PA: Elsevier; 2015.

20. Jin H, Subbarao K. Live attenuated influenza vaccine. *Current topics in microbiology and immunology*. 2015;386:181-204. Epub 2014/07/26. PubMed PMID: 25059893.

21. Wright PF, Neumann G, Kawaoka Y. Orthomyxoviruses. In: Knipe DM, Howley, Peter M., editor. *Fields Virology*. 6th ed. Philadelphia: Lippincott Williams & Wilkins; 2013. p. 1186-243.

22. Grabenstein JD, Pittman PR, Greenwood JT, Engler RJ. Immunization to protect the US Armed Forces: heritage, current practice, and prospects. *Epidemiologic reviews*. 2006;28:3-26. Epub 2006/06/10. PubMed PMID: 16763072.

23. Rota PA, Wallis TR, Harmon MW, Rota JS, Kendal AP, Nerome K. Cocirculation of two distinct evolutionary lineages of influenza type B virus since 1983. *Virology*. 1990;175(1):59-68. Epub 1990/03/01. PubMed PMID: 2309452.
24. Maassab HF. Adaptation and growth characteristics of influenza virus at 25 degrees c. *Nature*. 1967;213(5076):612-4. Epub 1967/02/11. PubMed PMID: 6040602.
25. Cox NJ, Kitame F, Kendal AP, Maassab HF, Naeve C. Identification of sequence changes in the cold-adapted, live attenuated influenza vaccine strain, A/Ann Arbor/6/60 (H2N2). *Virology*. 1988;167(2):554-67. Epub 1988/12/01. PubMed PMID: 2974219.
26. Jin H, Lu B, Zhou H, Ma C, Zhao J, Yang C-f, Kemble G, Greenberg H. Multiple amino acid residues confer temperature sensitivity to human influenza virus vaccine strains (flumist) derived from cold-adapted a/ann arbor/6/60. *Virology*. 2003;306(1):18-24.
27. Jin H, Zhou H, Lu B, Kemble G. Imparting Temperature Sensitivity and Attenuation in Ferrets to A/Puerto Rico/8/34 Influenza Virus by Transferring the Genetic Signature for Temperature Sensitivity from Cold-Adapted A/Ann Arbor/6/60. *Journal of virology*. 2004;78(2):995-8.
28. Snyder MH, Clements ML, De Borde D, Maassab HF, Murphy BR. Attenuation of wild-type human influenza A virus by acquisition of the PA polymerase and matrix protein genes of influenza A/Ann Arbor/6/60 cold-

adapted donor virus. *Journal of clinical microbiology*. 1985;22(5):719-25.

Epub 1985/11/01. PubMed PMID: 4056002 PMCID: PMCPMC268513.

29. Snyder MH, Betts RF, DeBorde D, Tierney EL, Clements ML, Herrington D, Sears SD, Dolin R, Maassab HF, Murphy BR. Four viral genes independently contribute to attenuation of live influenza A/Ann Arbor/6/60 (H2N2) cold-adapted reassortant virus vaccines. *Journal of virology*.

1988;62(2):488-95. Epub 1988/02/01. PubMed PMID: 3336068 PMCID: PMCPMC250559.

30. Fischer WA, 2nd, Chason KD, Brighton M, Jaspers I. Live attenuated influenza vaccine strains elicit a greater innate immune response than antigenically-matched seasonal influenza viruses during infection of human nasal epithelial cell cultures. *Vaccine*. 2014;32(15):1761-7. Epub 2014/02/04. PubMed PMID: 24486351 PMCID: PMCPMC3979967.

31. Fischer WA, 2nd, King LS, Lane AP, Pekosz A. Restricted replication of the live attenuated influenza A virus vaccine during infection of primary differentiated human nasal epithelial cells. *Vaccine*. 2015;33(36):4495-504. Epub 2015/07/22. PubMed PMID: 26196325 PMCID: PMCPMC4547880.

32. Forero A, Fenstermacher K, Wohlgemuth N, Nishida A, Carter V, Smith EA, Peng X, Hayes M, Francis D, Treanor J, Morrison J, Klein SL, Lane A, Katze MG, Pekosz A. Evaluation of the innate immune responses to influenza and live-attenuated influenza vaccine infection in primary

- differentiated human nasal epithelial cells. *Vaccine*. 2017. Epub 2017/10/03. PubMed PMID: 28967519.
33. Wohlgenuth N, Ye Y, Fenstermacher K, Liu H, Lane A, Pekosz A. The M2 protein of live, attenuated influenza vaccine encodes a mutation that reduces replication in human nasal epithelial cells. *Vaccine*. 2017. Epub 2017 Oct 24 PMID: PMC29079099.
34. Chen Z, Aspelund A, Kemble G, Jin H. Molecular studies of temperature-sensitive replication of the cold-adapted B/Ann Arbor/1/66, the master donor virus for live attenuated influenza FluMist vaccines. *Virology*. 2008;380(2):354-62. Epub 2008/09/23. PubMed PMID: 18804834.
35. Hoffmann E, Mahmood K, Chen Z, Yang CF, Spaete J, Greenberg HB, Herlocher ML, Jin H, Kemble G. Multiple gene segments control the temperature sensitivity and attenuation phenotypes of ca B/Ann Arbor/1/66. *Journal of virology*. 2005;79(17):11014-21. Epub 2005/08/17. PubMed PMID: 16103152 PMID: PMCPMC1193632.
36. Grohskopf LA, Sokolow LZ, Broder KR, Olsen SJ, Karron RA, Jernigan DB, Bresee JS. Prevention and Control of Seasonal Influenza with Vaccines. *MMWR Recomm Rep*. 2016;65(5):1-54.
37. Singanayagam A, Zambon M, Lalvani A, Barclay W. Urgent challenges in implementing live attenuated influenza vaccine. *The Lancet Infectious diseases*. 2017. Epub 2017/08/07. PubMed PMID: 28780285.

38. Miller DJ, Ahlquist P. Flock house virus RNA polymerase is a transmembrane protein with amino-terminal sequences sufficient for mitochondrial localization and membrane insertion. *Journal of virology*. 2002;76(19):9856-67. Epub 2002/09/05. PubMed PMID: 12208963 PMCID: PMCPMC136485.
39. Lontok E, Corse E, Machamer CE. Intracellular targeting signals contribute to localization of coronavirus spike proteins near the virus assembly site. *Journal of virology*. 2004;78(11):5913-22. Epub 2004/05/14. PubMed PMID: 15140989 PMCID: PMCPMC415842.
40. Alberts B, Johnson A, Lewis J, Morgan D, Raff M, Roberts K, Walter P. *Molecular Biology of the Cell*. 6 ed. New York: Garland Science; 2015.
41. Stoops EH, Caplan MJ. Trafficking to the Apical and Basolateral Membranes in Polarized Epithelial Cells. *Journal of the American Society of Nephrology*. 2014;25(7):1375-86.
42. Wohlgemuth N, Lane A, Pekosz A. Influenza A virus M2 protein apical targeting is required for efficient virus budding and replication. Unpublished results. 2017.
43. Jackson MR, Nilsson T, Peterson PA. Identification of a consensus motif for retention of transmembrane proteins in the endoplasmic reticulum. *The EMBO journal*. 1990;9(10):3153-62. Epub 1990/10/01. PubMed PMID: 2120038 PMCID: PMCPMC552044.

44. Jackson MR, Nilsson T, Peterson PA. Retrieval of transmembrane proteins to the endoplasmic reticulum. *The Journal of cell biology*. 1993;121(2):317-33. Epub 1993/04/01. PubMed PMID: 8468349 PMCID: PMC2200111.
45. Woolhouse M, Scott F, Hudson Z, Howey R, Chase-Topping M. Human viruses: discovery and emergence. *Philosophical Transactions of the Royal Society B: Biological Sciences*. 2012;367(1604):2864-71. PubMed PMID: PMC3427559.
46. Pekosz A, Glass GE. Emerging Viral Diseases. *Maryland medicine : MM : a publication of MEDCHI, the Maryland State Medical Society*. 2008;9(1):11-6. PubMed PMID: PMC2496997.
47. Anthony SJ, Epstein JH, Murray KA, Navarrete-Macias I, Zambrana-Torrel CM, Solovyov A, Ojeda-Flores R, Arrigo NC, Islam A, Ali Khan S, Hosseini P, Bogich TL, Olival KJ, Sanchez-Leon MD, Karesh WB, Goldstein T, Luby SP, Morse SS, Mazet JAK, Daszak P, Lipkin WI. A Strategy To Estimate Unknown Viral Diversity in Mammals. *mBio*. 2013;4(5).
48. Menachery VD, Graham RL, Baric RS. Jumping species—a mechanism for coronavirus persistence and survival. *Current Opinion in Virology*. 2017;23:1-7.
49. Nieva JL, Madan V, Carrasco L. Viroporins: structure and biological functions. *Nat Rev Micro*. 2012;10(8):563-74.

50. Davies WL, Grunert RR, Haff RF, McGahen JW, Neumayer EM, Paulshock M, Watts JC, Wood TR, Hermann EC, Hoffmann CE. ANTIVIRAL ACTIVITY OF 1-ADAMANTANAMINE (AMANTADINE). *Science (New York, NY)*. 1964;144(3620):862-3. Epub 1964/05/15. PubMed PMID: 14151624.
51. Sabin AB. Amantadine hydrochloride. Analysis of data related to its proposed use for prevention of A2 influenza virus disease in human beings. *JAMA*. 1967;200(11):943-50. Epub 1967/06/12. PubMed PMID: 5337680.
52. Togo Y, Hornick RB, Dawkins AT, Jr. Studies on induced influenza in man. I. Double-blind studies designed to assess prophylactic efficacy of amantadine hydrochloride against a2/Rockville/1/65 strain. *JAMA*. 1968;203(13):1089-94. Epub 1968/03/25. PubMed PMID: 4868123.
53. Dawkins AT, Jr., Gallager LR, Togo Y, Hornick RB, Harris BA. Studies on induced influenza in man. II. Double-blind study designed to assess the prophylactic efficacy of an analogue of amantadine hydrochloride. *JAMA*. 1968;203(13):1095-9. Epub 1968/03/25. PubMed PMID: 4870515.
54. Wingfield WL, Pollack D, Grunert RR. Therapeutic efficacy of amantadine HCl and rimantadine HCl in naturally occurring influenza A2 respiratory illness in man. *The New England journal of medicine*. 1969;281(11):579-84. Epub 1969/09/11. PubMed PMID: 4897137.

55. Couch RB. Use of amantadine in the therapy and prophylaxis of A2 influenza. *Bulletin of the World Health Organization*. 1969;41(3):695-6. Epub 1969/01/01. PubMed PMID: 5309494 PMCID: PMC2427709.
56. Scott C, Griffin S. Viroporins: structure, function and potential as antiviral targets. *The Journal of general virology*. 2015;96(8):2000-27. Epub 2015/05/30. PubMed PMID: 26023149.
57. Gonzalez ME, Carrasco L. Viroporins. *FEBS Lett*. 2003;552(1):28-34. Epub 2003/09/16. PubMed PMID: 12972148.
58. Plugge B, Gazzarrini S, Nelson M, Cerana R, Van JL, Etten, Derst C, DiFrancesco D, Moroni A, Thiel G. A Potassium Channel Protein Encoded by Chlorella Virus PBCV-1. *Science (New York, NY)*. 2000;287(5458):1641-4.
59. Pinto LH, Holsinger LJ, Lamb RA. Influenza virus M2 protein has ion channel activity. *Cell*. 1992;69(3):517-28.
60. Ewart GD, Sutherland T, Gage PW, Cox GB. The Vpu protein of human immunodeficiency virus type 1 forms cation-selective ion channels. *Journal of virology*. 1996;70(10):7108-15. Epub 1996/10/01. PubMed PMID: 8794357 PMCID: PMC190763.
61. Premkumar A, Wilson L, Ewart GD, Gage PW. Cation-selective ion channels formed by p7 of hepatitis C virus are blocked by hexamethylene amiloride. *FEBS Lett*. 2004;557(1-3):99-103. Epub 2004/01/27. PubMed PMID: 14741348.

62. Li Y, To J, Verdia-Baguena C, Dossena S, Surya W, Huang M, Paulmichl M, Liu DX, Aguilera VM, Torres J. Inhibition of the human respiratory syncytial virus small hydrophobic protein and structural variations in a bicelle environment. *Journal of virology*. 2014;88(20):11899-914. Epub 2014/08/08. PubMed PMID: 25100835 PMCID: PMC4178740.
63. Moffat JC, Vijayvergiya V, Gao PF, Cross TA, Woodbury DJ, Busath DD. Proton transport through influenza A virus M2 protein reconstituted in vesicles. *Biophysical journal*. 2008;94(2):434-45. Epub 2007/09/11. PubMed PMID: 17827230 PMCID: PMC2157240.
64. Pinto LH, Lamb RA. The M2 proton channels of influenza A and B viruses. *The Journal of biological chemistry*. 2006;281(14):8997-9000. Epub 2006/01/13. PubMed PMID: 16407184.
65. Pielak RM, Chou JJ. Influenza M2 proton channels. *Biochimica et biophysica acta*. 2011;1808(2):522-9. Epub 2010/05/11. PubMed PMID: 20451491 PMCID: PMC3108042.
66. Acharya R, Carnevale V, Fiorin G, Levine BG, Polishchuk AL, Balannik V, Samish I, Lamb RA, Pinto LH, DeGrado WF, Klein ML. Structure and mechanism of proton transport through the transmembrane tetrameric M2 protein bundle of the influenza A virus. *Proceedings of the National Academy of Sciences of the United States of America*. 2010;107(34):15075-80. Epub 2010/08/07. PubMed PMID: 20689043 PMCID: PMC2930543.

67. Schnell JR, Chou JJ. Structure and mechanism of the M2 proton channel of influenza A virus. *Nature*. 2008;451(7178):591-5. Epub 2008/02/01. PubMed PMID: 18235503 PMCID: PMC3108054.
68. Stouffer AL, Acharya R, Salom D, Levine AS, Di Costanzo L, Soto CS, Tereshko V, Nanda V, Stayrook S, DeGrado WF. Structural basis for the function and inhibition of an influenza virus proton channel. *Nature*. 2008;451(7178):596-9. Epub 2008/02/01. PubMed PMID: 18235504 PMCID: PMC3889492.
69. Wang J, Qiu JX, Soto C, DeGrado WF. Structural and dynamic mechanisms for the function and inhibition of the M2 proton channel from influenza A virus. *Current opinion in structural biology*. 2011;21(1):68-80. Epub 2011/01/21. PubMed PMID: 21247754 PMCID: PMC3039100.
70. Torres J, Surya W, Li Y, Liu DX. Protein-Protein Interactions of Viroporins in Coronaviruses and Paramyxoviruses: New Targets for Antivirals? *Viruses*. 2015;7(6):2858-83. Epub 2015/06/09. PubMed PMID: 26053927 PMCID: PMC4488717.
71. Verdia-Baguena C, Nieto-Torres JL, Alcaraz A, DeDiego ML, Torres J, Aguilella VM, Enjuanes L. Coronavirus E protein forms ion channels with functionally and structurally-involved membrane lipids. *Virology*. 2012;432(2):485-94. Epub 2012/07/27. PubMed PMID: 22832120 PMCID: PMC3438407.

72. Verdia-Baguena C, Nieto-Torres JL, Alcaraz A, Dediego ML, Enjuanes L, Aguilera VM. Analysis of SARS-CoV E protein ion channel activity by tuning the protein and lipid charge. *Biochimica et biophysica acta*. 2013;1828(9):2026-31. Epub 2013/05/22. PubMed PMID: 23688394 PMCID: PMC3715572.
73. Malev VV, Schagina LV, Gurnev PA, Takemoto JY, Nestorovich EM, Bezrukov SM. Syringomycin E channel: a lipidic pore stabilized by lipopeptide? *Biophysical journal*. 2002;82(4):1985-94. Epub 2002/03/28. PubMed PMID: 11916856 PMCID: PMC1301994.
74. Aldabe R, Barco A, Carrasco L. Membrane permeabilization by poliovirus proteins 2B and 2BC. *The Journal of biological chemistry*. 1996;271(38):23134-7. Epub 1996/09/20. PubMed PMID: 8798506.
75. Hyser JM, Collinson-Pautz MR, Utama B, Estes MK. Rotavirus disrupts calcium homeostasis by NSP4 viroporin activity. *MBio*. 2010;1(5). Epub 2010/12/15. PubMed PMID: 21151776 PMCID: PMC2999940.
76. Diaz Y, Chemello ME, Pena F, Aristimuno OC, Zambrano JL, Rojas H, Bartoli F, Salazar L, Chwetzoff S, Sapin C, Trugnan G, Michelangeli F, Ruiz MC. Expression of nonstructural rotavirus protein NSP4 mimics Ca²⁺ homeostasis changes induced by rotavirus infection in cultured cells. *Journal of virology*. 2008;82(22):11331-43. Epub 2008/09/13. PubMed PMID: 18787006 PMCID: PMC2573286.

77. Ehrenfeld E, Domingo E, Roos RP. *The Picornaviruses*: American Society of Microbiology; 2010.
78. Flint J, Racaniello VR, Rall GF, Skalka AM. *Principles of Virology*, Fourth Edition, Bundle: American Society of Microbiology; 2015.
79. Ciampor F, Bayley PM, Nermut MV, Hirst EM, Sugrue RJ, Hay AJ. Evidence that the amantadine-induced, M2-mediated conversion of influenza A virus hemagglutinin to the low pH conformation occurs in an acidic trans Golgi compartment. *Virology*. 1992;188(1):14-24. Epub 1992/05/01. PubMed PMID: 1566569.
80. Ciampor F, Thompson CA, Grambas S, Hay AJ. Regulation of pH by the M2 protein of influenza A viruses. *Virus research*. 1992;22(3):247-58. Epub 1992/03/01. PubMed PMID: 1626420.
81. Ciampor F, Cmarko D, Cmarkova J, Zavodska E. Influenza virus M2 protein and haemagglutinin conformation changes during intracellular transport. *Acta virologica*. 1995;39(3):171-81. Epub 1995/06/01. PubMed PMID: 8579000.
82. Sakaguchi T, Leser GP, Lamb RA. The ion channel activity of the influenza virus M2 protein affects transport through the Golgi apparatus. *The Journal of cell biology*. 1996;133(4):733-47. Epub 1996/05/01. PubMed PMID: 8666660 PMCID: PMCPMC2120830.
83. Takeuchi K, Lamb RA. Influenza virus M2 protein ion channel activity stabilizes the native form of fowl plague virus hemagglutinin during

intracellular transport. *Journal of virology*. 1994;68(2):911-9. Epub 1994/02/01. PubMed PMID: 7507186 PMCID: PMC236528.

84. Takeuchi K, Shaughnessy MA, Lamb RA. Influenza virus M2 protein ion channel activity is not required to maintain the equine-1 hemagglutinin in its native form in infected cells. *Virology*. 1994;202(2):1007-11. Epub 1994/08/01. PubMed PMID: 7518161.

85. Griffin SD, Harvey R, Clarke DS, Barclay WS, Harris M, Rowlands DJ. A conserved basic loop in hepatitis C virus p7 protein is required for amantadine-sensitive ion channel activity in mammalian cells but is dispensable for localization to mitochondria. *The Journal of general virology*. 2004;85(Pt 2):451-61. Epub 2004/02/11. PubMed PMID: 14769903.

86. Wozniak AL, Griffin S, Rowlands D, Harris M, Yi M, Lemon SM, Weinman SA. Intracellular proton conductance of the hepatitis C virus p7 protein and its contribution to infectious virus production. *PLoS pathogens*. 2010;6(9):e1001087. Epub 2010/09/09. PubMed PMID: 20824094 PMCID: PMC2932723.

87. Ichinohe T, Pang IK, Iwasaki A. Influenza virus activates inflammasomes via its intracellular M2 ion channel. *Nature immunology*. 2010;11(5):404-10. Epub 2010/04/13. PubMed PMID: 20383149 PMCID: PMC2857582.

88. Triantafilou K, Kar S, Vakakis E, Kotecha S, Triantafilou M. Human respiratory syncytial virus viroporin SH: a viral recognition pathway used by

the host to signal inflammasome activation. *Thorax*. 2013;68(1):66-75. Epub 2012/12/12. PubMed PMID: 23229815.

89. Shrivastava S, Mukherjee A, Ray R, Ray RB. Hepatitis C virus induces interleukin-1beta (IL-1beta)/IL-18 in circulatory and resident liver macrophages. *Journal of virology*. 2013;87(22):12284-90. Epub 2013/09/06. PubMed PMID: 24006444 PMCID: PMC3807883.

90. Perregaux D, Gabel CA. Interleukin-1 beta maturation and release in response to ATP and nigericin. Evidence that potassium depletion mediated by these agents is a necessary and common feature of their activity. *The Journal of biological chemistry*. 1994;269(21):15195-203. Epub 1994/05/27. PubMed PMID: 8195155.

91. Petrilli V, Papin S, Dostert C, Mayor A, Martinon F, Tschopp J. Activation of the NALP3 inflammasome is triggered by low intracellular potassium concentration. *Cell death and differentiation*. 2007;14(9):1583-9. Epub 2007/06/30. PubMed PMID: 17599094.

92. To J, Surya W, Torres J. Targeting the Channel Activity of Viroporins. *Advances in protein chemistry and structural biology*. 2016;104:307-55. Epub 2016/04/03. PubMed PMID: 27038378.

93. Alvarado-Facundo E, Gao Y, Ribas-Aparicio RM, Jiménez-Alberto A, Weiss CD, Wang W. Influenza Virus M2 Protein Ion Channel Activity Helps To Maintain Pandemic 2009 H1N1 Virus Hemagglutinin Fusion Competence during Transport to the Cell Surface. *Journal of virology*. 2015;89(4):1975-85.

94. Grambas S, Bennett MS, Hay AJ. Influence of amantadine resistance mutations on the pH regulatory function of the M2 protein of influenza A viruses. *Virology*. 1992;191(2):541-9.
95. Grambas S, Hay AJ. Maturation of influenza a virus hemagglutinin—Estimates of the pH encountered during transport and its regulation by the M2 protein. *Virology*. 1992;190(1):11-8.
96. McKay T, Patel M, Pickles RJ, Johnson LG, Olsen JC. Influenza M2 envelope protein augments avian influenza hemagglutinin pseudotyping of lentiviral vectors. *Gene Ther*. 2006;13(8):715-24.
97. Tobler K, Kelly ML, Pinto LH, Lamb RA. Effect of cytoplasmic tail truncations on the activity of the M(2) ion channel of influenza A virus. *Journal of virology*. 1999;73(12):9695-701. Epub 1999/11/13. PubMed PMID: 10559278 PMCID: PMC113015.
98. Rossman JS, Jing X, Leser GP, Balannik V, Pinto LH, Lamb RA. Influenza virus m2 ion channel protein is necessary for filamentous virion formation. *Journal of virology*. 2010;84(10):5078-88. Epub 2010/03/12. PubMed PMID: 20219914 PMCID: PMC2863831.
99. Rossman JS, Jing X, Leser GP, Lamb RA. Influenza virus M2 protein mediates ESCRT-independent membrane scission. *Cell*. 2010;142(6):902-13. Epub 2010/09/21. PubMed PMID: 20850012 PMCID: PMC3059587.
100. Stewart SM, Wu W-H, Lalime EN, Pekosz A. The cholesterol recognition/interaction amino acid consensus motif of the influenza A virus

M2 protein is not required for virus replication but contributes to virulence. *Virology*. 2010;405(2):530-8.

101. Stewart SM, Pekosz A. Mutations in the membrane-proximal region of the influenza A virus M2 protein cytoplasmic tail have modest effects on virus replication. *Journal of virology*. 2011;85(23):12179-87. Epub 2011/09/16. PubMed PMID: 21917980 PMCID: PMC3209349.

102. Thaa B, Tievesch C, Moller L, Schmitt AO, Wolff T, Bannert N, Herrmann A, Veit M. Growth of influenza A virus is not impeded by simultaneous removal of the cholesterol-binding and acylation sites in the M2 protein. *The Journal of general virology*. 2012;93(Pt 2):282-92. Epub 2011/10/21. PubMed PMID: 22012459.

103. Roberts KL, Leser GP, Ma C, Lamb RA. The amphipathic helix of influenza A virus M2 protein is required for filamentous bud formation and scission of filamentous and spherical particles. *Journal of virology*. 2013;87(18):9973-82. Epub 2013/07/12. PubMed PMID: 23843641 PMCID: PMC3754012.

104. Schroeder C, Heider H, Moncke-Buchner E, Lin TI. The influenza virus ion channel and maturation cofactor M2 is a cholesterol-binding protein. *European biophysics journal : EBJ*. 2005;34(1):52-66. Epub 2004/06/29. PubMed PMID: 15221235.

105. Leser GP, Lamb RA. Influenza virus assembly and budding in raft-derived microdomains: a quantitative analysis of the surface distribution of

HA, NA and M2 proteins. *Virology*. 2005;342(2):215-27. Epub 2005/10/27.
PubMed PMID: 16249012.

106. Zhang J, Pekosz A, Lamb RA. Influenza virus assembly and lipid raft microdomains: a role for the cytoplasmic tails of the spike glycoproteins. *Journal of virology*. 2000;74(10):4634-44. Epub 2000/04/25. PubMed PMID: 10775599 PMCID: PMCPMC111983.

107. Thaa B, Siche S, Herrmann A, Veit M. Acylation and cholesterol binding are not required for targeting of influenza A virus M2 protein to the hemagglutinin-defined budzone. *FEBS Lett*. 2014;588(6):1031-6. Epub 2014/02/25. PubMed PMID: 24561202.

108. Grantham ML, Wu WH, Lalime EN, Lorenzo ME, Klein SL, Pekosz A. Palmitoylation of the influenza A virus M2 protein is not required for virus replication in vitro but contributes to virus virulence. *Journal of virology*. 2009;83(17):8655-61. Epub 2009/06/26. PubMed PMID: 19553312 PMCID: PMCPMC2738213.

109. Sun L, Hemgard GV, Susanto SA, Wirth M. Caveolin-1 influences human influenza A virus (H1N1) multiplication in cell culture. *Virology journal*. 2010;7:108. Epub 2010/05/28. PubMed PMID: 20504340 PMCID: PMCPMC2889940.

110. Zou P, Wu F, Lu L, Huang JH, Chen YH. The cytoplasmic domain of influenza M2 protein interacts with caveolin-1. *Archives of biochemistry and biophysics*. 2009;486(2):150-4. Epub 2009/06/11. PubMed PMID: 19514132.

111. McCown MF, Pekosz A. The influenza A virus M2 cytoplasmic tail is required for infectious virus production and efficient genome packaging. *Journal of virology*. 2005;79(6):3595-605. Epub 2005/02/26. PubMed PMID: 15731254 PMCID: PMCPMC1075690.
112. McCown MF, Pekosz A. Distinct domains of the influenza a virus M2 protein cytoplasmic tail mediate binding to the M1 protein and facilitate infectious virus production. *Journal of virology*. 2006;80(16):8178-89. Epub 2006/07/29. PubMed PMID: 16873274 PMCID: PMCPMC1563831.
113. Grantham ML, Stewart SM, Lalime EN, Pekosz A. Tyrosines in the Influenza A Virus M2 Protein Cytoplasmic Tail Are Critical for Production of Infectious Virus Particles. *Journal of virology*. 2010;84(17):8765-76.
114. Chen BJ, Leser GP, Jackson D, Lamb RA. The influenza virus M2 protein cytoplasmic tail interacts with the M1 protein and influences virus assembly at the site of virus budding. *Journal of virology*. 2008;82(20):10059-70. Epub 2008/08/15. PubMed PMID: 18701586 PMCID: PMCPMC2566248.
115. Iwatsuki-Horimoto K, Horimoto T, Noda T, Kiso M, Maeda J, Watanabe S, Muramoto Y, Fujii K, Kawaoka Y. The Cytoplasmic Tail of the Influenza A Virus M2 Protein Plays a Role in Viral Assembly. *Journal of virology*. 2006;80(11):5233-40.
116. Liu H, Grantham M, Pekosz A. Unpublished results. 2017.
117. Beale R, Wise H, Stuart A, Ravenhill BJ, Digard P, Randow F. A LC3-interacting motif in the influenza A virus M2 protein is required to subvert

- autophagy and maintain virion stability. *Cell host & microbe*. 2014;15(2):239-47. Epub 2014/02/18. PubMed PMID: 24528869 PMCID: PMC3991421.
118. Munz C. Influenza A virus lures autophagic protein LC3 to budding sites. *Cell host & microbe*. 2014;15(2):130-1. Epub 2014/02/18. PubMed PMID: 24528859.
119. Gannagé M, Dormann D, Albrecht R, Dengjel J, Torossi T, Rämer PC, Lee M, Strowig T, Arrey F, Conenello G, Pypaert M, Andersen J, García-Sastre A, Münz C. Matrix Protein 2 of Influenza A Virus Blocks Autophagosome Fusion with Lysosomes. *Cell host & microbe*. 6(4):367-80.
120. Ren Y, Li C, Feng L, Pan W, Li L, Wang Q, Li J, Li N, Han L, Zheng X, Niu X, Sun C, Chen L. Proton Channel Activity of Influenza A Virus Matrix Protein 2 Contributes to Autophagy Arrest. *Journal of virology*. 2015;90(1):591-8. Epub 2015/10/16. PubMed PMID: 26468520 PMCID: PMC4702553.
121. Paterson RG, Takeda M, Ohigashi Y, Pinto LH, Lamb RA. Influenza B virus BM2 protein is an oligomeric integral membrane protein expressed at the cell surface. *Virology*. 2003;306(1):7-17.
122. Balannik V, Lamb RA, Pinto LH. The oligomeric state of the active BM2 ion channel protein of influenza B virus. *The Journal of biological chemistry*. 2008;283(8):4895-904. Epub 2007/12/13. PubMed PMID: 18073201.

123. Hongo S, Sugawara K, Muraki Y, Kitame F, Nakamura K. Characterization of a second protein (CM2) encoded by RNA segment 6 of influenza C virus. *Journal of virology*. 1997;71(4):2786-92. Epub 1997/04/01. PubMed PMID: 9060633 PMCID: PMCPMC191402.
124. Pekosz A, Lamb RA. The CM2 protein of influenza C virus is an oligomeric integral membrane glycoprotein structurally analogous to influenza A virus M2 and influenza B virus NB proteins. *Virology*. 1997;237(2):439-51. Epub 1997/11/14. PubMed PMID: 9356355.
125. Imai M, Watanabe S, Ninomiya A, Obuchi M, Odagiri T. Influenza B virus BM2 protein is a crucial component for incorporation of viral ribonucleoprotein complex into virions during virus assembly. *Journal of virology*. 2004;78(20):11007-15. Epub 2004/09/29. PubMed PMID: 15452221 PMCID: PMCPMC521833.
126. Furukawa T, Muraki Y, Noda T, Takashita E, Sho R, Sugawara K, Matsuzaki Y, Shimotai Y, Hongo S. Role of the CM2 protein in the influenza C virus replication cycle. *Journal of virology*. 2011;85(3):1322-9. Epub 2010/11/26. PubMed PMID: 21106743 PMCID: PMCPMC3020500.
127. Stewart SM, Pekosz A. The influenza C virus CM2 protein can alter intracellular pH, and its transmembrane domain can substitute for that of the influenza A virus M2 protein and support infectious virus production. *Journal of virology*. 2012;86(2):1277-81. Epub 2011/09/16. PubMed PMID: 21917958 PMCID: PMCPMC3255851.

128. Wanitchang A, Wongthida P, Jongkaewwattana A. Influenza B virus M2 protein can functionally replace its influenza A virus counterpart in promoting virus replication. *Virology*. 2016;498:99-108. Epub 2016/08/28. PubMed PMID: 27567258.
129. Zhang H, Yu H, Wang J, Zhang M, Wang X, Ahmad W, Duan M, Guan Z. The BM2 protein of influenza B virus interacts with p53 and inhibits its transcriptional and apoptotic activities. *Molecular and cellular biochemistry*. 2015;403(1-2):187-97. Epub 2015/02/12. PubMed PMID: 25670017.
130. Dazza MC, Ekwalinga M, Nende M, Shamamba KB, Bitshi P, Paraskevis D, Saragosti S. Characterization of a novel vpu-harboring simian immunodeficiency virus from a Dent's Mona monkey (*Cercopithecus mona denti*). *Journal of virology*. 2005;79(13):8560-71. Epub 2005/06/16. PubMed PMID: 15956597 PMCID: PMC1143702.
131. Andrew A, Strebel K. HIV-1 Vpu targets cell surface markers CD4 and BST-2 through distinct mechanisms. *Molecular aspects of medicine*. 2010;31(5):407-17. Epub 2010/09/23. PubMed PMID: 20858517 PMCID: PMC2967615.
132. Coadou G, Evrard-Todeschi N, Gharbi-Benarous J, Benarous R, Girault JP. HIV-1 encoded virus protein U (Vpu) solution structure of the 41-62 hydrophilic region containing the phosphorylated sites Ser52 and Ser56. *International journal of biological macromolecules*. 2002;30(1):23-40. Epub 2002/03/15. PubMed PMID: 11893391.

133. Wray V, Federau T, Henklein P, Klabunde S, Kunert O, Schomburg D, Schubert U. Solution structure of the hydrophilic region of HIV-1 encoded virus protein U (Vpu) by CD and ¹H NMR spectroscopy. *International journal of peptide and protein research*. 1995;45(1):35-43. Epub 1995/01/01. PubMed PMID: 7775007.
134. Greiner T, Bolduan S, Hertel B, Gross C, Hamacher K, Schubert U, Moroni A, Thiel G. Ion Channel Activity of Vpu Proteins Is Conserved throughout Evolution of HIV-1 and SIV. *Viruses*. 2016;8(12). Epub 2016/12/06. PubMed PMID: 27916968 PMCID: PMC5192386.
135. Hsu K, Han J, Shinlapawittayatorn K, Deschenes I, Marban E. Membrane potential depolarization as a triggering mechanism for Vpu-mediated HIV-1 release. *Biophysical journal*. 2010;99(6):1718-25. Epub 2010/09/23. PubMed PMID: 20858415 PMCID: PMC2941015.
136. Hout DR, Gomez ML, Pacyniak E, Gomez LM, Inbody SH, Mulcahy ER, Culley N, Pinson DM, Powers MF, Wong SW, Stephens EB. Scrambling of the amino acids within the transmembrane domain of Vpu results in a simian-human immunodeficiency virus (SHIV_{TM}) that is less pathogenic for pig-tailed macaques. *Virology*. 2005;339(1):56-69. Epub 2005/06/25. PubMed PMID: 15975620.
137. Schubert U, Bour S, Ferrer-Montiel AV, Montal M, Maldarell F, Strebel K. The two biological activities of human immunodeficiency virus type 1 Vpu protein involve two separable structural domains. *Journal of*

virology. 1996;70(2):809-19. Epub 1996/02/01. PubMed PMID: 8551619
PMCID: PMC189883.

138. Hout DR, Gomez ML, Pacyniak E, Gomez LM, Fegley B, Mulcahy ER, Hill MS, Culley N, Pinson DM, Nothnick W, Powers MF, Wong SW, Stephens EB. Substitution of the transmembrane domain of Vpu in simian-human immunodeficiency virus (SHIVKU1bMC33) with that of M2 of influenza A results in a virus that is sensitive to inhibitors of the M2 ion channel and is pathogenic for pig-tailed macaques. *Virology*. 2006;344(2):541-59.

139. Park SH, Mrse AA, Nevzorov AA, Mesleh MF, Oblatt-Montal M, Montal M, Opella SJ. Three-dimensional structure of the channel-forming trans-membrane domain of virus protein "u" (Vpu) from HIV-1. *Journal of molecular biology*. 2003;333(2):409-24. Epub 2003/10/08. PubMed PMID: 14529626.

140. Lu JX, Sharpe S, Ghirlando R, Yau WM, Tycko R. Oligomerization state and supramolecular structure of the HIV-1 Vpu protein transmembrane segment in phospholipid bilayers. *Protein science : a publication of the Protein Society*. 2010;19(10):1877-96. Epub 2010/07/30. PubMed PMID: 20669237 PMCID: PMC2998723.

141. Cordes FS, Tustian AD, Sansom MS, Watts A, Fischer WB. Bundles consisting of extended transmembrane segments of Vpu from HIV-1: computer simulations and conductance measurements. *Biochemistry*. 2002;41(23):7359-65. Epub 2002/06/05. PubMed PMID: 12044168.

142. Lopez CF, Montal M, Blasie JK, Klein ML, Moore PB. Molecular dynamics investigation of membrane-bound bundles of the channel-forming transmembrane domain of viral protein U from the human immunodeficiency virus HIV-1. *Biophysical journal*. 2002;83(3):1259-67. Epub 2002/08/31. PubMed PMID: 12202353 PMCID: PMC1302226.
143. Willey RL, Maldarelli F, Martin MA, Strebel K. Human immunodeficiency virus type 1 Vpu protein induces rapid degradation of CD4. *Journal of virology*. 1992;66(12):7193-200. Epub 1992/12/01. PubMed PMID: 1433512 PMCID: PMC240416.
144. Bour S, Schubert U, Strebel K. The human immunodeficiency virus type 1 Vpu protein specifically binds to the cytoplasmic domain of CD4: implications for the mechanism of degradation. *Journal of virology*. 1995;69(3):1510-20. Epub 1995/03/01. PubMed PMID: 7853484 PMCID: PMC188742.
145. Margottin F, Benichou S, Durand H, Richard V, Liu LX, Gomas E, Benarous R. Interaction between the cytoplasmic domains of HIV-1 Vpu and CD4: role of Vpu residues involved in CD4 interaction and in vitro CD4 degradation. *Virology*. 1996;223(2):381-6. Epub 1996/09/15. PubMed PMID: 8806575.
146. Gonzalez ME. Vpu Protein: The Viroporin Encoded by HIV-1. *Viruses*. 2015;7(8):4352-68. Epub 2015/08/08. PubMed PMID: 26247957 PMCID: PMC4576185.

147. Chen MY, Maldarelli F, Karczewski MK, Willey RL, Strebel K. Human immunodeficiency virus type 1 Vpu protein induces degradation of CD4 in vitro: the cytoplasmic domain of CD4 contributes to Vpu sensitivity. *Journal of virology*. 1993;67(7):3877-84. Epub 1993/07/01. PubMed PMID: 8510209
PMCID: PMCPMC237753.
148. Schubert U, Strebel K. Differential activities of the human immunodeficiency virus type 1-encoded Vpu protein are regulated by phosphorylation and occur in different cellular compartments. *Journal of virology*. 1994;68(4):2260-71. Epub 1994/04/01. PubMed PMID: 8139011
PMCID: PMCPMC236702.
149. Margottin F, Bour SP, Durand H, Selig L, Benichou S, Richard V, Thomas D, Strebel K, Benarous R. A novel human WD protein, h-beta TrCp, that interacts with HIV-1 Vpu connects CD4 to the ER degradation pathway through an F-box motif. *Molecular cell*. 1998;1(4):565-74. Epub 1998/07/14. PubMed PMID: 9660940.
150. Bai C, Sen P, Hofmann K, Ma L, Goebel M, Harper JW, Elledge SJ. SKP1 connects cell cycle regulators to the ubiquitin proteolysis machinery through a novel motif, the F-box. *Cell*. 1996;86(2):263-74. Epub 1996/07/26. PubMed PMID: 8706131.
151. Strebel K, Klimkait T, Martin MA. A novel gene of HIV-1, vpu, and its 16-kilodalton product. *Science (New York, NY)*. 1988;241(4870):1221-3. Epub 1988/09/02. PubMed PMID: 3261888.

152. Terwilliger EF, Cohen EA, Lu YC, Sodroski JG, Haseltine WA. Functional role of human immunodeficiency virus type 1 vpu. *Proceedings of the National Academy of Sciences of the United States of America*. 1989;86(13):5163-7. Epub 1989/07/01. PubMed PMID: 2472639 PMCID: PMC297578.
153. Swiecki M, Omattage NS, Brett TJ. BST-2/tetherin: structural biology, viral antagonism, and immunobiology of a potent host antiviral factor. *Molecular immunology*. 2013;54(2):132-9. Epub 2013/01/01. PubMed PMID: 23274150.
154. Neil SJ. The antiviral activities of tetherin. *Current topics in microbiology and immunology*. 2013;371:67-104. Epub 2013/05/21. PubMed PMID: 23686232.
155. Billcliff PG, Rollason R, Prior I, Owen DM, Gaus K, Banting G. CD317/tetherin is an organiser of membrane microdomains. *J Cell Sci*. 2013;126(Pt 7):1553-64. Epub 2013/02/05. PubMed PMID: 23378022 PMCID: PMC3647434.
156. Roy N, Pacini G, Berlioz-Torrent C, Janvier K. Mechanisms underlying HIV-1 Vpu-mediated viral egress. *Front Microbiol*. 2014;5:177. Epub 2014/05/14. PubMed PMID: 24822052 PMCID: PMC4013480.
157. Van Damme N, Goff D, Katsura C, Jorgenson RL, Mitchell R, Johnson MC, Stephens EB, Guatelli J. The interferon-induced protein BST-2 restricts HIV-1 release and is downregulated from the cell surface by the viral Vpu

protein. *Cell host & microbe*. 2008;3(4):245-52. Epub 2008/03/18. PubMed PMID: 18342597 PMCID: PMC2474773.

158. Neil SJ, Zang T, Bieniasz PD. Tetherin inhibits retrovirus release and is antagonized by HIV-1 Vpu. *Nature*. 2008;451(7177):425-30. Epub 2008/01/18. PubMed PMID: 18200009.

159. Perez-Caballero D, Zang T, Ebrahimi A, McNatt MW, Gregory DA, Johnson MC, Bieniasz PD. Tetherin inhibits HIV-1 release by directly tethering virions to cells. *Cell*. 2009;139(3):499-511. Epub 2009/11/03. PubMed PMID: 19879838 PMCID: PMC2844890.

160. Hu S, Yin L, Mei S, Li J, Xu F, Sun H, Liu X, Cen S, Liang C, Li A, Guo F. BST-2 restricts IAV release and is countered by the viral M2 protein. *The Biochemical journal*. 2017;474(5):715-30. Epub 2017/01/15. PubMed PMID: 28087685.

161. Pan XB, Han JC, Cong X, Wei L. BST2/tetherin inhibits dengue virus release from human hepatoma cells. *PLoS One*. 2012;7(12):e51033. Epub 2012/12/14. PubMed PMID: 23236425 PMCID: PMC3517589.

162. Rollason R, Korolchuk V, Hamilton C, Schu P, Banting G. Clathrin-mediated endocytosis of a lipid-raft-associated protein is mediated through a dual tyrosine motif. *J Cell Sci*. 2007;120(Pt 21):3850-8. Epub 2007/10/18. PubMed PMID: 17940069.

163. Masuyama N, Kuronita T, Tanaka R, Muto T, Hirota Y, Takigawa A, Fujita H, Aso Y, Amano J, Tanaka Y. HM1.24 is internalized from lipid rafts

- by clathrin-mediated endocytosis through interaction with alpha-adaptin. *The Journal of biological chemistry*. 2009;284(23):15927-41. Epub 2009/04/11. PubMed PMID: 19359243 PMCID: PMC2708888.
164. Vigan R, Neil SJ. Determinants of tetherin antagonism in the transmembrane domain of the human immunodeficiency virus type 1 Vpu protein. *Journal of virology*. 2010;84(24):12958-70. Epub 2010/10/12. PubMed PMID: 20926557 PMCID: PMC3004320.
165. Kobayashi T, Ode H, Yoshida T, Sato K, Gee P, Yamamoto SP, Ebina H, Strebel K, Sato H, Koyanagi Y. Identification of amino acids in the human tetherin transmembrane domain responsible for HIV-1 Vpu interaction and susceptibility. *Journal of virology*. 2011;85(2):932-45. Epub 2010/11/12. PubMed PMID: 21068238 PMCID: PMC3020002.
166. Skasko M, Wang Y, Tian Y, Tokarev A, Munguia J, Ruiz A, Stephens EB, Opella SJ, Guatelli J. HIV-1 Vpu protein antagonizes innate restriction factor BST-2 via lipid-embedded helix-helix interactions. *The Journal of biological chemistry*. 2012;287(1):58-67. Epub 2011/11/11. PubMed PMID: 22072710 PMCID: PMC3249111.
167. McNatt MW, Zang T, Bieniasz PD. Vpu binds directly to tetherin and displaces it from nascent virions. *PLoS pathogens*. 2013;9(4):e1003299. Epub 2013/05/02. PubMed PMID: 23633949 PMCID: PMC3635990.
168. Pickering S, Hue S, Kim EY, Reddy S, Wolinsky SM, Neil SJ. Preservation of tetherin and CD4 counter-activities in circulating Vpu alleles

despite extensive sequence variation within HIV-1 infected individuals. PLoS pathogens. 2014;10(1):e1003895. Epub 2014/01/28. PubMed PMID: 24465210 PMCID: PMC3900648.

169. Mitchell RS, Katsura C, Skasko MA, Fitzpatrick K, Lau D, Ruiz A, Stephens EB, Margottin-Goguet F, Benarous R, Guatelli JC. Vpu antagonizes BST-2-mediated restriction of HIV-1 release via beta-TrCP and endo-lysosomal trafficking. PLoS pathogens. 2009;5(5):e1000450. Epub 2009/05/30. PubMed PMID: 19478868 PMCID: PMC2679223.

170. Dube M, Paquay C, Roy BB, Bego MG, Mercier J, Cohen EA. HIV-1 Vpu antagonizes BST-2 by interfering mainly with the trafficking of newly synthesized BST-2 to the cell surface. Traffic (Copenhagen, Denmark). 2011;12(12):1714-29. Epub 2011/09/10. PubMed PMID: 21902775 PMCID: PMC3955191.

171. Lau D, Kwan W, Guatelli J. Role of the endocytic pathway in the counteraction of BST-2 by human lentiviral pathogens. Journal of virology. 2011;85(19):9834-46. Epub 2011/08/05. PubMed PMID: 21813615 PMCID: PMC3196438.

172. Schmidt S, Fritz JV, Bitzegeio J, Fackler OT, Keppler OT. HIV-1 Vpu blocks recycling and biosynthetic transport of the intrinsic immunity factor CD317/tetherin to overcome the virion release restriction. MBio. 2011;2(3):e00036-11. Epub 2011/05/26. PubMed PMID: 21610122 PMCID: PMC3101777.

173. Caillet M, Janvier K, Pelchen-Matthews A, Delcroix-Genete D, Camus G, Marsh M, Berlioz-Torrent C. Rab7A is required for efficient production of infectious HIV-1. *PLoS pathogens*. 2011;7(11):e1002347. Epub 2011/11/11. PubMed PMID: 22072966 PMCID: PMC3207927.
174. Janvier K, Pelchen-Matthews A, Renaud JB, Caillet M, Marsh M, Berlioz-Torrent C. The ESCRT-0 component HRS is required for HIV-1 Vpu-mediated BST-2/tetherin down-regulation. *PLoS pathogens*. 2011;7(2):e1001265. Epub 2011/02/10. PubMed PMID: 21304933 PMCID: PMC3033365.
175. Janvier K, Roy N, Berlioz-Torrent C. Role of the endosomal ESCRT machinery in HIV-1 Vpu-induced down-regulation of BST2/tetherin. *Current HIV research*. 2012;10(4):315-20. Epub 2012/04/25. PubMed PMID: 22524180.
176. Madan V, Bartenschlager R. Structural and Functional Properties of the Hepatitis C Virus p7 Viroporin. *Viruses*. 2015;7(8):4461-81. Epub 2015/08/11. PubMed PMID: 26258788 PMCID: PMC4576187.
177. Luik P, Chew C, Aittoniemi J, Chang J, Wentworth P, Jr., Dwek RA, Biggin PC, Venien-Bryan C, Zitzmann N. The 3-dimensional structure of a hepatitis C virus p7 ion channel by electron microscopy. *Proceedings of the National Academy of Sciences of the United States of America*. 2009;106(31):12712-6. Epub 2009/07/11. PubMed PMID: 19590017 PMCID: PMC2722341.

178. Carrère-Kremer S, Montpellier-Pala C, Cocquerel L, Wychowski C, Penin F, Dubuisson J. Subcellular Localization and Topology of the p7 Polypeptide of Hepatitis C Virus. *Journal of virology*. 2002;76(8):3720-30.
179. Patargias G, Zitzmann N, Dwek R, Fischer WB. Protein-Protein Interactions: Modeling the Hepatitis C Virus Ion Channel p7. *Journal of Medicinal Chemistry*. 2006;49(2):648-55.
180. Steinmann E, Pietschmann T. Hepatitis C virus p7-a viroporin crucial for virus assembly and an emerging target for antiviral therapy. *Viruses*. 2010;2(9):2078-95. Epub 2011/10/14. PubMed PMID: 21994720 PMCID: PMC3185753.
181. Montserret R, Saint N, Vanbelle C, Salvay AG, Simorre JP, Ebel C, Sapay N, Renisio JG, Bockmann A, Steinmann E, Pietschmann T, Dubuisson J, Chipot C, Penin F. NMR structure and ion channel activity of the p7 protein from hepatitis C virus. *The Journal of biological chemistry*. 2010;285(41):31446-61. Epub 2010/07/30. PubMed PMID: 20667830 PMCID: PMC2951219.
182. Griffin S, Stgelais C, Owsianka AM, Patel AH, Rowlands D, Harris M. Genotype-dependent sensitivity of hepatitis C virus to inhibitors of the p7 ion channel. *Hepatology (Baltimore, Md)*. 2008;48(6):1779-90. Epub 2008/10/02. PubMed PMID: 18828153.
183. Griffin SD, Beales LP, Clarke DS, Worsfold O, Evans SD, Jaeger J, Harris MP, Rowlands DJ. The p7 protein of hepatitis C virus forms an ion

- channel that is blocked by the antiviral drug, Amantadine. *FEBS Lett.* 2003;535(1-3):34-8. Epub 2003/02/01. PubMed PMID: 12560074.
184. Pavlovic D, Neville DC, Argaud O, Blumberg B, Dwek RA, Fischer WB, Zitzmann N. The hepatitis C virus p7 protein forms an ion channel that is inhibited by long-alkyl-chain iminosugar derivatives. *Proceedings of the National Academy of Sciences of the United States of America.* 2003;100(10):6104-8. Epub 2003/04/30. PubMed PMID: 12719519 PMCID: PMC156333.
185. Clarke D, Griffin S, Beales L, Gelais CS, Burgess S, Harris M, Rowlands D. Evidence for the formation of a heptameric ion channel complex by the hepatitis C virus p7 protein in vitro. *The Journal of biological chemistry.* 2006;281(48):37057-68. Epub 2006/10/13. PubMed PMID: 17032656.
186. OuYang B, Xie S, Berardi MJ, Zhao X, Dev J, Yu W, Sun B, Chou JJ. Unusual architecture of the p7 channel from hepatitis C virus. *Nature.* 2013;498(7455):521-5. Epub 2013/06/07. PubMed PMID: 23739335 PMCID: PMC3725310.
187. StGelais C, Tuthill TJ, Clarke DS, Rowlands DJ, Harris M, Griffin S. Inhibition of hepatitis C virus p7 membrane channels in a liposome-based assay system. *Antiviral research.* 2007;76(1):48-58. Epub 2007/06/19. PubMed PMID: 17574688.

188. Atoom AM, Jones DM, Russell RS. Evidence suggesting that HCV p7 protects E2 glycoprotein from premature degradation during virus production. *Virus research*. 2013;176(1-2):199-210. Epub 2013/07/03. PubMed PMID: 23816605.
189. Bentham MJ, Foster TL, McCormick C, Griffin S. Mutations in hepatitis C virus p7 reduce both the egress and infectivity of assembled particles via impaired proton channel function. *The Journal of general virology*. 2013;94(Pt 10):2236-48. Epub 2013/08/03. PubMed PMID: 23907396.
190. Farag NS, Breiting U, El-Azizi M, Breiting HG. The p7 viroporin of the hepatitis C virus contributes to liver inflammation by stimulating production of Interleukin-1beta. *Biochimica et biophysica acta*. 2017;1863(3):712-20. Epub 2016/12/17. PubMed PMID: 27979709.
191. Vieyres G, Brohm C, Friesland M, Gentzsch J, Wolk B, Roingeard P, Steinmann E, Pietschmann T. Subcellular localization and function of an epitope-tagged p7 viroporin in hepatitis C virus-producing cells. *Journal of virology*. 2013;87(3):1664-78. Epub 2012/11/24. PubMed PMID: 23175364 PMCID: PMC3554161.
192. Jirasko V, Montserret R, Appel N, Janvier A, Eustachi L, Brohm C, Steinmann E, Pietschmann T, Penin F, Bartenschlager R. Structural and functional characterization of nonstructural protein 2 for its role in hepatitis C virus assembly. *The Journal of biological chemistry*. 2008;283(42):28546-62. Epub 2008/07/23. PubMed PMID: 18644781 PMCID: PMC2661407.

193. Jirasko V, Montserret R, Lee JY, Gouttenoire J, Moradpour D, Penin F, Bartenschlager R. Structural and functional studies of nonstructural protein 2 of the hepatitis C virus reveal its key role as organizer of virion assembly. *PLoS pathogens*. 2010;6(12):e1001233. Epub 2010/12/29. PubMed PMID: 21187906 PMCID: PMC3002993.
194. Ma Y, Anantpadma M, Timpe JM, Shanmugam S, Singh SM, Lemon SM, Yi M. Hepatitis C virus NS2 protein serves as a scaffold for virus assembly by interacting with both structural and nonstructural proteins. *Journal of virology*. 2011;85(1):86-97. Epub 2010/10/22. PubMed PMID: 20962101 PMCID: PMC3014171.
195. Popescu CI, Callens N, Trinel D, Roingeard P, Moradpour D, Descamps V, Duverlie G, Penin F, Heliot L, Rouille Y, Dubuisson J. NS2 protein of hepatitis C virus interacts with structural and non-structural proteins towards virus assembly. *PLoS pathogens*. 2011;7(2):e1001278. Epub 2011/02/25. PubMed PMID: 21347350 PMCID: PMC3037360.
196. Stapleford KA, Lindenbach BD. Hepatitis C virus NS2 coordinates virus particle assembly through physical interactions with the E1-E2 glycoprotein and NS3-NS4A enzyme complexes. *Journal of virology*. 2011;85(4):1706-17. Epub 2010/12/15. PubMed PMID: 21147927 PMCID: PMC3028914.
197. Tedbury P, Welbourn S, Pause A, King B, Griffin S, Harris M. The subcellular localization of the hepatitis C virus non-structural protein NS2 is

regulated by an ion channel-independent function of the p7 protein. The Journal of general virology. 2011;92(Pt 4):819-30. Epub 2010/12/24. PubMed PMID: 21177929 PMCID: PMC3133701.

198. Boson B, Granio O, Bartenschlager R, Cosset FL. A concerted action of hepatitis C virus p7 and nonstructural protein 2 regulates core localization at the endoplasmic reticulum and virus assembly. PLoS pathogens. 2011;7(7):e1002144. Epub 2011/08/05. PubMed PMID: 21814513 PMCID: PMC3141040.

199. Lee GY, Lee S, Lee HR, Yoo YD. Hepatitis C virus p7 mediates membrane-to-membrane adhesion. Biochimica et biophysica acta. 2016;1861(9 Pt A):1096-101. Epub 2016/06/21. PubMed PMID: 27320856.

200. Gentsch J, Brohm C, Steinmann E, Friesland M, Menzel N, Vieyres G, Perin PM, Frentzen A, Kaderali L, Pietschmann T. hepatitis c Virus p7 is critical for capsid assembly and envelopment. PLoS pathogens. 2013;9(5):e1003355. Epub 2013/05/10. PubMed PMID: 23658526 PMCID: PMC3642076.

201. Ruch TR, Machamer CE. The coronavirus E protein: assembly and beyond. Viruses. 2012;4(3):363-82. Epub 2012/05/17. PubMed PMID: 22590676 PMCID: PMC3347032.

202. Torres J, Wang J, Parthasarathy K, Liu DX. The transmembrane oligomers of coronavirus protein E. Biophysical journal. 2005;88(2):1283-90. Epub 2005/02/17. PubMed PMID: 15713601 PMCID: PMC1305130.

203. Torres J, Maheswari U, Parthasarathy K, Ng L, Liu DX, Gong X. Conductance and amantadine binding of a pore formed by a lysine-flanked transmembrane domain of SARS coronavirus envelope protein. *Protein science : a publication of the Protein Society*. 2007;16(9):2065-71. Epub 2007/09/04. PubMed PMID: 17766393 PMCID: PMC2206980.
204. Parthasarathy K, Ng L, Lin X, Liu DX, Pervushin K, Gong X, Torres J. Structural flexibility of the pentameric SARS coronavirus envelope protein ion channel. *Biophysical journal*. 2008;95(6):L39-41. Epub 2008/07/29. PubMed PMID: 18658207 PMCID: PMC2527252.
205. Pervushin K, Tan E, Parthasarathy K, Lin X, Jiang FL, Yu D, Vararattanavech A, Soong TW, Liu DX, Torres J. Structure and inhibition of the SARS coronavirus envelope protein ion channel. *PLoS pathogens*. 2009;5(7):e1000511. Epub 2009/07/14. PubMed PMID: 19593379 PMCID: PMC2702000.
206. Yuan Q, Liao Y, Torres J, Tam JP, Liu DX. Biochemical evidence for the presence of mixed membrane topologies of the severe acute respiratory syndrome coronavirus envelope protein expressed in mammalian cells. *FEBS Lett*. 2006;580(13):3192-200. Epub 2006/05/11. PubMed PMID: 16684538.
207. Maeda J, Repass JF, Maeda A, Makino S. Membrane topology of coronavirus E protein. *Virology*. 2001;281(2):163-9. Epub 2001/03/30. PubMed PMID: 11277690.

208. Liao Y, Yuan Q, Torres J, Tam JP, Liu DX. Biochemical and functional characterization of the membrane association and membrane permeabilizing activity of the severe acute respiratory syndrome coronavirus envelope protein. *Virology*. 2006;349(2):264-75. Epub 2006/03/02. PubMed PMID: 16507314.
209. Corse E, Machamer CE. The cytoplasmic tail of infectious bronchitis virus E protein directs Golgi targeting. *Journal of virology*. 2002;76(3):1273-84. Epub 2002/01/05. PubMed PMID: 11773403 PMCID: PMC135861.
210. Boscarino JA, Logan HL, Lacny JJ, Gallagher TM. Envelope protein palmitoylations are crucial for murine coronavirus assembly. *Journal of virology*. 2008;82(6):2989-99. Epub 2008/01/11. PubMed PMID: 18184706 PMCID: PMC2258982.
211. Lopez LA, Riffle AJ, Pike SL, Gardner D, Hogue BG. Importance of conserved cysteine residues in the coronavirus envelope protein. *Journal of virology*. 2008;82(6):3000-10. Epub 2008/01/11. PubMed PMID: 18184703 PMCID: PMC2258990.
212. Wilson L, Gage P, Ewart G. Hexamethylene amiloride blocks E protein ion channels and inhibits coronavirus replication. *Virology*. 2006;353(2):294-306. Epub 2006/07/04. PubMed PMID: 16815524.
213. Wilson L, McKinlay C, Gage P, Ewart G. SARS coronavirus E protein forms cation-selective ion channels. *Virology*. 2004;330(1):322-31. Epub 2004/11/06. PubMed PMID: 15527857.

214. Ruch TR, Machamer CE. The hydrophobic domain of infectious bronchitis virus E protein alters the host secretory pathway and is important for release of infectious virus. *Journal of virology*. 2011;85(2):675-85. Epub 2010/11/05. PubMed PMID: 21047962 PMCID: PMC3020032.
215. Ye Y, Hogue BG. Role of the coronavirus E viroporin protein transmembrane domain in virus assembly. *Journal of virology*. 2007;81(7):3597-607. Epub 2007/01/19. PubMed PMID: 17229680 PMCID: PMC1866030.
216. Tooze J, Tooze S, Warren G. Replication of coronavirus MHV-A59 in sac- cells: determination of the first site of budding of progeny virions. *Eur J Cell Biol*. 1984;33(2):281-93. Epub 1984/03/01. PubMed PMID: 6325194.
217. Klumperman J, Locker JK, Meijer A, Horzinek MC, Geuze HJ, Rottier PJ. Coronavirus M proteins accumulate in the Golgi complex beyond the site of virion budding. *Journal of virology*. 1994;68(10):6523-34. Epub 1994/10/01. PubMed PMID: 8083990 PMCID: PMC237073.
218. Hogue BG, Machamer CE. Coronavirus Structural Proteins and Virus Assembly. *Nidoviruses: American Society of Microbiology*; 2008.
219. Vennema H, Godeke GJ, Rossen JW, Voorhout WF, Horzinek MC, Opstelten DJ, Rottier PJ. Nucleocapsid-independent assembly of coronavirus-like particles by co-expression of viral envelope protein genes. *The EMBO journal*. 1996;15(8):2020-8. Epub 1996/04/15. PubMed PMID: 8617249 PMCID: PMC450121.

220. Corse E, Machamer CE. Infectious bronchitis virus E protein is targeted to the Golgi complex and directs release of virus-like particles. *Journal of virology*. 2000;74(9):4319-26. Epub 2001/02/07. PubMed PMID: 10756047 PMCID: PMCPMC111949.
221. Baudoux P, Carrat C, Besnardeau L, Charley B, Laude H. Coronavirus pseudoparticles formed with recombinant M and E proteins induce alpha interferon synthesis by leukocytes. *Journal of virology*. 1998;72(11):8636-43. Epub 1998/10/10. PubMed PMID: 9765403 PMCID: PMCPMC110275.
222. Fischer F, Stegen CF, Masters PS, Samsonoff WA. Analysis of constructed E gene mutants of mouse hepatitis virus confirms a pivotal role for E protein in coronavirus assembly. *Journal of virology*. 1998;72(10):7885-94. Epub 1998/09/12. PubMed PMID: 9733825 PMCID: PMCPMC110113.
223. Kuo L, Masters PS. The small envelope protein E is not essential for murine coronavirus replication. *Journal of virology*. 2003;77(8):4597-608. Epub 2003/03/29. PubMed PMID: 12663766 PMCID: PMCPMC152126.
224. DeDiego ML, Alvarez E, Almazan F, Rejas MT, Lamirande E, Roberts A, Shieh WJ, Zaki SR, Subbarao K, Enjuanes L. A severe acute respiratory syndrome coronavirus that lacks the E gene is attenuated in vitro and in vivo. *Journal of virology*. 2007;81(4):1701-13. Epub 2006/11/17. PubMed PMID: 17108030 PMCID: PMCPMC1797558.
225. Ortego J, Ceriani JE, Patino C, Plana J, Enjuanes L. Absence of E protein arrests transmissible gastroenteritis coronavirus maturation in the

secretory pathway. *Virology*. 2007;368(2):296-308. Epub 2007/08/19. PubMed PMID: 17692883.

226. Teoh KT, Siu YL, Chan WL, Schluter MA, Liu CJ, Peiris JS, Bruzzone R, Margolis B, Nal B. The SARS coronavirus E protein interacts with PALS1 and alters tight junction formation and epithelial morphogenesis. *Mol Biol Cell*. 2010;21(22):3838-52. Epub 2010/09/24. PubMed PMID: 20861307
PMCID: PMC2982091.

227. Ye F, Zhang M. Structures and target recognition modes of PDZ domains: recurring themes and emerging pictures. *The Biochemical journal*. 2013;455(1):1-14. Epub 2013/09/14. PubMed PMID: 24028161.

228. Lavi E, Wang Q, Weiss SR, Gonatas NK. Syncytia formation induced by coronavirus infection is associated with fragmentation and rearrangement of the Golgi apparatus. *Virology*. 1996;221(2):325-34. Epub 1996/07/15. PubMed PMID: 8661443.

229. Ulasli M, Verheije MH, de Haan CA, Reggiori F. Qualitative and quantitative ultrastructural analysis of the membrane rearrangements induced by coronavirus. *Cellular microbiology*. 2010;12(6):844-61. Epub 2010/01/22. PubMed PMID: 20088951.

230. Bonfanti L, Mironov AA, Jr., Martinez-Menarguez JA, Martella O, Fusella A, Baldassarre M, Buccione R, Geuze HJ, Mironov AA, Luini A. Procollagen traverses the Golgi stack without leaving the lumen of cisternae:

- evidence for cisternal maturation. *Cell*. 1998;95(7):993-1003. Epub 1999/01/06. PubMed PMID: 9875853.
231. Mironov AA, Beznoussenko GV, Nicoziani P, Martella O, Trucco A, Kweon HS, Di Giandomenico D, Polishchuk RS, Fusella A, Lupetti P, Berger EG, Geerts WJ, Koster AJ, Burger KN, Luini A. Small cargo proteins and large aggregates can traverse the Golgi by a common mechanism without leaving the lumen of cisternae. *The Journal of cell biology*. 2001;155(7):1225-38. Epub 2002/01/05. PubMed PMID: 11756473 PMCID: PMC2199327.
232. Wilson WH, Van Etten JL, Allen MJ. The Phycodnaviridae: the story of how tiny giants rule the world. *Current topics in microbiology and immunology*. 2009;328:1-42. Epub 2009/02/17. PubMed PMID: 19216434 PMCID: PMC2908299.
233. Van Etten JL. Unusual life style of giant chlorella viruses. *Annual review of genetics*. 2003;37:153-95. Epub 2003/11/18. PubMed PMID: 14616059.
234. Gazzarrini S, Severino M, Lombardi M, Morandi M, DiFrancesco D, Van Etten JL, Thiel G, Moroni A. The viral potassium channel Kcv: structural and functional features. *FEBS Letters*. 2003;552(1):12-6.
235. Moroni A, Viscomi C, Sangiorgio V, Pagliuca C, Meckel T, Horvath F, Gazzarrini S, Valbuzzi P, Van Etten JL, DiFrancesco D, Thiel G. The short N-terminus is required for functional expression of the virus-encoded

- miniature K(+) channel Kcv. FEBS Lett. 2002;530(1-3):65-9. Epub 2002/10/22. PubMed PMID: 12387867.
236. Gazzarrini S, Kang M, Abenavoli A, Romani G, Olivari C, Gaslini D, Ferrara G, van Etten JL, Kreim M, Kast SM, Thiel G, Moroni A. Chlorella virus ATCV-1 encodes a functional potassium channel of 82 amino acids. The Biochemical journal. 2009;420(2):295-303. Epub 2009/03/10. PubMed PMID: 19267691 PMCID: PMCPMC2903877.
237. Pagliuca C, Goetze TA, Wagner R, Thiel G, Moroni A, Parcej D. Molecular properties of Kcv, a virus encoded K⁺ channel. Biochemistry. 2007;46(4):1079-90. Epub 2007/01/24. PubMed PMID: 17240991.
238. Greiner T, Frohns F, Kang M, Van Etten JL, Kasmann A, Moroni A, Hertel B, Thiel G. Chlorella viruses prevent multiple infections by depolarizing the host membrane. The Journal of general virology. 2009;90(Pt 8):2033-9. Epub 2009/04/24. PubMed PMID: 19386783 PMCID: PMCPMC2887576.
239. Hyser JM, Utama B, Crawford SE, Estes MK. Genetic divergence of rotavirus nonstructural protein 4 results in distinct serogroup-specific viroporin activity and intracellular punctate structure morphologies. Journal of virology. 2012;86(9):4921-34. Epub 2012/02/24. PubMed PMID: 22357281 PMCID: PMCPMC3347366.
240. Pham T, Perry JL, Dosey TL, Delcour AH, Hyser JM. The Rotavirus NSP4 Viroporin Domain is a Calcium-conducting Ion Channel. Scientific

reports. 2017;7:43487. Epub 2017/03/04. PubMed PMID: 28256607 PMCID: PMCPMC5335360.

241. Hyser JM, Utama B, Crawford SE, Broughman JR, Estes MK.

Activation of the Endoplasmic Reticulum Calcium Sensor STIM1 and Store-Operated Calcium Entry by Rotavirus Requires NSP4 Viroporin Activity.

Journal of virology. 2013;87(24):13579-88.

242. Tian P, Ball JM, Zeng CQ, Estes MK. Rotavirus protein expression is important for virus assembly and pathogenesis. Archives of virology Supplementum. 1996;12:69-77. Epub 1996/01/01. PubMed PMID: 9015103.

243. Estes MK, Morris AP. A viral enterotoxin. A new mechanism of virus-

induced pathogenesis. Advances in experimental medicine and biology. 1999;473:73-82. Epub 2000/02/05. PubMed PMID: 10659345.

244. Ball JM, Mitchell DM, Gibbons TF, Parr RD. Rotavirus NSP4: a

multifunctional viral enterotoxin. Viral immunology. 2005;18(1):27-40. Epub 2005/04/02. PubMed PMID: 15802952.

245. Crawford SE, Hyser JM, Utama B, Estes MK. Autophagy hijacked

through viroporin-activated calcium/calmodulin-dependent kinase kinase- β signaling is required for rotavirus replication. Proceedings of the National

Academy of Sciences. 2012;109(50):E3405-E13.

246. Volchkova VA, Klenk HD, Volchkov VE. Delta-peptide is the carboxy-terminal cleavage fragment of the nonstructural small glycoprotein sGP of

Ebola virus. *Virology*. 1999;265(1):164-71. Epub 1999/12/22. PubMed PMID: 10603327.

247. Radoshitzky SR, Warfield KL, Chi X, Dong L, Kota K, Bradfute SB, Gearhart JD, Retterer C, Kranzusch PJ, Misasi JN, Hogenbirk MA, Wahl-Jensen V, Volchkov VE, Cunningham JM, Jahrling PB, Aman MJ, Bavari S, Farzan M, Kuhn JH. Ebolavirus delta-peptide immunoadhesins inhibit marburgvirus and ebolavirus cell entry. *Journal of virology*. 2011;85(17):8502-13. Epub 2011/06/24. PubMed PMID: 21697477 PMCID: PMC3165852.

248. Gallaher WR, Garry RF. Modeling of the Ebola virus delta peptide reveals a potential lytic sequence motif. *Viruses*. 2015;7(1):285-305. Epub 2015/01/23. PubMed PMID: 25609303 PMCID: PMC4306839.

249. He J, Melnik LI, Komin A, Wiedman G, Fuselier T, Morris CF, Starr CG, Searson PC, Gallaher WR, Hristova K, Garry RF, Wimley WC. Ebola Virus Delta Peptide is a Viroporin. *Journal of virology*. 2017.

250. Ding Q, Heller B, Capuccino JM, Song B, Nimgaonkar I, Hrebikova G, Contreras JE, Ploss A. Hepatitis E virus ORF3 is a functional ion channel required for release of infectious particles. *Proceedings of the National Academy of Sciences of the United States of America*. 2017;114(5):1147-52. Epub 2017/01/18. PubMed PMID: 28096411 PMCID: PMC5293053.

251. Graff J, Nguyen H, Yu C, Elkins WR, St Claire M, Purcell RH, Emerson SU. The open reading frame 3 gene of hepatitis E virus contains a

cis-reactive element and encodes a protein required for infection of macaques. *Journal of virology*. 2005;79(11):6680-9. Epub 2005/05/14. PubMed PMID: 15890906 PMCID: PMCPMC1112134.

252. Emerson SU, Nguyen HT, Torian U, Burke D, Engle R, Purcell RH. Release of genotype 1 hepatitis E virus from cultured hepatoma and polarized intestinal cells depends on open reading frame 3 protein and requires an intact PXXP motif. *Journal of virology*. 2010;84(18):9059-69. Epub 2010/07/09. PubMed PMID: 20610720 PMCID: PMCPMC2937629.

253. Kenney SP, Pudupakam RS, Huang YW, Pierson FW, LeRoith T, Meng XJ. The PSAP motif within the ORF3 protein of an avian strain of the hepatitis E virus is not critical for viral infectivity in vivo but plays a role in virus release. *Journal of virology*. 2012;86(10):5637-46. Epub 2012/03/23. PubMed PMID: 22438540 PMCID: PMCPMC3347299.

254. Nagashima S, Takahashi M, Jirintai, Tanaka T, Yamada K, Nishizawa T, Okamoto H. A PSAP motif in the ORF3 protein of hepatitis E virus is necessary for virion release from infected cells. *The Journal of general virology*. 2011;92(Pt 2):269-78. Epub 2010/11/12. PubMed PMID: 21068219.

255. Yamada K, Takahashi M, Hoshino Y, Takahashi H, Ichiyama K, Nagashima S, Tanaka T, Okamoto H. ORF3 protein of hepatitis E virus is essential for virion release from infected cells. *The Journal of general virology*. 2009;90(Pt 8):1880-91. Epub 2009/04/03. PubMed PMID: 19339479.

256. Lei Q, Li L, Cai J, Huang W, Qin B, Zhang S. ORF3 of Hepatitis E Virus Inhibits the Expression of Proinflammatory Cytokines and Chemotactic Factors in LPS-Stimulated Human PMA-THP1 Cells by Inhibiting NF-kappaB Pathway. *Viral immunology*. 2016;29(2):105-11. Epub 2016/01/16. PubMed PMID: 26771290.
257. Welch WJ, Sefton BM. Characterization of a small, nonstructural viral polypeptide present late during infection of BHK cells by Semliki Forest virus. *Journal of virology*. 1980;33(1):230-7. Epub 1980/01/01. PubMed PMID: 7365868 PMCID: PMCPMC288539.
258. Sanz MA, Perez L, Carrasco L. Semliki Forest virus 6K protein modifies membrane permeability after inducible expression in *Escherichia coli* cells. *The Journal of biological chemistry*. 1994;269(16):12106-10. Epub 1994/04/22. PubMed PMID: 8163515.
259. Melton JV, Ewart GD, Weir RC, Board PG, Lee E, Gage PW. Alphavirus 6K proteins form ion channels. *The Journal of biological chemistry*. 2002;277(49):46923-31. Epub 2002/09/14. PubMed PMID: 12228229.
260. Gaedigk-Nitschko K, Ding MX, Levy MA, Schlesinger MJ. Site-directed mutations in the Sindbis virus 6K protein reveal sites for fatty acylation and the underacylated protein affects virus release and virion structure. *Virology*. 1990;175(1):282-91. Epub 1990/03/01. PubMed PMID: 2309447.

261. Ivanova L, Lustig S, Schlesinger MJ. A pseudo-revertant of a Sindbis virus 6K protein mutant, which corrects for aberrant particle formation, contains two new mutations that map to the ectodomain of the E2 glycoprotein. *Virology*. 1995;206(2):1027-34. Epub 1995/02/01. PubMed PMID: 7856077.
262. Liljestrom P, Lusa S, Huylebroeck D, Garoff H. In vitro mutagenesis of a full-length cDNA clone of Semliki Forest virus: the small 6,000-molecular-weight membrane protein modulates virus release. *Journal of virology*. 1991;65(8):4107-13. Epub 1991/08/01. PubMed PMID: 2072446 PMCID: PMC248843.
263. Loewy A, Smyth J, von Bonsdorff CH, Liljestrom P, Schlesinger MJ. The 6-kilodalton membrane protein of Semliki Forest virus is involved in the budding process. *Journal of virology*. 1995;69(1):469-75. Epub 1995/01/01. PubMed PMID: 7983743 PMCID: PMC188595.
264. Sanz MA, Madan V, Nieva JL, Carrasco L. The Alphavirus 6K Protein. In: Fischer WB, editor. *Viral Membrane Proteins: Structure, Function, and Drug Design*. Boston, MA: Springer US; 2005. p. 233-44.
265. Snyder JE, Kulcsar KA, Schultz KLW, Riley CP, Neary JT, Marr S, Jose J, Griffin DE, Kuhn RJ. Functional Characterization of the Alphavirus TF Protein. *Journal of virology*. 2013;87(15):8511-23.
266. Karron RA, Buonagurio DA, Georgiu AF, Whitehead SS, Adamus JE, Clements-Mann ML, Harris DO, Randolph VB, Udem SA, Murphy BR, Sidhu

MS. Respiratory syncytial virus (RSV) SH and G proteins are not essential for viral replication in vitro: clinical evaluation and molecular characterization of a cold-passaged, attenuated RSV subgroup B mutant. Proceedings of the National Academy of Sciences of the United States of America. 1997;94(25):13961-6. Epub 1998/02/12. PubMed PMID: 9391135 PMCID: PMCPMC28415.

267. Techaarpornkul S, Barretto N, Peeples ME. Functional analysis of recombinant respiratory syncytial virus deletion mutants lacking the small hydrophobic and/or attachment glycoprotein gene. Journal of virology. 2001;75(15):6825-34. Epub 2001/07/04. PubMed PMID: 11435561 PMCID: PMCPMC114409.

268. Bukreyev A, Whitehead SS, Murphy BR, Collins PL. Recombinant respiratory syncytial virus from which the entire SH gene has been deleted grows efficiently in cell culture and exhibits site-specific attenuation in the respiratory tract of the mouse. Journal of virology. 1997;71(12):8973-82. Epub 1997/11/26. PubMed PMID: 9371553 PMCID: PMCPMC230197.

269. Fuentes S, Tran KC, Luthra P, Teng MN, He B. Function of the respiratory syncytial virus small hydrophobic protein. Journal of virology. 2007;81(15):8361-6. Epub 2007/05/12. PubMed PMID: 17494063 PMCID: PMCPMC1951288.

270. Lin Y, Bright AC, Rothermel TA, He B. Induction of apoptosis by paramyxovirus simian virus 5 lacking a small hydrophobic gene. Journal of

virology. 2003;77(6):3371-83. Epub 2003/03/01. PubMed PMID: 12610112
PMCID: PMCPMC149502.

271. Ao D, Sun S-Q, Guo H-C. Topology and biological function of enterovirus non-structural protein 2B as a member of the viroporin family. *Veterinary Research*. 2014;45(1):87. PubMed PMID: PMC4155101.

272. de Jong AS, Wessels E, Dijkman HB, Galama JM, Melchers WJ, Willems PH, van Kuppeveld FJ. Determinants for membrane association and permeabilization of the coxsackievirus 2B protein and the identification of the Golgi complex as the target organelle. *The Journal of biological chemistry*. 2003;278(2):1012-21. Epub 2002/09/24. PubMed PMID: 12244057.

273. Nieva JL, Agirre A, Nir S, Carrasco L. Mechanisms of membrane permeabilization by picornavirus 2B viroporin. *FEBS Lett*. 2003;552(1):68-73. Epub 2003/09/16. PubMed PMID: 12972154.

274. Doedens JR, Kirkegaard K. Inhibition of cellular protein secretion by poliovirus proteins 2B and 3A. *The EMBO journal*. 1995;14(5):894-907. Epub 1995/03/01. PubMed PMID: 7889939 PMCID: PMCPMC398162.

275. Bodelon G, Labrada L, Martinez-Costas J, Benavente J. Modification of late membrane permeability in avian reovirus-infected cells: viroporin activity of the S1-encoded nonstructural p10 protein. *The Journal of biological chemistry*. 2002;277(20):17789-96. Epub 2002/03/15. PubMed PMID: 11893756.

276. Hsu HW, Su HY, Huang PH, Lee BL, Liu HJ. Sequence and phylogenetic analysis of P10- and P17-encoding genes of avian reovirus. *Avian diseases*. 2005;49(1):36-42. Epub 2005/04/21. PubMed PMID: 15839410.
277. Wu H, He Z, Tang J, Li X, Cao H, Wang Y, Zheng SJ. A critical role of LAMP-1 in avian reovirus P10 degradation associated with inhibition of apoptosis and virus release. *Archives of virology*. 2016;161(4):899-911. Epub 2016/01/09. PubMed PMID: 26744063.
278. Salsman J, Top D, Boutilier J, Duncan R. Extensive Syncytium Formation Mediated by the Reovirus FAST Proteins Triggers Apoptosis-Induced Membrane Instability. *Journal of virology*. 2005;79(13):8090-100.
279. Hay AJ, Wolstenholme AJ, Skehel JJ, Smith MH. The molecular basis of the specific anti-influenza action of amantadine. *The EMBO journal*. 1985;4(11):3021-4. Epub 1985/11/01. PubMed PMID: 4065098 PMCID: PMC554613.
280. Steinmann E, Whitfield T, Kallis S, Dwek RA, Zitzmann N, Pietschmann T, Bartenschlager R. Antiviral effects of amantadine and iminosugar derivatives against hepatitis C virus. *Hepatology (Baltimore, Md)*. 2007;46(2):330-8. Epub 2007/06/30. PubMed PMID: 17599777.
281. Foster TL, Verow M, Wozniak AL, Bentham MJ, Thompson J, Atkins E, Weinman SA, Fishwick C, Foster R, Harris M, Griffin S. Resistance mutations define specific antiviral effects for inhibitors of the hepatitis C

- virus p7 ion channel. *Hepatology* (Baltimore, Md). 2011;54(1):79-90. Epub 2011/04/27. PubMed PMID: 21520195.
282. Ewart GD, Mills K, Cox GB, Gage PW. Amiloride derivatives block ion channel activity and enhancement of virus-like particle budding caused by HIV-1 protein Vpu. *European biophysics journal : EBJ*. 2002;31(1):26-35. Epub 2002/06/06. PubMed PMID: 12046895.
283. Kolpe A, Schepens B, Fiers W, Saelens X. M2-based influenza vaccines: recent advances and clinical potential. *Expert review of vaccines*. 2017;16(2):123-36. Epub 2016/09/23. PubMed PMID: 27653543.
284. Schotsaert M, De Filette M, Fiers W, Saelens X. Universal M2 ectodomain-based influenza A vaccines: preclinical and clinical developments. *Expert review of vaccines*. 2009;8(4):499-508. Epub 2009/04/08. PubMed PMID: 19348565 PMCID: PMC2706389.
285. Zebedee SL, Lamb RA. Influenza A virus M2 protein: monoclonal antibody restriction of virus growth and detection of M2 in virions. *Journal of virology*. 1988;62(8):2762-72. Epub 1988/08/01. PubMed PMID: 2455818 PMCID: PMC253710.
286. Treanor JJ, Tierney EL, Zebedee SL, Lamb RA, Murphy BR. Passively transferred monoclonal antibody to the M2 protein inhibits influenza A virus replication in mice. *Journal of virology*. 1990;64(3):1375-7. Epub 1990/03/01. PubMed PMID: 2304147 PMCID: PMC249260.

287. Neiryneck S, Deroo T, Saelens X, Vanlandschoot P, Jou WM, Fiers W. A universal influenza A vaccine based on the extracellular domain of the M2 protein. *Nature medicine*. 1999;5(10):1157-63. Epub 1999/09/30. PubMed PMID: 10502819.
288. Wu WH, Pekosz A. Extending the cytoplasmic tail of the influenza A virus M2 protein leads to reduced virus replication in vivo but not in vitro. *Journal of virology*. 2008;82(2):1059-63. Epub 2007/11/09. PubMed PMID: 17989186 PMCID: PMCPMC2224589.
289. Watanabe T, Watanabe S, Kim JH, Hatta M, Kawaoka Y. Novel approach to the development of effective H5N1 influenza A virus vaccines: use of M2 cytoplasmic tail mutants. *Journal of virology*. 2008;82(5):2486-92. Epub 2007/12/28. PubMed PMID: 18160446 PMCID: PMCPMC2258945.
290. Hatta Y, Hatta M, Bilsel P, Neumann G, Kawaoka Y. An M2 cytoplasmic tail mutant as a live attenuated influenza vaccine against pandemic (H1N1) 2009 influenza virus. *Vaccine*. 2011;29(12):2308-12. Epub 2011/01/29. PubMed PMID: 21272601 PMCID: PMCPMC3132197.
291. Watanabe T, Watanabe S, Kida H, Kawaoka Y. Influenza A virus with defective M2 ion channel activity as a live vaccine. *Virology*. 2002;299(2):266-70. Epub 2002/08/31. PubMed PMID: 12202229.
292. Watanabe S, Watanabe T, Kawaoka Y. Influenza A virus lacking M2 protein as a live attenuated vaccine. *Journal of virology*. 2009;83(11):5947-50. Epub 2009/03/27. PubMed PMID: 19321619 PMCID: PMCPMC2681926.

293. Sarawar S, Hatta Y, Watanabe S, Dias P, Neumann G, Kawaoka Y, Bilsel P. M2SR, a novel live single replication influenza virus vaccine, provides effective heterosubtypic protection in mice. *Vaccine*. 2016;34(42):5090-8. Epub 2016/09/07. PubMed PMID: 27595896 PMCID: PMC5038585.
294. Hatta Y, Boltz D, Sarawar S, Kawaoka Y, Neumann G, Bilsel P. M2SR, a novel live influenza vaccine, protects mice and ferrets against highly pathogenic avian influenza. *Vaccine*. 2017;35(33):4177-83. Epub 2017/07/03. PubMed PMID: 28668565.
295. Tompkins SM, Zhao ZS, Lo CY, Misplon JA, Liu T, Ye Z, Hogan RJ, Wu Z, Benton KA, Tumpey TM, Epstein SL. Matrix protein 2 vaccination and protection against influenza viruses, including subtype H5N1. *Emerging infectious diseases*. 2007;13(3):426-35. Epub 2007/06/08. PubMed PMID: 17552096 PMCID: PMC2725899.
296. Jameson J, Cruz J, Ennis FA. Human cytotoxic T-lymphocyte repertoire to influenza A viruses. *Journal of virology*. 1998;72(11):8682-9. Epub 1998/10/10. PubMed PMID: 9765409 PMCID: PMC110281.
297. Lalor PA, Webby RJ, Morrow J, Rusalov D, Kaslow DC, Rolland A, Smith LR. Plasmid DNA-based vaccines protect mice and ferrets against lethal challenge with A/Vietnam/1203/04 (H5N1) influenza virus. *The Journal of infectious diseases*. 2008;197(12):1643-52. Epub 2008/06/03. PubMed PMID: 18513153.

298. Lo CY, Wu Z, Mispion JA, Price GE, Pappas C, Kong WP, Tumpey TM, Epstein SL. Comparison of vaccines for induction of heterosubtypic immunity to influenza A virus: cold-adapted vaccine versus DNA prime-adenovirus boost strategies. *Vaccine*. 2008;26(17):2062-72. Epub 2008/04/02. PubMed PMID: 18378366.
299. Chen L, Zanker D, Xiao K, Wu C, Zou Q, Chen W. Immunodominant CD4+ T-cell responses to influenza A virus in healthy individuals focus on matrix 1 and nucleoprotein. *Journal of virology*. 2014;88(20):11760-73. Epub 2014/08/01. PubMed PMID: 25078703 PMCID: PMC4178733.
300. Grant E, Wu C, Chan KF, Eckle S, Bharadwaj M, Zou QM, Kedzierska K, Chen W. Nucleoprotein of influenza A virus is a major target of immunodominant CD8+ T-cell responses. *Immunology and cell biology*. 2013;91(2):184-94. Epub 2013/02/13. PubMed PMID: 23399741.
301. Noda T. Native Morphology of Influenza Virions. *Frontiers in Microbiology*. 2012;2(269).
302. Chan W, Zhou H, Kemble G, Jin H. The cold adapted and temperature sensitive influenza A/Ann Arbor/6/60 virus, the master donor virus for live attenuated influenza vaccines, has multiple defects in replication at the restrictive temperature. *Virology*. 2008;380(2):304-11.
303. Liu T, Ye Z. Attenuating mutations of the matrix gene of influenza A/WSN/33 virus. *Journal of virology*. 2005;79(3):1918-23. Epub 2005/01/15. PubMed PMID: 15650216 PMCID: PMC4178733.

304. Lamb RA, Choppin PW. Identification of a second protein (M2) encoded by RNA segment 7 of influenza virus. *Virology*. 1981;112(2):729-37. Epub 1981/07/30. PubMed PMID: 7257188.
305. Takeda M, Pekosz A, Shuck K, Pinto LH, Lamb RA. Influenza a virus M2 ion channel activity is essential for efficient replication in tissue culture. *Journal of virology*. 2002;76(3):1391-9. Epub 2002/01/05. PubMed PMID: 11773413 PMCID: PMC135863.
306. Holsinger LJ, Lamb RA. Influenza virus M2 integral membrane protein is a homotetramer stabilized by formation of disulfide bonds. *Virology*. 1991;183(1):32-43. Epub 1991/07/01. PubMed PMID: 2053285.
307. Helenius A. Unpacking the incoming influenza virus. *Cell*. 1992;69(4):577-8.
308. Martin K, Helenius A. Transport of incoming influenza virus nucleocapsids into the nucleus. *Journal of virology*. 1991;65(1):232-44.
309. Lane AP, Saatian B, Yu XY, Spannhake EW. mRNA for genes associated with antigen presentation are expressed by human middle meatal epithelial cells in culture. *The Laryngoscope*. 2004;114(10):1827-32. Epub 2004/09/30. PubMed PMID: 15454780.
310. Ramanathan M, Jr., Lane AP. Innate immunity of the sinonasal cavity and its role in chronic rhinosinusitis. *Otolaryngology--head and neck surgery : official journal of American Academy of Otolaryngology-Head and Neck Surgery*. 2007;136(3):348-56. Epub 2007/02/27. PubMed PMID: 17321858.

311. Ramanathan M, Jr., Lee WK, Dubin MG, Lin S, Spannhake EW, Lane AP. Sinonasal epithelial cell expression of toll-like receptor 9 is decreased in chronic rhinosinusitis with polyps. *American journal of rhinology*. 2007;21(1):110-6. Epub 2007/02/08. PubMed PMID: 17283572.
312. Neumann G, Watanabe T, Ito H, Watanabe S, Goto H, Gao P, Hughes M, Perez DR, Donis R, Hoffmann E, Hobom G, Kawaoka Y. Generation of influenza A viruses entirely from cloned cDNAs. *Proceedings of the National Academy of Sciences of the United States of America*. 1999;96(16):9345-50. Epub 1999/08/04. PubMed PMID: 10430945 PMCID: PMC17785.
313. Clark K, Karsch-Mizrachi I, Lipman DJ, Ostell J, Sayers EW. GenBank. *Nucleic Acids Research*. 2016;44(Database issue):D67-D72. PubMed PMID: PMC4702903.
314. Squires RB, Noronha J, Hunt V, García-Sastre A, Macken C, Baumgarth N, Suarez D, Pickett BE, Zhang Y, Larsen CN, Ramsey A, Zhou L, Zaremba S, Kumar S, Deitrich J, Klem E, Scheuermann RH. Influenza Research Database: an integrated bioinformatics resource for influenza research and surveillance. *Influenza and Other Respiratory Viruses*. 2012;6(6):404-16. PubMed PMID: PMC3345175.
315. Neumann G, Ozawa M, Kawaoka Y. Reverse genetics of influenza viruses. *Methods in molecular biology (Clifton, NJ)*. 2012;865:193-206. Epub 2012/04/25. PubMed PMID: 22528161.

316. Reed LJ, Muench H. A simple method of estimating fifty per cent endpoints. *American journal of epidemiology*. 1938;27(3):493-7.
317. Peretz J, Pekosz A, Lane AP, Klein SL. Estrogenic compounds reduce influenza A virus replication in primary human nasal epithelial cells derived from female, but not male, donors. *American journal of physiology Lung cellular and molecular physiology*. 2016;310(5):L415-25. Epub 2015/12/20. PubMed PMID: 26684252 PMCID: PMC4773846.
318. Hall OJ, Limjunyawong N, Vermillion MS, Robinson DP, Wohlgemuth N, Pekosz A, Mitzner W, Klein SL. Progesterone-Based Therapy Protects Against Influenza by Promoting Lung Repair and Recovery in Females. *PLoS pathogens*. 2016;12(9):e1005840. Epub 2016/09/16. PubMed PMID: 27631986 PMCID: PMC4773846.
319. Newby CM, Sabin L, Pekosz A. The RNA binding domain of influenza A virus NS1 protein affects secretion of tumor necrosis factor alpha, interleukin-6, and interferon in primary murine tracheal epithelial cells. *Journal of virology*. 2007;81(17):9469-80. Epub 2007/06/29. PubMed PMID: 17596305 PMCID: PMC1951395.
320. Ilyushina NA, Ikizler MR, Kawaoka Y, Rudenko LG, Treanor JJ, Subbarao K, Wright PF. Comparative study of influenza virus replication in MDCK cells and in primary cells derived from adenoids and airway epithelium. *Journal of virology*. 2012;86(21):11725-34. Epub 2012/08/24. PubMed PMID: 22915797 PMCID: PMC3486302.

321. Ibricevic A, Pekosz A, Walter MJ, Newby C, Battaile JT, Brown EG, Holtzman MJ, Brody SL. Influenza virus receptor specificity and cell tropism in mouse and human airway epithelial cells. *Journal of virology*. 2006;80(15):7469-80. Epub 2006/07/15. PubMed PMID: 16840327 PMCID: PMC1563738.
322. Newby CM, Rowe RK, Pekosz A. Influenza A virus infection of primary differentiated airway epithelial cell cultures derived from Syrian golden hamsters. *Virology*. 2006;354(1):80-90. Epub 2006/08/01. PubMed PMID: 16876846 PMCID: PMC1704084.
323. Adler KB, Cheng PW, Kim KC. Characterization of guinea pig tracheal epithelial cells maintained in biphasic organotypic culture: cellular composition and biochemical analysis of released glycoconjugates. *American journal of respiratory cell and molecular biology*. 1990;2(2):145-54. Epub 1990/02/01. PubMed PMID: 2306371.
324. You Y, Richer EJ, Huang T, Brody SL. Growth and differentiation of mouse tracheal epithelial cells: selection of a proliferative population. *American journal of physiology Lung cellular and molecular physiology*. 2002;283(6):L1315-21. Epub 2002/10/22. PubMed PMID: 12388377.
325. de Weerd NA, Nguyen T. The interferons and their receptors--distribution and regulation. *Immunology and cell biology*. 2012;90(5):483-91. Epub 2012/03/14. PubMed PMID: 22410872.

326. Sommereyns C, Paul S, Staeheli P, Michiels T. IFN-lambda (IFN-lambda) is expressed in a tissue-dependent fashion and primarily acts on epithelial cells in vivo. *PLoS pathogens*. 2008;4(3):e1000017. Epub 2008/03/29. PubMed PMID: 18369468 PMCID: PMCPMC2265414.
327. Odagiri T, Tanaka T, Tobita K. Temperature-sensitive defect of influenza A/Ann Arbor/6/60 cold-adapted variant leads to a blockage of matrix polypeptide incorporation into the plasma membrane of the infected cells. *Virus research*. 1987;7(3):203-18. Epub 1987/05/01. PubMed PMID: 3604455.
328. Belshe RB, Edwards KM, Vesikari T, Black SV, Walker RE, Hultquist M, Kemble G, Connor EM. Live attenuated versus inactivated influenza vaccine in infants and young children. *The New England journal of medicine*. 2007;356(7):685-96. Epub 2007/02/16. PubMed PMID: 17301299.
329. Nichol KL, Mendelman PM, Mallon KP, Jackson LA, Gorse GJ, Belshe RB, Glezen WP, Wittes J. Effectiveness of live, attenuated intranasal influenza virus vaccine in healthy, working adults: a randomized controlled trial. *JAMA*. 1999;282(2):137-44. Epub 1999/07/20. PubMed PMID: 10411194.
330. Treanor JJ, Kotloff K, Betts RF, Belshe R, Newman F, Iacuzio D, Wittes J, Bryant M. Evaluation of trivalent, live, cold-adapted (CAIV-T) and inactivated (TIV) influenza vaccines in prevention of virus infection and illness following challenge of adults with wild-type influenza A (H1N1), A

(H3N2), and B viruses. *Vaccine*. 1999;18(9-10):899-906. Epub 1999/12/02. PubMed PMID: 10580204.

331. Rodriguez Boulan E, Sabatini DD. Asymmetric budding of viruses in epithelial monolayers: a model system for study of epithelial polarity.

Proceedings of the National Academy of Sciences of the United States of America. 1978;75(10):5071-5. Epub 1978/10/01. PubMed PMID: 283416
PMCID: PMC336265.

332. Compans RW. Virus entry and release in polarized epithelial cells. *Current topics in microbiology and immunology*. 1995;202:209-19. Epub 1995/01/01. PubMed PMID: 7587364.

333. Roth MG, Compans RW, Giusti L, Davis AR, Nayak DP, Gething MJ, Sambrook J. Influenza virus hemagglutinin expression is polarized in cells infected with recombinant SV40 viruses carrying cloned hemagglutinin DNA. *Cell*. 1983;33(2):435-43. Epub 1983/06/01. PubMed PMID: 6305510.

334. Lin S, Naim HY, Rodriguez AC, Roth MG. Mutations in the middle of the transmembrane domain reverse the polarity of transport of the influenza virus hemagglutinin in MDCK epithelial cells. *The Journal of cell biology*. 1998;142(1):51-7. Epub 1998/07/14. PubMed PMID: 9660862 PMCID: PMC2133032.

335. Jones LV, Compans RW, Davis AR, Bos TJ, Nayak DP. Surface expression of influenza virus neuraminidase, an amino-terminally anchored viral membrane glycoprotein, in polarized epithelial cells. *Mol Cell Biol*.

1985;5(9):2181-9. Epub 1985/09/01. PubMed PMID: 3016520 PMCID: PMCPMC366942.

336. Barman S, Nayak DP. Analysis of the transmembrane domain of influenza virus neuraminidase, a type II transmembrane glycoprotein, for apical sorting and raft association. *Journal of virology*. 2000;74(14):6538-45. Epub 2000/06/23. PubMed PMID: 10864667 PMCID: PMCPMC112163.

337. Kundu A, Avalos RT, Sanderson CM, Nayak DP. Transmembrane domain of influenza virus neuraminidase, a type II protein, possesses an apical sorting signal in polarized MDCK cells. *Journal of virology*. 1996;70(9):6508-15. Epub 1996/09/01. PubMed PMID: 8709291 PMCID: PMCPMC190689.

338. Hughey PG, Compans RW, Zebedee SL, Lamb RA. Expression of the influenza A virus M2 protein is restricted to apical surfaces of polarized epithelial cells. *Journal of virology*. 1992;66(9):5542-52. Epub 1992/09/01. PubMed PMID: 1501289 PMCID: PMCPMC289113.

339. Ali A, Avalos RT, Ponimaskin E, Nayak DP. Influenza virus assembly: effect of influenza virus glycoproteins on the membrane association of M1 protein. *Journal of virology*. 2000;74(18):8709-19. Epub 2000/08/23. PubMed PMID: 10954572 PMCID: PMCPMC116382.

340. Enami M, Enami K. Influenza virus hemagglutinin and neuraminidase glycoproteins stimulate the membrane association of the matrix protein.

Journal of virology. 1996;70(10):6653-7. Epub 1996/10/01. PubMed PMID: 8794300 PMCID: PMCPMC190706.

341. Jin H, Leser GP, Zhang J, Lamb RA. Influenza virus hemagglutinin and neuraminidase cytoplasmic tails control particle shape. The EMBO journal. 1997;16(6):1236-47. Epub 1997/03/17. PubMed PMID: 9135140 PMCID: PMCPMC1169722.

342. Avalos RT, Yu Z, Nayak DP. Association of influenza virus NP and M1 proteins with cellular cytoskeletal elements in influenza virus-infected cells. Journal of virology. 1997;71(4):2947-58. Epub 1997/04/01. PubMed PMID: 9060654 PMCID: PMCPMC191423.

343. Carrasco M, Amorim MJ, Digard P. Lipid raft-dependent targeting of the influenza A virus nucleoprotein to the apical plasma membrane. Traffic (Copenhagen, Denmark). 2004;5(12):979-92. Epub 2004/11/04. PubMed PMID: 15522099.

344. Niwa H, Yamamura K, Miyazaki J. Efficient selection for high-expression transfectants with a novel eukaryotic vector. Gene. 1991;108(2):193-9. Epub 1991/12/15. PubMed PMID: 1660837.

345. McCown M, Diamond MS, Pekosz A. The utility of siRNA transcripts produced by RNA polymerase i in down regulating viral gene expression and replication of negative- and positive-strand RNA viruses. Virology. 2003;313(2):514-24. Epub 2003/09/05. PubMed PMID: 12954218.

346. Russier M, Yang G, Rehg JE, Wong SS, Mostafa HH, Fabrizio TP, Barman S, Krauss S, Webster RG, Webby RJ, Russell CJ. Molecular requirements for a pandemic influenza virus: An acid-stable hemagglutinin protein. *Proceedings of the National Academy of Sciences of the United States of America*. 2016;113(6):1636-41. Epub 2016/01/27. PubMed PMID: 26811446 PMCID: PMC4760800.
347. Bello V, Goding JW, Greengrass V, Sali A, Dubljevic V, Lenoir C, Trugnan G, Maurice M. Characterization of a Di-leucine-based Signal in the Cytoplasmic Tail of the Nucleotide-pyrophosphatase NPP1 That Mediates Basolateral Targeting but not Endocytosis. *Molecular Biology of the Cell*. 2001;12(10):3004-15.
348. Mora R, Rodriguez-Boulan E, Palese P, Garcia-Sastre A. Apical budding of a recombinant influenza A virus expressing a hemagglutinin protein with a basolateral localization signal. *Journal of virology*. 2002;76(7):3544-53. Epub 2002/03/09. PubMed PMID: 11884578 PMCID: PMC136015.
349. Barman S, Adhikary L, Kawaoka Y, Nayak DP. Influenza A virus hemagglutinin containing basolateral localization signal does not alter the apical budding of a recombinant influenza A virus in polarized MDCK cells. *Virology*. 2003;305(1):138-52. Epub 2002/12/31. PubMed PMID: 12504548.
350. Brewer CB, Roth MG. A single amino acid change in the cytoplasmic domain alters the polarized delivery of influenza virus hemagglutinin. *The*

Journal of cell biology. 1991;114(3):413-21. Epub 1991/08/01. PubMed PMID: 1860878 PMCID: PMCPMC2289095.

351. Zimmer G, Zimmer K-P, Trotz I, Herrler G. Vesicular Stomatitis Virus Glycoprotein Does Not Determine the Site of Virus Release in Polarized Epithelial Cells. Journal of virology. 2002;76(8):4103-7.

352. Maisner A, Klenk H-D, Herrler G. Polarized Budding of Measles Virus Is Not Determined by Viral Surface Glycoproteins. Journal of virology. 1998;72(6):5276-8.

353. Moll M, Pfeuffer J, Klenk HD, Niewiesk S, Maisner A. Polarized glycoprotein targeting affects the spread of measles virus in vitro and in vivo. The Journal of general virology. 2004;85(Pt 4):1019-27. Epub 2004/03/25. PubMed PMID: 15039544.

354. Naim HY, Ehler E, Billeter MA. Measles virus matrix protein specifies apical virus release and glycoprotein sorting in epithelial cells. The EMBO journal. 2000;19(14):3576-85. Epub 2000/07/19. PubMed PMID: 10899112 PMCID: PMCPMC313987.

355. Tripathi S, Pohl MO, Zhou Y, Rodriguez-Frandsen A, Wang G, Stein DA, Moulton HM, DeJesus P, Che J, Mulder LC, Yanguéz E, Andenmatten D, Pache L, Manicassamy B, Albrecht RA, Gonzalez MG, Nguyen Q, Brass A, Elledge S, White M, Shapira S, Hacohen N, Karlas A, Meyer TF, Shales M, Gatorano A, Johnson JR, Jang G, Johnson T, Verschueren E, Sanders D, Krogan N, Shaw M, König R, Stertz S, Garcia-Sastre A, Chanda SK. Meta-

and Orthogonal Integration of Influenza "OMICs" Data Defines a Role for UBR4 in Virus Budding. *Cell host & microbe*. 2015;18(6):723-35. Epub 2015/12/15. PubMed PMID: 26651948 PMCID: PMC4829074.

356. Ma H, Kien F, Maniere M, Zhang Y, Lagarde N, Tse KS, Poon LL, Nal B. Human annexin A6 interacts with influenza A virus protein M2 and negatively modulates infection. *Journal of virology*. 2012;86(3):1789-801. Epub 2011/11/25. PubMed PMID: 22114333 PMCID: PMC3264383.

357. Bruce EA, Digard P, Stuart AD. The Rab11 Pathway Is Required for Influenza A Virus Budding and Filament Formation. *Journal of virology*. 2010;84(12):5848-59.

358. Gorai T, Goto H, Noda T, Watanabe T, Kozuka-Hata H, Oyama M, Takano R, Neumann G, Watanabe S, Kawaoka Y. F1Fo-ATPase, F-type proton-translocating ATPase, at the plasma membrane is critical for efficient influenza virus budding. *Proceedings of the National Academy of Sciences*. 2012;109(12):4615-20.

359. Tashiro M, Pritzer E, Khoshnan MA, Yamakawa M, Kuroda K, Klenk HD, Rott R, Seto JT. Characterization of a pantropic variant of Sendai virus derived from a host range mutant. *Virology*. 1988;165(2):577-83. Epub 1988/08/01. PubMed PMID: 2841801.

360. Tashiro M, Yamakawa M, Tobita K, Seto JT, Klenk HD, Rott R. Altered budding site of a pantropic mutant of Sendai virus, F1-R, in polarized epithelial cells. *Journal of virology*. 1990;64(10):4672-7.

361. Tashiro M, James I, Karri S, Wahn K, Tobita JK, Klenk HD, Rott R, Seto JT. Pneumotropic revertants derived from a pantropic mutant, F1-R, of Sendai virus. *Virology*. 1991;184(1):227-34.
362. Tashiro M, Seto JT, Choosakul S, Yamakawa M, Klenk HD, Rott R. Budding site of Sendai virus in polarized epithelial cells is one of the determinants for tropism and pathogenicity in mice. *Virology*. 1992;187(2):413-22. Epub 1992/04/01. PubMed PMID: 1312267.
363. Rossen JW, Horzinek MC, Rottier PJ. Coronavirus infection of polarized epithelial cells. *Trends in microbiology*. 1995;3(12):486-90. Epub 1995/12/01. PubMed PMID: 8800844.
364. Cong Y, Ren X. Coronavirus entry and release in polarized epithelial cells: a review. *Reviews in medical virology*. 2014;24(5):308-15. Epub 2014/04/17. PubMed PMID: 24737708.
365. Thompson CI, Barclay WS, Zambon MC, Pickles RJ. Infection of human airway epithelium by human and avian strains of influenza A virus. *Journal of virology*. 2006;80(16):8060-8. Epub 2006/07/29. PubMed PMID: 16873262 PMCID: PMC1563802.
366. Chan MC, Chan RW, Yu WC, Ho CC, Chui WH, Lo CK, Yuen KM, Guan YI, Nicholls JM, Peiris JS. Influenza H5N1 virus infection of polarized human alveolar epithelial cells and lung microvascular endothelial cells. *Respiratory research*. 2009;10:102. Epub 2009/10/31. PubMed PMID: 19874627 PMCID: PMC2780994.

367. Webster RG, Rott R. Influenza virus A pathogenicity: the pivotal role of hemagglutinin. *Cell*. 1987;50(5):665-6. Epub 1987/08/28. PubMed PMID: 3304656.
368. Klenk HD, Garten W. Host cell proteases controlling virus pathogenicity. *Trends in microbiology*. 1994;2(2):39-43. Epub 1994/02/01. PubMed PMID: 8162439.
369. Hatta M, Gao P, Halfmann P, Kawaoka Y. Molecular basis for high virulence of Hong Kong H5N1 influenza A viruses. *Science (New York, NY)*. 2001;293(5536):1840-2. Epub 2001/09/08. PubMed PMID: 11546875.
370. Schrauwen EJ, Bestebroer TM, Munster VJ, de Wit E, Herfst S, Rimmelzwaan GF, Osterhaus AD, Fouchier RA. Insertion of a multibasic cleavage site in the haemagglutinin of human influenza H3N2 virus does not increase pathogenicity in ferrets. *The Journal of general virology*. 2011;92(Pt 6):1410-5. Epub 2011/02/25. PubMed PMID: 21346026 PMCID: PMC3168280.
371. Schrauwen EJ, Herfst S, Leijten LM, van Run P, Bestebroer TM, Linster M, Bodewes R, Kreijtz JH, Rimmelzwaan GF, Osterhaus AD, Fouchier RA, Kuiken T, van Riel D. The multibasic cleavage site in H5N1 virus is critical for systemic spread along the olfactory and hematogenous routes in ferrets. *Journal of virology*. 2012;86(7):3975-84. Epub 2012/01/27. PubMed PMID: 22278228 PMCID: PMC3302532.

372. Rhorer J, Ambrose CS, Dickinson S, Hamilton H, Oleka NA, Malinoski FJ, Wittes J. Efficacy of live attenuated influenza vaccine in children: A meta-analysis of nine randomized clinical trials. *Vaccine*. 2009;27(7):1101-10. Epub 2008/12/20. PubMed PMID: 19095024.
373. Chung JR, Flannery B, Thompson MG, Gaglani M, Jackson ML, Monto AS, Nowalk MP, Talbot HK, Treanor JJ, Belongia EA, Murthy K, Jackson LA, Petrie JG, Zimmerman RK, Griffin MR, McLean HQ, Fry AM. Seasonal Effectiveness of Live Attenuated and Inactivated Influenza Vaccine. *Pediatrics*. 2016;137(2):e20153279. Epub 2016/01/08. PubMed PMID: 26738884 PMCID: PMC4732363.
374. Pebody R, Warburton F, Ellis J, Andrews N, Potts A, Cottrell S, Johnston J, Reynolds A, Gunson R, Thompson C, Galiano M, Robertson C, Byford R, Gallagher N, Sinnathamby M, Yonova I, Pathirannehelage S, Donati M, Moore C, de Lusignan S, McMenemy J, Zambon M. Effectiveness of seasonal influenza vaccine for adults and children in preventing laboratory-confirmed influenza in primary care in the United Kingdom: 2015/16 end-of-season results. *Euro surveillance : bulletin Europeen sur les maladies transmissibles = European communicable disease bulletin*. 2016;21(38). Epub 2016/09/30. PubMed PMID: 27684603 PMCID: PMC5073201.
375. Nohynek H, Baum U, Syrjanen R, Ikonen N, Sundman J, Jokinen J. Effectiveness of the live attenuated and the inactivated influenza vaccine in

two-year-olds - a nationwide cohort study Finland, influenza season 2015/16.

Euro surveillance : bulletin Europeen sur les maladies transmissibles =

European communicable disease bulletin. 2016;21(38). Epub 2016/09/30.

PubMed PMID: 27684447 PMCID: PMCPMC5073199.

376. Sullivan SG, Feng S, Cowling BJ. Potential of the test-negative design for measuring influenza vaccine effectiveness: a systematic review. *Expert review of vaccines*. 2014;13(12):1571-91. Epub 2014/10/29. PubMed PMID: 25348015 PMCID: PMCPMC4277796.

377. Sullivan SG, Tchetgen Tchetgen EJ, Cowling BJ. Theoretical Basis of the Test-Negative Study Design for Assessment of Influenza Vaccine Effectiveness. *American journal of epidemiology*. 2016;184(5):345-53. Epub 2016/09/03. PubMed PMID: 27587721 PMCID: PMCPMC5013887.

378. Valenciano M, Ciancio B. I-MOVE: a European network to measure the effectiveness of influenza vaccines. *Euro surveillance : bulletin Europeen sur les maladies transmissibles = European communicable disease bulletin*. 2012;17(39). Epub 2012/10/09. PubMed PMID: 23041022.

379. Ambrose CS, Levin MJ, Belshe RB. The relative efficacy of trivalent live attenuated and inactivated influenza vaccines in children and adults. *Influenza Other Respir Viruses*. 2011;5(2):67-75. Epub 2011/02/11. PubMed PMID: 21306569 PMCID: PMCPMC3151550.

380. Monto AS, Ohmit SE, Petrie JG, Johnson E, Truscon R, Teich E, Rotthoff J, Boulton M, Victor JC. Comparative efficacy of inactivated and live

- attenuated influenza vaccines. *The New England journal of medicine*. 2009;361(13):1260-7. Epub 2009/09/25. PubMed PMID: 19776407.
381. Caspard H, Heikkinen T, Belshe RB, Ambrose CS. A systematic review of the efficacy of live attenuated influenza vaccine upon revaccination of children. *Human vaccines & immunotherapeutics*. 2016;12(7):1721-7. Epub 2016/01/12. PubMed PMID: 26751513 PMCID: PMC4964816.
382. Easterbrook JD, Kash JC, Sheng ZM, Qi L, Gao J, Kilbourne ED, Eichelberger MC, Taubenberger JK. Immunization with 1976 swine H1N1- or 2009 pandemic H1N1-inactivated vaccines protects mice from a lethal 1918 influenza infection. *Influenza Other Respir Viruses*. 2011;5(3):198-205. Epub 2011/04/12. PubMed PMID: 21477139 PMCID: PMC3073596.
383. Morens DM, Taubenberger JK, Fauci AS. The persistent legacy of the 1918 influenza virus. *The New England journal of medicine*. 2009;361(3):225-9. Epub 2009/07/01. PubMed PMID: 19564629 PMCID: PMC2749954.
384. Dawood FS, Jain S, Finelli L, Shaw MW, Lindstrom S, Garten RJ, Gubareva LV, Xu X, Bridges CB, Uyeki TM. Emergence of a novel swine-origin influenza A (H1N1) virus in humans. *The New England journal of medicine*. 2009;360(25):2605-15. Epub 2009/05/09. PubMed PMID: 19423869.
385. Cauldwell AV, Long JS, Moncorge O, Barclay WS. Viral determinants of influenza A virus host range. *The Journal of general virology*. 2014;95(Pt 6):1193-210. Epub 2014/03/04. PubMed PMID: 24584475.

386. Neumann G, Kawaoka Y. Host range restriction and pathogenicity in the context of influenza pandemic. *Emerging infectious diseases*. 2006;12(6):881-6. Epub 2006/05/19. PubMed PMID: 16707041 PMCID: PMC3373033.
387. Boonnak K, Paskel M, Matsuoka Y, Vogel L, Subbarao K. Evaluation of replication, immunogenicity and protective efficacy of a live attenuated cold-adapted pandemic H1N1 influenza virus vaccine in non-human primates. *Vaccine*. 2012;30(38):5603-10. Epub 2012/07/14. PubMed PMID: 22789506 PMCID: PMC3412900.
388. Cotter CR, Jin H, Chen Z. A Single Amino Acid in the Stalk Region of the H1N1pdm Influenza Virus HA Protein Affects Viral Fusion, Stability and Infectivity. *PLoS pathogens*. 2014;10(1):e1003831.
389. Caspard H, Coelingh KL, Mallory RM, Ambrose CS. Association of vaccine handling conditions with effectiveness of live attenuated influenza vaccine against H1N1pdm09 viruses in the United States. *Vaccine*. 2016;34(42):5066-72.
390. Pebody R, McMenamin J, Nohynek H. Live attenuated influenza vaccine (LAIV): recent effectiveness results from the USA and implications for LAIV programmes elsewhere. *Arch Dis Child*. 2017. Epub 2017/09/01. PubMed PMID: 28855230.

391. Ye Y. Characterization of Influenza A Virus M2 Cytoplasmic Tail Amino Acid Residue Position 83 and 86 Mutations: Johns Hopkins University; 2016.
392. Syedbasha M, Egli A. Interferon Lambda: Modulating Immunity in Infectious Diseases. *Frontiers in immunology*. 2017;8:119. Epub 2017/03/16. PubMed PMID: 28293236 PMCID: PMC5328987.
393. Egli A, Santer DM, O'Shea D, Tyrrell DL, Houghton M. The impact of the interferon-lambda family on the innate and adaptive immune response to viral infections. *Emerging microbes & infections*. 2014;3(7):e51. Epub 2015/06/04. PubMed PMID: 26038748 PMCID: PMC4126180.
394. Bolen CR, Ding S, Robek MD, Kleinstein SH. Dynamic expression profiling of type I and type III interferon-stimulated hepatocytes reveals a stable hierarchy of gene expression. *Hepatology (Baltimore, Md)*. 2014;59(4):1262-72. Epub 2013/08/10. PubMed PMID: 23929627 PMCID: PMC3938553.
395. Stanton J. Characterization of Mutations in the C-terminal Domain of the NS1 Protein of Influenza A Virus and Live Attenuated Influenza Vaccine: Johns Hopkins University; 2017.
396. Fink AL, Klein SL. Sex and Gender Impact Immune Responses to Vaccines Among the Elderly. *Physiology (Bethesda, Md)*. 2015;30(6):408-16. Epub 2015/11/04. PubMed PMID: 26525340 PMCID: PMC4630198.

397. Klein SL, Pekosz A. Sex-based biology and the rational design of influenza vaccination strategies. *The Journal of infectious diseases*. 2014;209 Suppl 3:S114-9. Epub 2014/06/27. PubMed PMID: 24966191 PMCID: PMC4157517.
398. Weisz OA, Rodriguez-Boulan E. Apical trafficking in epithelial cells: signals, clusters and motors. *Journal of Cell Science*. 2009;122(23):4253-66.
399. Wiley CA, Bhardwaj N, Ross TM, Bissel SJ. Emerging Infections of CNS: Avian Influenza A Virus, Rift Valley Fever Virus and Human Parechovirus. *Brain pathology (Zurich, Switzerland)*. 2015;25(5):634-50. Epub 2015/08/16. PubMed PMID: 26276027 PMCID: PMC4538697.
400. Studahl M. Influenza virus and CNS manifestations. *Journal of Clinical Virology*. 28(3):225-32.
401. Toovey S. Influenza-associated central nervous system dysfunction: A literature review. *Travel Medicine and Infectious Disease*. 6(3):114-24.
402. Surtees R, DeSousa C. Influenza virus associated encephalopathy. *Archives of Disease in Childhood*. 2006;91(6):455-6. PubMed PMID: PMC2082798.
403. Smith W, Andrewes CH, Laidlaw PP. A virus obtained from influenza patients. *The Lancet*. 1933;222(5732):66-8.
404. Francis T, Moore AE. A STUDY OF THE NEUROTROPIC TENDENCY IN STRAINS OF THE VIRUS OF EPIDEMIC INFLUENZA.

The Journal of experimental medicine. 1940;72(6):717-28. Epub 1940/11/30.

PubMed PMID: 19871056 PMCID: PMCPMC2135049.

405. Claas ECJ, Osterhaus ADME. New clues to the emergence of flu pandemics. Nature medicine. 1998;4(10):1122-3.

406. Castrucci MR, Kawaoka Y. Biologic importance of neuraminidase stalk length in influenza A virus. Journal of virology. 1993;67(2):759-64. Epub 1993/02/01. PubMed PMID: 8419645 PMCID: PMCPMC237428.

407. Bouvier NM, Lowen AC. Animal Models for Influenza Virus Pathogenesis and Transmission. Viruses. 2010;2(8):1530-63. PubMed PMID: PMC3063653.

408. Langlois RA, Albrecht RA, Kimble B, Sutton T, Shapiro JS, Finch C, Angel M, Chua MA, Gonzalez-Reiche AS, Xu K, Perez D, Garcia-Sastre A, tenOever BR. MicroRNA-based strategy to mitigate the risk of gain-of-function influenza studies. Nat Biotech. 2013;31(9):844-7.

409. Kamboj M, Sepkowitz KA. Risk of transmission associated with live attenuated vaccines given to healthy persons caring for or residing with an immunocompromised patient. Infection control and hospital epidemiology. 2007;28(6):702-7. Epub 2007/05/24. PubMed PMID: 17520544.

410. Harper S, KFukuda K, Cox N, Bridges C. Using Live, Attenuated Influenza Vaccine for Prevention and Control of Influenza. MMWR Recomm Rep. 2003;52(13):8.

411. Fauci AS. An Accelerated Pathway Towards a Universal Vaccine. June 8 2017 NIAID Advisory Committee to the Director [cited 2017 September 4].

Available from:

<https://acd.od.nih.gov/documents/presentations/06082017Fauci.pdf>.

412. Nabel GJ, Fauci AS. Induction of unnatural immunity: prospects for a broadly protective universal influenza vaccine. *Nature medicine*.

2010;16(12):1389-91.

413. Paules CI, Marston HD, Eisinger RW, Baltimore D, Fauci AS. The Pathway to a Universal Influenza Vaccine. *Immunity*. 2017;47(4):599-603.

CURRICULUM VITAE

NICHOLAS WOHLGEMUTH

Work

615 N. Wolfe Street, Rm W2104-1
Baltimore, MD 21205
443-287-8750
nwohlge1@jhu.edu

Home

3409 Bank Street
Baltimore, MD 21224
443-990-1197
nicholasjameswohlgemuth@gmail.com

EDUCATION

August 2012 – Present

Johns Hopkins University, Johns Hopkins Bloomberg School of Public Health
PhD Candidate in Molecular Microbiology and Immunology GPA: 3.96
Thesis: “Apical M2 Protein is required for efficient influenza A virus replication”
Laboratory of Dr. Andrew Pekosz

August 2007 – May 2011

University of Nebraska - Lincoln
Bachelor of Science Degree with Highest Distinction 2011
Major: Biochemistry Minors: Psychology, Chemistry GPA: 4.0
Honors Thesis: “Analysis of Chlorella NC64A and PBCV-1 genomes for secreted
proteins using computer-based prediction algorithms and progress
towards isolation of secreted proteins in Chlorella NC64A”
Laboratory of Dr. James L. Van Etten

EMPLOYMENT

July 2011 – August 2012

Research Technologist, Johns Hopkins University, Baltimore, MD
Stanley Division of Developmental Neurovirology
Advisors: Assistant Professor Lorraine V. Jones-Brando and Robert Yolken,
Theodore and Vada Stanley Distinguished Professor of Neurovirology in
Pediatrics

December 2007 – August 2008

Laboratory Technician, Archer Daniels Midland, Columbus, NE

PUBLICATIONS

*Co-first author

Wohlgemuth N*, Ye E*, Fenstermacher K, Liu H, Lane A, Pekosz A. 2017. The M2 protein of live, attenuated influenza vaccine encodes a mutation that reduced virus replication in human nasal epithelial cells, *Vaccine*: <http://doi.org/10.1016/j.vaccine.2017.10.018>.

Forero A*, Fenstermacher K*, **Wohlgemuth N**, Nishida A, Carter V, Smith EA, Peng X, Hayes M, Francis D, Treanor J, Morrison J, Klein SL, Lane A, Katze MG, Pekosz A. 2017. Evaluation of the innate immune responses to influenza and live-attenuated influenza vaccine infection in primary differentiated human nasal epithelial cells, *Vaccine*: <http://doi.org/10.1016/j.vaccine.2017.09.058>.

Hall OJ, Limjunyawong N, Vermillion MS, Robinson DP, **Wohlgemuth N**, Pekosz A, Mitzner W, Klein SL. 2016. Progesterone-Based Therapy Protects Against Influenza by Promoting Lung Repair and Recovery in Females, *PLoS Pathogens*: <http://dx.doi.org/10.1371/journal.ppat.1005840>.

Wohlgemuth N, Lane A, Pekosz A. Influenza A virus M2 protein apical targeting is required for efficient virus budding and replication. Submitted.

RESEARCH PRESENTATIONS

Poster Presentation at the Centers of Excellence for Influenza Research and Surveillance Annual Meeting. Title: The M2 protein of live, attenuated influenza vaccine encodes a mutation that reduces replication in human nasal epithelial cells. **Wohlgemuth N**, Ye Y, Fenstermacher KJ, Liu H, Lane AP, and Pekosz A. July 2016, Atlanta, GA.

Oral Presentation at the Annual Meeting of the American Society for Virology. Title: The M2 protein of live, attenuated influenza vaccine encodes a mutation that reduces replication in human nasal epithelial cells. **Wohlgemuth N**, Ye Y, Fenstermacher KJ, Liu H, Lane AP, and Pekosz A. June 2017, Madison, WI.

Poster Presentation at the Nebraska Center for Virology Annual Symposium in Virology. Title: Influenza A virus M2 protein apical targeting is required for efficient virus assembly and replication. **Wohlgemuth N** and Pekosz A. October 2016, Lincoln, NE.

Poster Presentation at the Centers of Excellence for Influenza Research and Surveillance Annual Meeting. Title: Influenza A virus M2 protein apical targeting is required for efficient virus assembly and replication. **Wohlgemuth N** and Pekosz A. June 2016, Memphis, TN.

Oral Presentation at the Annual Meeting of the American Society for Virology. Title: Influenza A virus M2 protein apical targeting is required for efficient virus assembly and replication. **Wohlgemuth N** and Pekosz A. June 2016, Blacksburg, VA.

Poster Presentation at the Annual Meeting of the American Society for Cell Biology. Title: Apical targeting of the influenza A virus M2 protein is required for virus production. **Wohlgemuth N** and Pekosz A. December 2015, San Deigo, CA.

Webinar Presentation for the Centers for Excellence for Influenza Research and Surveillance. Title: Apical targeting of M2 is required for influenza A virus replication in polarized epithelial cells. **Wohlgemuth N**. September 2015.

Poster Presentation at UNL Undergraduate Research Conference. Title: Chlorella NC64A and PBCV-1 predicted secreted proteins and progress towards isolation of secreted proteins in Chlorella NC64A. **Wohlgemuth N**, Lane L, Van Etten JL. April 2011, Lincoln, NE.

Oral Presentation at ASM Missouri Valley Branch Meeting. Title: Analysis of Chlorella NC64A and PBCV-1 genomes for secreted proteins using computer-based prediction algorithms and progress towards isolation of secreted proteins. April 2011, **Wohlgemuth N**, Lane L, Van Etten JL. Lincoln, NE.

Poster Presentation at UNL Undergraduate Research Conference. Title: Proteins Secreted by Chlorella NC64A. April 2010, **Wohlgemuth N**, Lane L, Van Etten JL. Lincoln, NE.

PROFESSIONAL AND TEACHING EXPERIENCE

PLOS One 2015 – Present
Ad Hoc Reviewer

Johns Hopkins University 1st Term 2014, 2015, & 2016
Teaching Assistant – Fundamental Virology: 260.623.01
Collaborated in design of course assessments. Graded assessments. Provided office hours and review sessions.

Johns Hopkins University August 2016 – October 2016

AWARDS AND HONORS

| | |
|--|-------------------------|
| JHSPH Student Assembly Conference Fund Award | October 2016 |
| American Society for Virology Student Travel Grant | May 2016 |
| American Society for Cell Biology Student Travel Award | December 2015 |
| Eleanor Bliss Honorary Fellowship, JHSPH | March 2014 |
| Dr. J. Harold Drudge Scholarship, JHSPH | March 2013 |
| UNL Chancellor's Scholar | Spring 2011 |
| Dean's List Award, UNL College of Arts and Sciences | Fall 2007 – Spring 2011 |
| Schuler-Mills Scholarship, UNL | August 2010 – May 2011 |
| University Honors Program, UNL | August 2008 – May 2011 |
| UNL Regents Scholarship | August 2007 – May 2011 |
| Corporate National Merit Scholarship | August 2007 – May 2011 |
| NE Bankers Association Grant, UNL | August 2007 – May 2011 |
| Phi Beta Kappa, Honor Society | April 2011 |
| Degering Trust Fund Scholarship, UNL | August 2009 – May 2010 |
| UCARE Award, UNL | August 2008– May 2010 |
| Alpha Epsilon Delta Honors Society | April 2009 |
| Alpha Lambda Delta and Phi Eta Sigma Honor Societies | January 2009 |

SCHOOL AND STUDENT ORGANIZATIONS

| | |
|---|--------------------------|
| Public Health United: A podcast about improving public health dialogue Website manager, Podcast Cohost, Blog Contributor | April 2013 – August 2016 |
| Johns Hopkins School of Public Health School-Wide Committees | |
| Academics Ethics Board | August 2015 – May 2016 |
| Honors and Awards Committee | August 2014 – May 2015 |
| Johns Hopkins School of Public Health Student Assembly | |
| Vice-President of Communications and External Affairs | May 2015 – May 2016 |
| Vice-President of Honors and Awards | May 2014 – May 2015 |
| Member-at-Large | October 2013 – May 2014 |
| Departmental Newsletter – MMI, Johns Hopkins University Editor | October 2013 – May 2014 |
| Biochemistry Club, University of Nebraska-Lincoln | |
| Organized/participated in variety of major-related activities and social events. | |
| President | May 2010 – May 2011 |
| Vice-President | May 2009 – May 2010 |
| Information Specialist | May 2008 – May 2009 |
| Member | August 2007 – May 2008 |

ASSOCIATION MEMBERSHIPS

| | |
|---|----------------|
| American Society for Virology | 2013 – Present |
| American Society for Microbiology | 2013 – Present |
| American Association for the Advancement of Science | 2013 – Present |
| American Society for Cell Biology | 2014 – Present |
| Society for Molecular Biology and Evolution | 2014 – Present |

PROFESSIONAL SKILLS

Basic Spanish language competence
Perl programming for biological applications
Website management

PRIMAY AREAS OF RESEARCH INTEREST

Viral pathogenesis, molecular virology, emerging and zoonotic viruses, virus-host interactions, animal models of viral infections, primary cell culture models, viral bioinformatics.